Project Review Committee

Each research project has an advisory committee appointed by the LTRC Director. The Project Review Committee (PRC) is responsible for assisting the LTRC Administrator or Manager in the development of acceptable research problem statements, requests for proposals, review of research proposals, oversight of approved research projects, and implementation of findings.

LTRC appreciates the dedication of the following Project Review Committee members in guiding this research study to fruition.

LTRC Manager

Walid R. Alaywan
Senior Structures Research Engineer

Members

Kian Yap, DOTD
Doug Hood, DOTD
Nick Fagerburg, DOTD
Mike Boudreaux, LTRC
Mark Morvant, LTRC
Arturo Aguirre, FHWA

Directorate Implementation Sponsor

William T. Temple, DOTD Chief Engineer

Report No. **FHWA/LA.05/397**	2. Government Accession No.	3. Recipient's Catalog No.
4. Title and Subtitle **Evaluation of DOTD Semi-Integral Bridge and Abutment System**	5. Report Date **March 2005** 6. Performing Organization Code	
7. Author(s) **Reda M. Bakeer, Ph.D., P.E., Norma Jean Mattei, Ph.D., P.E., Bashar K. Almalik, Stacey P. Carr, P.E., David Homes**	8. Performing Organization Report No.	
9. Performing Organization Name and Address **Department of Civil and Environmental Engineering** **Tulane University** **New Orleans, Louisiana 70118**	10. Work Unit No. 11. Contract or Grant No. **State Project Number: 736-99-0916** **LTRC Project Number: 01-3ST**	
12. Sponsoring Agency Name and Address **Louisiana Transportation Research Center** **4101 Gourrier Avenue** **Baton Rouge, LA 70809**	13. Type of Report and Period Covered **Final Report** **Period April 2002 – June 2004** 14. Sponsoring Agency Code	
15. Supplementary Notes		

16. Abstract

The Louisiana Department of Transportation and Development (LADOTD) designed and constructed its first prototype semi-integral abutment bridge in 1989. In this design, large longitudinal movements due to expansion and contraction, creep, shrinkage, and settlement are mitigated with an annular space, or gap, constructed between the backwall and the roadway embankment. This annular space is created using a geosynthetic-reinforced embankment constructed underneath the approach slab on the roadway side. To date, DOTD has constructed six prototype semi-integral bridges. These bridges are located in the north, central, and western parts of the state. All six-prototype bridges were replacement projects in areas of the state where soil conditions are relatively good and, therefore, settlement was not a concern. The approach slab in the DOTD prototype design is cast integral with the bridge making it one continuous structure. Construction of a geosynthetic-reinforced embankment would eliminate the lateral pressure transfer to the backwall of the semi-integral bridge. The prototype design addresses the problem of the loss of soil support under the approach slab due to settlement or lateral movement. A gap created between the backwall and the reinforced embankment would eliminate the passive pressure from developing on the backwall due to bridge movement into the backfill. Permitting free backwall movement would also eliminate the potential for abutment rotation.

In view of the review of existing records, field inspections, conventional structural and geotechnical analyses, and the finite element parametric study, the researches concluded that the present DOTD design for semi-integral bridges is structurally sound. Based on the results of a cost/benefit analysis, the researchers concluded that the present design is also cost effective. Therefore, the present design could be continued by DOTD in areas with fair to good subsoil conditions. Future designs should consider the effect of settlement and the potential for deep-seated slope stability at sites with thick, soft cohesive and/or highly compressible subsoils, specifically when the grades require relatively high embankments. At these sites, preload surcharge programs, possibly with wick drains, could be considered. Alternatively, lightweight aggregate or EPS geofoam could be used for the construction of the embankment to minimize detrimental effects of settlements.

17. Key Words	18. Distribution Statement
Integral abutment bridge, semi-integral abutment bridge, jointless bridge, approach slabs, headwall, finite element analysis, field performance.	**Unrestricted. This document is available through the National Technical Information Service, Springfield, VA 21161.**

19. Security Classif. (of this report)	20. Security Classif. (of this page)	21. No. of Pages	22. Price
N/A	**N/A**	**148**	**N/A**

Evaluation of DOTD Semi-Integral Bridge and Abutment System

by

Reda M. Bakeer, Ph.D., P.E.
Bashar K. Almalik
Stacey P. Carr, P.E.

Department of Civil & Environmental Engineering
Tulane University
New Orleans, Louisiana 70118

Norma Jean Mattei, Ph.D., P.E.
David Homes

Department of Civil & Environmental Engineering
University of New Orleans
New Orleans, Louisiana 70148

LTRC Project No. 01-3ST
State Project No. 736-99-0916

conducted for
Louisiana Department of Transportation and Development
Louisiana Transportation Research Center

March 2005

ABSTRACT

An integral abutment bridge does not have deck joints at the abutments. The backwall is integral with the superstructure and dimensionally the same as the diaphragms cast to the girders. This design eliminates both the need for joints and sealers and the maintenance associated with their use generally resulting in a more economical bridge to construct with lower long-term maintenance costs. Elimination of joints also improves rideability for drivers. However, because of structural continuity, integral construction may introduce secondary stresses into the superstructure. Additional secondary stresses could develop due to thermal changes and gradients, creep and shrinkage of concrete, and settlement. Flexibility and free movement are essential factors in the design of a jointless bridge. Also noteworthy is the fact that integral bridges experience less overall movement than what is theoretically assumed.

Thirty-five states in the U.S. have constructed jointless bridges and eleven have reported a very good to excellent overall experience. Another twenty-one states indicated a good to satisfactory experience. However, Minnesota reported poor experiences, and Arizona has discontinued the use of jointless bridges. Sixteen states indicated that there is a strong need for further research on jointless bridge design and construction.

The Louisiana Department of Transportation and Development (LADOTD) designed and constructed its first prototype semi-integral abutment bridge in 1989. In this design, large longitudinal movements due to expansion and contraction, creep, shrinkage, and settlement are mitigated with an annular space, or gap, constructed between the backwall and the roadway embankment. This annular space is created using a geosynthetic-reinforced embankment constructed underneath the approach slab on the roadway side. To date, DOTD has constructed six prototype semi-integral bridges. These bridges are located in the north, central, and western parts of the state. All six-prototype bridges were replacement projects in areas of the state where soil conditions are relatively good and, therefore, settlement was not a concern.

The approach slab in the DOTD prototype design is cast integral with the bridge making it one continuous structure. Construction of a geosynthetic- reinforced embankment would eliminate the lateral pressure transfer to the backwall of the semi-integral bridge. The prototype design addresses the problem of the loss of soil support under the approach slab due to settlement or lateral movement. A gap created between the backwall and the reinforced embankment would eliminate the passive pressure from developing on the backwall due to bridge movement into the backfill. Permitting free backwall movement

would also eliminate the potential for abutment rotation. Specifically, in the absence of a gap on the typical integral bridge, large movements would develop because of two factors:

- Rotation/movement of the backwall that would cause the development of higher lateral pressure that is closer in magnitude to the passive value, which is possibly higher than the design value (active or at rest).
- Rotation could cause the earth pressure distribution to become non-hydrostatic. Accordingly, the earth pressure resultant would act at a higher location. This results in higher overturning moments that may exceed the design values.

Field inspection of the six prototype semi-integral abutment bridges confirmed that they are all performing well, with a few exceptions. The presence of a gap was confirmed in all bridges. Some hairline cracks were found in several of the bridge decks, specifically at the connection between the approach slab and the backwall. These are expected and should be of no concern.

Bridge SP 39-04-31 does not include an open joint at the interface of the approach slab with the roadway. Over the years, the bridge repeatedly expanded and contracted due to thermal variations. As a result, it pushed the adjacent asphalt pavement away from the approach slab, forming a noticeable mound of asphalt and an open joint. This problem produced a bump that motorist felt when driving over the bridge ends. Periodically, the DOTD district office removed the asphalt mound and filled the joint with asphalt. This problem was corrected in all subsequent semi-integral bridges.

Bridges SP 129-02-1799-1 and 129-02-1338-1 are presently in good condition, but may experience future problems due to the placement of incompressible gravel fill in the annular space between the geosynthetic-reinforced embankment and the backwall according to the design plans. This was confirmed by field inspections. The short spans of these bridges, and the fact that the fill material was probably not fully compacted, have reduced the impact of longitudinal movements. However, more frequent inspections of these two bridges should be made focusing the backwalls and the connection of the backwall with the approach slab.

In view of the review of existing records, field inspections, conventional structural and geotechnical analyses, and the finite element parametric study, the researchers concluded that the present DOTD design for semi-integral bridges is structurally sound. Based on the results of a cost/benefit analysis, the researchers concluded that the present design is also cost effective. Therefore, the present design could be continued by DOTD in areas with fair to

good subsoil conditions. Future designs should consider the effect of settlement and the potential for deep-seated slope stability at sites with thick, soft cohesive and/or highly compressible subsoils, specifically when the grades require relatively high embankments

A continuous gap should be established between the embankment and backwall in all future semi-integral bridge designs or to fill it with a soft compressible material, such as EPS geofoam. Attention should be given during construction to eliminate or minimize the potential for fallen debris inside the gap. Also, a weak joint should be created in the approach slab at some distance away from the backwall, e.g., 10 feet (3 m) on a 40 foot (12 m) long approach slab, to maintain a smooth transition between the bridge and roadway if excessive settlement does develop under the roadway embankment with time.

ACKNOWLEDGMENTS

The Departments of Civil and Environmental Engineering at Tulane University (Tulane) and the University of New Orleans (UNO) conducted this study. The Louisiana Transportation Research Center (LTRC) in cooperation with the Louisiana Department of Transportation and Development (DOTD) sponsored the study. Their financial support is greatly appreciated. William B. Conway and Modjeski and Masters, Inc. (M & M) are also acknowledged for their initial willingness to assist with this project, even though their assistance was not required. Modjeski and Masters were also supportive of Stacey Carr and her work on this project.

Fieldwork was performed by the principal investigators and graduate students of Tulane (2) and UNO (1) under the administrative direction of Walid Alaywan, Structural Research Engineer at LTRC. Several personnel from DOTD districts 07, 08, and 58 under the supervision of Stacey White, Kent Hardin, and Tommy Hale assisted in this effort. Archie Ezell and Monty Bradley from district 58 assisted in this effort too.

Appreciation is also expressed to Drs. Robert N. Bruce, Jr. and San Hla Aung of Tulane University, Drs. Mike Folse, Paul Herrington, Mysore Nataraj, and Ken McManis of UNO, and other Tulane and UNO personnel including Tony Jensen, Mickey Alexander, and Duane Johnson.

IMPLEMENTATION STATEMENT

Results of this research will benefit DOTD's designers by providing a systematic evaluation of the performance of the existing semi-integral prototype bridges constructed in Louisiana. This research will assist in evaluating the present DOTD semi-integral abutment bridge design. It will also provide guidelines and recommendations for future use of semi-integral abutment bridges in other areas of the state. Since the semi-integral abutment bridge system has proven to be a viable and cost-effective solution, this conceptual design could be implemented on a wider scale in areas with good soil conditions. However, consideration should be given to the effect of settlement at sites with thick, soft cohesive and/or highly compressible soils and relatively high embankments.

TABLE OF CONTENTS

LIST OF TABLES

LIST OF FIGURES

INTRODUCTION

Integral Abutment Bridges

An integral abutment bridge system is constructed without deck joints, particularly at the abutments. Integral abutment bridges have also been referred to as integral, jointless, rigid-frame and U-frame bridges. First built in the United States during the 1930s, integral abutment bridges have experienced extensive worldwide use in the 1990s.

Integral bridges can be single or multiple spans, and are built in an integral or a semi-integral configuration. The superstructures of integral bridges are cast integrally with the abutments. Piers can be cast integrally or kept independent from the superstructure. In a jointless bridge, the backwall is integral with the superstructure and dimensionally the same as the diaphragms cast to the girders. This type of construction eliminates costly joints and sealers as well as maintenance costs associated with their use, resulting in a more economical and low maintenance structure and better overall rideability.

A slight modification of the integral abutment bridge is the semi-integral design, which eliminates joints, but still uses conventional bearings. However, unlike conventional bridges, the jointless slab protects these moveable bearings. Semi-integral bridges have end diaphragms that are integral with the superstructure, but non-integral with the foundation. Semi-integral bridges require a horizontal joint separating the superstructure and the abutment. Stub abutments (short height), one type of semi-integral abutment, have worked well in limiting abutment cracking. Figure 1 shows examples of integral and semi-integral abutment designs [1]. Louisiana uses the semi-integral type jointless bridge design.

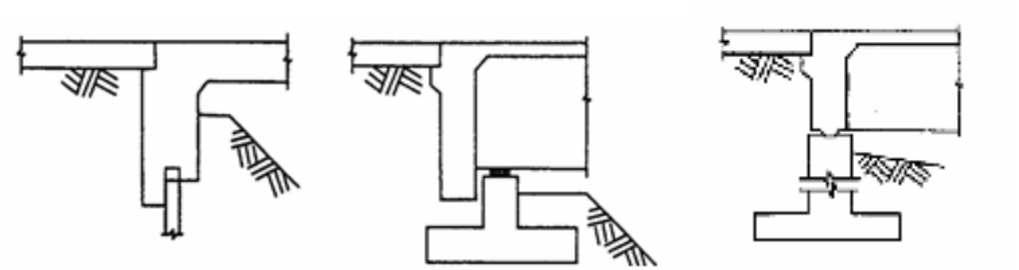

Figure 1
Integral and semi-integral abutments

Integral or semi-integral bridges can incorporate precast concrete girders, cast-in-place concrete girders or steel girders. Precast, prestressed concrete experiences less thermal movement than steel and lower long-term movement due to creep and shrinkage than cast-in-place concrete. In moderate climates, concrete expands about 0.5 inch (13 mm) over a 100 feet (30.5 m) span length. Steel superstructures generally expand at twice this rate [1].

Approach slabs are generally used with integral and semi-integral bridges. Their primary function is to transfer the bridge movement to an open joint at the roadway interface. Sleeper slabs or grade beams are typically used to support the approach slabs at the roadway interface. In some instances, plastic sheets or similar materials are placed over the soil backfill beneath the approach slab to permit longitudinal movement when the superstructure expands or contracts. Mild reinforcement keeps the approach slab attached to the abutment and prevents the development of a crack between the slab and abutment. Typical approach slabs are about 20 to 25 feet (6.0 to 7.6 m) in length.

Jointless bridges may not be completely jointless if the designers only change the number of joints and/or their locations. In addition, the continuity achieved by integral construction may introduce secondary stresses into the superstructure that could affect long-term performance and rideability. These secondary stresses could be due to thermal and moisture changes, gradients, concrete creep and shrinkage, or long-term subsoil consolidation settlement. Therefore, open joints are required at the end of the approach slabs to accommodate longitudinal movement of the superstructure. Expansion dams may also be used at midspan of long span bridges.

Advantages and Disadvantages of Integral Bridges

The main advantage of integral bridge design is the elimination of many, if not all, of the bridge joints, which reduces construction, maintenance, and repair costs. Jointless bridges were originally developed to eliminate expansion joints in short to moderate length bridge design. Expansion joints can develop major maintenance concerns over time, including expansion joints that leak and expansion materials that work their way out of the joints. Broken debris associated with expansion joints can be dangerous to motorists, and joint maintenance is expensive, especially because it disrupts traffic flow. In addition, fewer construction joints are required with integral abutments, further reducing construction time. Large expansion bearings are often eliminated, again reducing construction costs. Expansion bearings may freeze over time, so eliminating them whenever possible reduces the cost of future repair or replacement and eliminates possible earthquake damage to bearings.

One row of vertical piles is typically used at the end of the bridge bents, reducing construction cost and time. Integral bridges require a simplistic analysis as a continuous frame with one horizontal member representing the bridge deck. Loads on the substructure are distributed over the total number of supports. This redundancy is also carried over for catastrophic events, such as earthquakes. The last advantage of jointless bridges is its improved rideability over that of a jointed bridge design. A noticeably smoother surface is provided for bridge traffic, and bumps are eliminated, especially at the bridge abutments.

The problems associated with integral bridges include minor longitudinal and transverse cracking, poor drainage at the abutments, cracking and spalling in bearing areas, and settlement of the approach slabs. Backfill may settle in the gap between the backfill and abutment when the superstructure contracts. Wingwalls may crack due to superstructure movement, joints could open between the bridge and approach pavement, and the use of improper size joints at the end of approach slab has caused problems.

Similar to a conventional bridge, an integral abutment bridge will also experience length changes due to seasonal temperature variations. However, the integral abutment bridge accommodates this length change differently. A conventional bridge has a thermally active bridge superstructure and thermally inactive substructure, while an integral abutment bridge connects this thermally active superstructure to the substructure. The resulting problem in a conventional bridge is structural, since joints and bearings are used to accommodate temperature movement. On the other hand, the resulting problems in an integral abutment bridge are geotechnical in nature, due to the thermally induced movement against the roadway embankment. Because of soil structure interaction, this geotechnical problem can cause significant structural damage to the bridge. Thus, integral abutment bridges can exhibit long-term problems and high maintenance costs. A semi-integral abutment bridge with an open gap behind the backwall, as in the DOTD prototype design, keeps the thermally active superstructure separate from the thermally inactive substructure. Figure 2 shows a semi-integral bridge abutment configuration, similar to the DOTD prototype design.

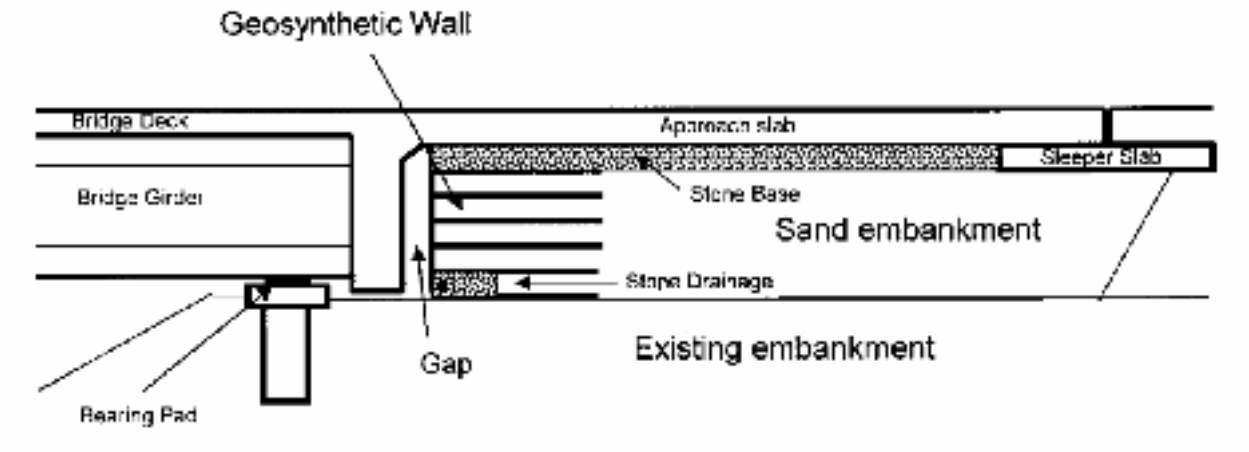

Figure 2
Semi-integral abutment configuration

Integral abutments move against the embankment in the summer and away from the retained soil in the winter. This movement gets progressively worse with time, with large lateral earth pressures developing behind the abutment during the summer expansion of the superstructure. The abutment may not only translate, but also rotate about its base with larger movements at the upper portion of the abutment. During winter, the abutment moves away form the retained soil, but a soil wedge from the unsupported retained soil may fall toward the abutment. This soil wedge causes additional pressure on the abutment during the following summer when the bridge expands again. This long-term process is called "ratcheting" [2]. Ultimately, this additional pressure could cause the abutment to fail over many years of repeated cyclic movement. Alternatively, the construction cost of the abutment would increase if it were designed to withstand this additional pressure. This potential problem is addressed in the DOTD design where a gap is constructed between the roadway embankment and the backwall.

Another effect of the soil wedge movement into the abutment during winter months is the resulting settlement or "void" of soil that could develop at the soil surface behind the abutment of an integral bridge. This settlement could result into one of two consequences. First, if the approach slab were to be constructed integral with the bridge superstructure, the approach slab would have to span over this void and, therefore, could fail in flexure. If the approach slab were not attached to the superstructure, a difference in elevation could develop between the approach slab and the road surface, resulting in a bump at the end of the bridge similar to those experienced with conventional bridges. As a testimony to this problem, South Dakota detected a void under the approach slab in 140 of its integral bridges [2]. The severity of this void depends on the quality of the backfill material. This void development is a fairly short-term problem, developing within only a few years of construction.

Ratcheting is a long-term problem, sometimes taking decades to produce severe problems. Again, this potential problem is addressed in the DOTD semi-integral abutment bridge design.

Other basic disadvantages of jointless bridge design are the special requirement for the foundation system such as the need for flexible foundations, limits on the length to restrict bridge movement, and restrictions on skew angles to limit secondary forces. If a bridge cannot be constructed with flexible foundations, or if it has an excessive length or a large skew angle, a jointless bridge may not be the appropriate design choice.

U.S. Experience with Integral Bridges

As of 2001, 35 of the 50 states had constructed jointless bridges [1]. Eleven states reported their overall experience with integral bridges as either very good or excellent. Another 21 say their experience has been good to satisfactory. However, Minnesota reported poor experiences and Arizona has discontinued the use of jointless bridges. Of the 35 states, 16 say there is definitely a need for future research of jointless bridge design and construction. Figure 3 shows the states with jointless bridges and their reported experiences of bridge performance.

Virginia has reported more than 10 years of satisfactory performance with their more than 25 integral bridges. California, Kansas, Tennessee, Washington and Wyoming have each constructed over 1,000 integral bridges [3]. All have had at least satisfactory experiences. Kansas and Tennessee rate their best experiences as being very good. Arizona discontinued the use of integral bridges because of the expensive repairs to all the approaches of their more than 50 integral bridges. Alaska is another state that had problems with integral bridges. Frozen soil has adhered to integral backwalls and caused hairline cracking.

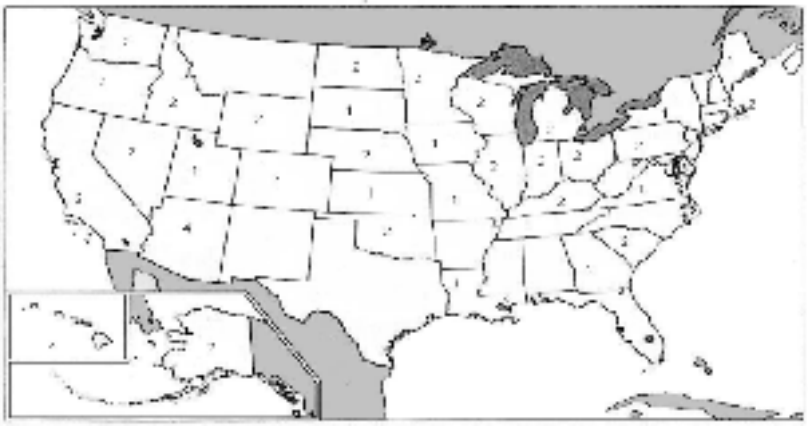

1- Very Good to Excellent 2- Satisfactory to Good 3- Poor to Fair 4- Discontinued

Figure 3
States with jointless bridges and their reported performance

Approach slabs are the most common problem reported with integral bridges. In North Dakota, approach slabs were resting on lips protruding from the abutments. This has allowed runoff to deteriorate the concrete abutment. North Dakota has since modified this detail. However, when states have connected slabs rigidly to the abutments, cracks have often formed at the far end of the approach slab near the roadway. Washington State has reported having problems with their approach slabs on bridges longer than 350 feet (107 m).

Design Considerations of Integral Bridges

Jointless bridges do not have standard design procedures. Presently, only California, Colorado, Idaho, Iowa, Kentucky, Massachusetts, Michigan, Minnesota, Missouri, New York, Pennsylvania, South Carolina, Tennessee, Virginia, Oregon, and Washington have their own temperature, creep and shrinkage criteria, a design methodology, and abutment design parameters. Some of the success that has been achieved with integral bridges is because they experience less overall movements than what is theoretically anticipated. Flexibility and free movement are very important factors in the design of jointless bridges. Some lessons learned from the use of jointless bridges include [1]:

- Designing the bridge with details that allow sufficient movement,
- Using stub abutment or semi-integral abutments to avoid abutment cracking,
- Limiting span length,

- Limiting skew angle,
- Using a single row of flexible piling (possibly with predrilled holes),
- Using sleeper slabs to reduce the effects of settlement, and
- Using granular backfill with sufficient drainage.

States have identified the establishment of integral bridge design criteria and guidelines as an issue that needs to be addressed. Other topics that need to be addressed are structural limitations, seismic resistance, approach slab and wingwall design, effects of earth pressure behind the abutments, pile stresses due to the bridge's longitudinal movement, and deck cracking potential.

Table 1 includes a list of the maximum bridge length limitations imposed by 31 states. These states have restrictions on skew angles that vary from 0 to 45 degrees, with most states limiting them to about 30 degrees [1]. Tennessee has constructed the longest jointless integral bridge at just over 1,175 feet (358 m) in length. The bridge has nine spans of precast, prestressed concrete bulb-tee girders with no expansion bearings. The bridge was constructed in 1997 and has performed satisfactorily. Table 1 also lists the year each state recorded the construction of its first integral/semi-integral bridge. For the purpose of comparison, a summary of the jointless bridge design requirements in five states with available published data is given in tables 2 and 3 [1].

International Experience with Integral Bridges

The United Kingdom has had so much success with integral abutment bridges that the British Highways Agency Standard now recommends that any new bridge less than 200 feet (60 m) long should be integral. This is primarily due to the overall cost effectiveness of integral bridges, especially the elimination of the cost of replacement of failed expansion joints. In addition, this recommendation is due to the longer life expectancy of integral bridges, as compared with jointed bridges.

Canada has several provinces with integral experience. Alberta, Quebec, Nova Scotia, and Ontario have jointless bridges, and most have reported good to satisfactory experiences with their use. Nova Scotia built its first integral bridge in 1986, and Quebec built its first integral bridge in 1988. Ontario limits its integral bridge span to less than 325 feet (100 m) and a 20-degree skew angle. Ontario's recommendations for their integral bridges are similar to those used by many U.S. states. These include a weak joint between

the approach slab and roadway pavement, granular backfill with a 6-inch (150 mm) diameter perforated drain pipe, and a single row of vertical steel H-piles.

Table 1
Maximum integral bridge length and skew constraints

State	First Year Built	Length Limit in feet (m)	Skew Angle (degrees)
Arkansas	1996	260 (79)	33
California	1950	1 inch (25 mm) movement	45
Georgia	1975	410/260 (125/79)	0/40
Hawaii	NA	250 (76)	NA
Illinois	1983	300 (92)	30
Indiana	NA	300 (92)	30
Idaho	NA	400 (122)	30
Iowa	1962	300 (92)	30
Kansas	1935	450 (137)	NA
Kentucky	1970	400 (122)	30
Louisiana	1989	1,000 (305)	0
Maine	1983	150 (46)	30
Michigan	1990	None	30
Missouri	NA	600 (183)	NA
Massachusetts	1930	300 (92)	30
North Dakota	1960	400 (122)	30
Nevada	1980	200 (61)	45
New York	1980	300 (92)	30
Ohio	NA	375 (114)	30
Oklahoma	1980	210 (64)	0
Pennsylvania	1946	600 (183)	20
Oregon	1940	200 (61)	25
South Dakota	1948	700 (214)	35
South Carolina	NA	500 (153)	30
Tennessee	1965	2 inches (50 mm) movement	No limit
Utah	NA	300 (92)	20
Virginia	1982	500 (153)	NA
Wyoming	1957	360 (110)	30
Washington	1965	450 (137)	40
Wisconsin	NA	300 (92)	30

Table 2
DOT's guidelines for integral bridges

SUPERSTRUCTURE	
Illinois	• No thermal force analysis for concrete structures < 300 feet (91.5 m) & steel < 200 feet (61 m)
Indiana	• Maximum steel structures 250 feet (76 m), concrete 300 feet (91.5 m), slab bridges 200 feet (61 m) • Longer structures permitted if analysis shows feasibility
New York	• Maximum steel or precast concrete structures 300 feet (91.5 m), and with approval < 400 feet (122 m) • Not recommended > 400 feet (122 m)
Pennsylvania	• Maximum steel structures 400 feet (122 m) & concrete 600 feet (183 m) • Not recommended > 600 feet (183 m) • Maximum temperature range 120°F (49°C) for concrete and 90°F (32°C) for steel
Tennessee	• Constructed maximum steel structures 535 feet (163 m) & concrete structures 1,175 feet (358 m) • Special approval for steel structures > 425 feet (129.5 m) & concrete 800 feet (244 m) • Maximum temperature range –18 to 49°C (0 to 120°F) for concrete and 25 to 95°F (–4 to 35°C) for steel
APPROACH SLABS / SUBGRADE	
Illinois	• Required non-compacted porous granular backfill, geotextile & 6 inches (150 mm) perforated drain pipe
Indiana	• Required approach slab • Required 2 layers of minimum 6 mil (0.15 mm) PE sheeting between approach slab & subgrade • Required Indiana's "type B" backfill & 6 inches (150 mm) perforated drain pipe
New York	• Required approach slab with saw cut or construction joint between approach slab & backwall for controlled crack location • Required geotextile & 6 inches (150 mm) perforated drain pipe • Required sleeper slab • Required expansion joint at end of approach slab for spans > 150 feet (45.7 m) and < 150 feet (45.7 m) for rigid pavements
Pennsylvania	• Required 25 feet (7.6 m) approach slab • Required 2 layers of minimum 6 mil (0.15 mm) PE sheeting between approach slab & subgrade • Required joint between approach slab & backwall for controlled crack location • Required granular backfill, geotextile & 6 inches (150 mm) perforated drain pipe • Required sleeper slab • Required expansion joint at end of approach slab for spans > 150 feet (45.7

	m) and < 150 feet (45.7 m) for rigid pavements
Tennessee	• Required constructed joint between approach slab & backwall • Required Granular backfill, geotextile & 6 inches (150 mm) perforated drain pipe Required expansion joint at end of approach slab

ABUTMENTS / PIERS	
Illinois	• Required parallel abutment & piers
Indiana	• NA
New York	• Required parallel abutment & beams
Pennsylvania	• Required parallel abutment & beams
Tennessee	• NA
WINGWALLS	
Illinois	• "dog ear" wingwalls
Indiana	• NA
New York	• NA
Pennsylvania	• Avoid wingwalls > 10 feet (3 m)
Tennessee	• NA
PILES / FOUNDATIONS	
Illinois	• Concrete pile permitted for 200 feet (61 m) structure • Required steel H-piles for 200 to 300 feet (61 to 91.5 m) structure
Indiana	• Steel H-piles or steel encased concrete piles at end bents, H-piles preferred • Piles require 8 feet (2.4 m) predrilled hole filled with pea gravel if stiff clay is found within 10 feet (3 m) of cap
New York	• Cast-in-place piles allowed for spans < 150 feet (45.7 m), otherwise H-piles required • Only single line of piles, orientated for weak axis bending • Top 8 feet (2.4 m) of pile predrilled & filled with sand
Pennsylvania	• Steel encased concrete piles allowed for spans < 150 feet (45.7 m), otherwise H-piles required • Only single line of piles, orientated for weak axis bending • Top 10 to 20 feet (3 to 6 m) of pile predrilled & filled with sand
Tennessee	• Spread footing allowed for < 0.25 inch (6 mm) movement • Required one row of piles for movement > 0.25 inch (6 mm)

Louisiana Prototype Semi-Integral Bridges

The Louisiana Department of Transportation and Development (DOTD) designed and constructed its first prototype semi-integral abutment bridge in 1989. To date, DOTD has constructed six such prototype semi-integral bridges. The approach slab in the DOTD prototype design is cast integral with the bridge, thus making them one continuous structure. All six-prototype bridges were replacement projects in areas of the state with relatively good soil conditions. Therefore, settlement was not deemed a potential problem at these sites. The six prototype semi-integral abutment bridges are located in the north, central, and western parts of the state, as shown in figures 4-6.

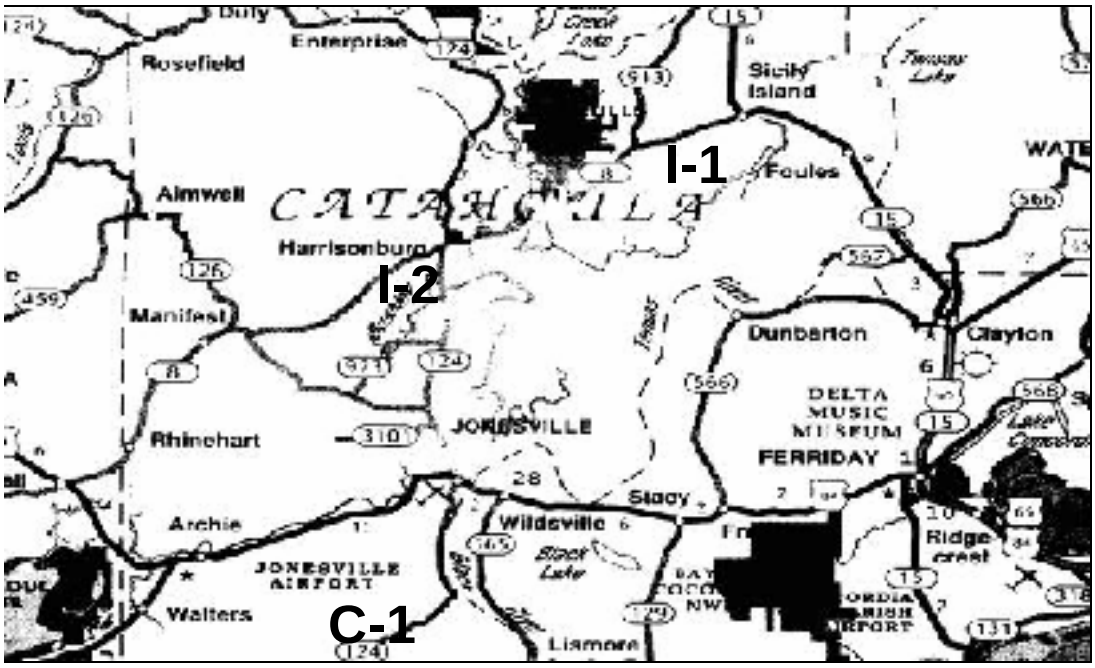

Figure 4
District 58 semi-integral and conventional bridges considered in the study

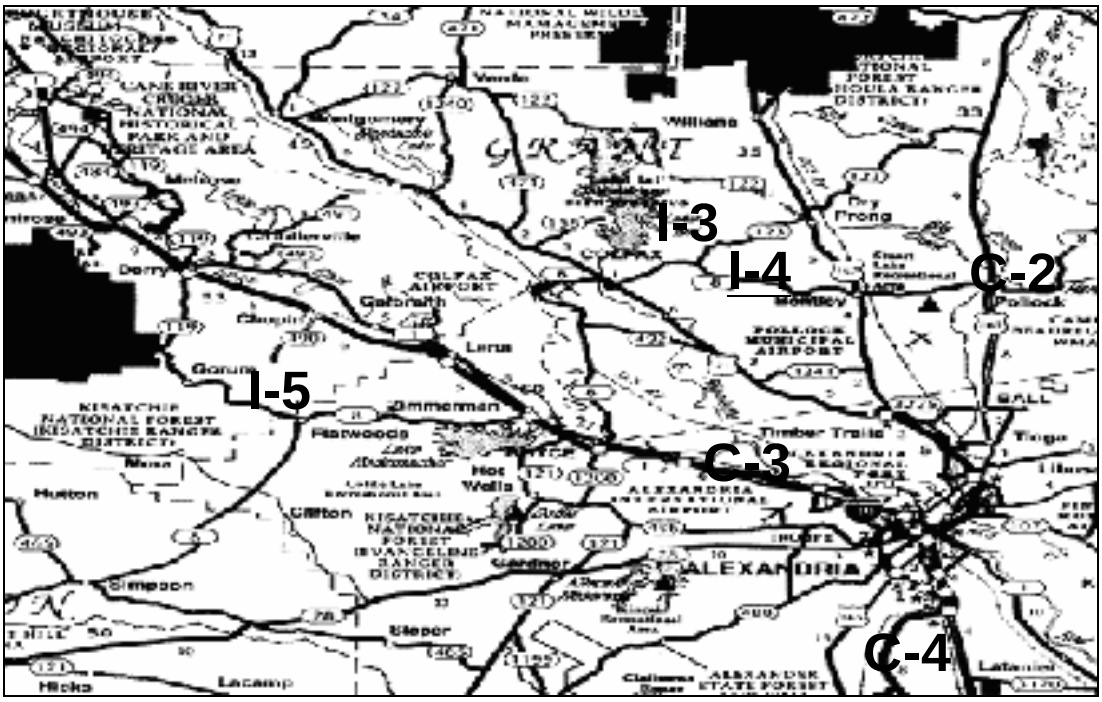

Figure 5
District 8 semi-integral and conventional bridges considered in the study

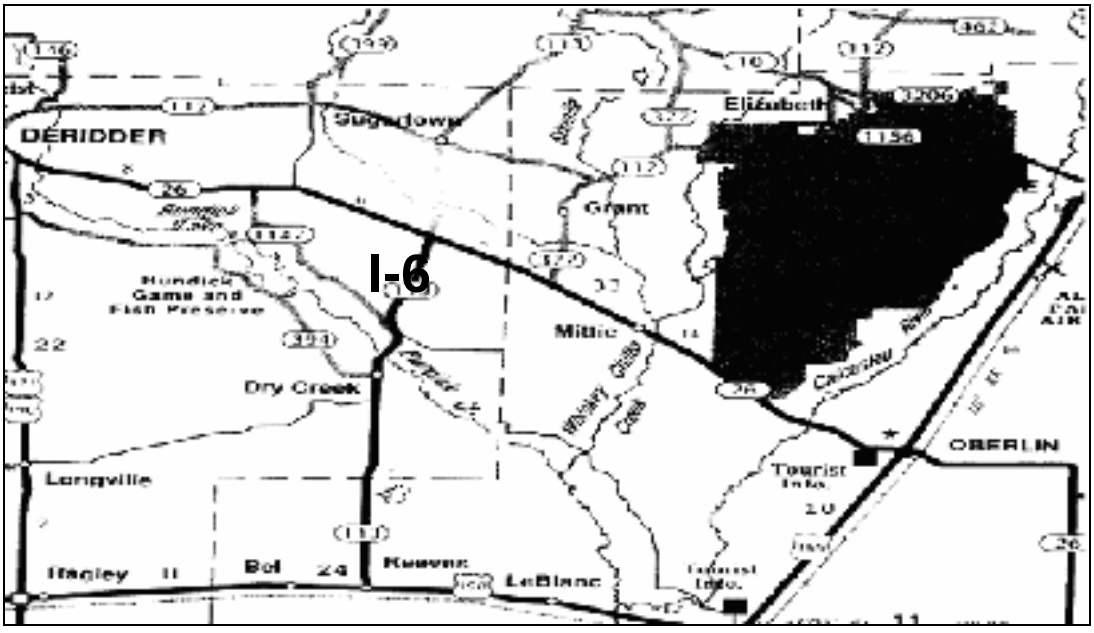

Figure 6
District 7 semi-integral bridge considered in the study

Details of the approach slab, gap, and backwall of the DOTD semi-integral bridge are illustrated in figure 7. In this design, large longitudinal movements due to expansion and contraction from thermal movements, creep, shrinkage, and settlement are all mitigated with an annular space, or vertical gap, established between the abutment and the roadway embankment. The face of the geosynthetic-reinforced roadway embankment is located about 6 inches (150 mm) away from the backwall creating a continuous gap to accommodate lateral movement of the semi-integral superstructure. The embankment is constructed of a non-plastic granular fill, but the first 6 to 10 feet (1.8 to 3.1 m) of the top lift and the first 3 feet (0.91 m) of the bottom lift of the embankment are filled with gravel/crushed stone. A perforated drainage pipe is placed in the gravel in the bottom lift. Geogrid sheets are used to construct the reinforced embankment, and a geotextile fabric is included in the lift in the segment near the embankment face to prevent flow of the fill material from the wall face into the gap.

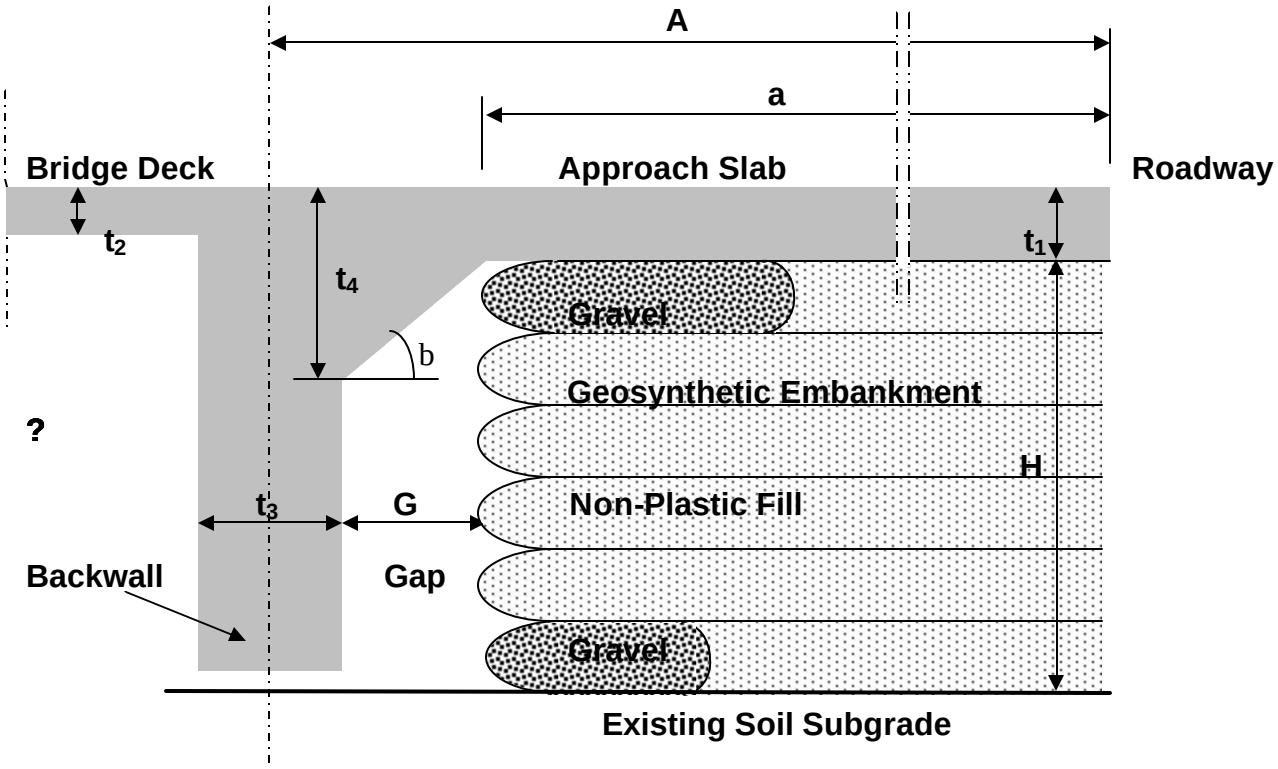

Note: Girders and abutment are not shown for clarity.

Figure 7
Details of DOTD prototype semi-integral bridge design

OBJECTIVES

The objective of this project was to evaluate the present design of the DOTD prototype semi-integral abutment bridge design. This objective was accomplished through the following specific tasks:

- Review existing design and maintenance records of the six semi-integral abutment bridges.
- Compare the performance of the semi-integral abutment bridges with that of a representative set of four comparable conventional bridges in terms of design, performance, rideability, and construction cost.
- Perform conventional structural and geotechnical analyses on one of the semi-integral bridges.
- Perform a parametric study on one of the semi-integral abutment bridges using the finite element method to examine the effect of some of the design parameters on the bridge performance.
- Perform cost/benefit analysis on a selected semi-integral abutment bridge and a comparable conventional bridge of the same span and dimensions.
- Develop guidelines and recommendations for future designs of semi-integral abutment bridges.

The project tasks were performed as a collaborative effort between Tulane University (Tulane), University of New Orleans (UNO), LTRC, and DOTD.

SCOPE

The Louisiana Department of Transportation and Development (DOTD) has designed and constructed a prototype semi-integral abutment bridge that is cast continuously from abutment to abutment. This eliminates the need for joints and sealers. The present DOTD design includes the construction of a gap between the backwall and the roadway embankment. However, a conventional jointed bridge with abutments is still the standard design used by DOTD statewide. To date, DOTD has built six prototype semi-integral bridges in north, central, and western Louisiana, but the performance of these semi-integral abutment bridges has not been evaluated. Consequently, the main components of this research project included the following:

1. Collect information regarding the nationwide and international use of integral abutment bridges.
2. Compare these designs with DOTD's design and assess the applicability of some of the design concepts for use in Louisiana.
3. Assess performance of the six semi-integral abutment bridges already constructed by DOTD and compare it with the performance of a representative set of comparable conventional bridges of similar design and age and within the same geographical area. This included:
    - Examination of the construction and maintenance records of the semi-integral and the representative set of conventional bridges,
    - Field evaluation of the condition and performance of these bridges, and
    - Performing finite element computer modeling of the DOTD prototype semi-integral bridge design.
4. Compare materials, construction and maintenance costs of a prototype semi-integral abutment bridge to the cost of a conventional bridge of similar dimensions, loads, soil conditions, etc.
5. Recommend methods for improving the DOTD design of the prototype semi-integral abutment bridge.
6. Provide guidelines and recommendations for selection of the appropriate bridge type, a semi-integral abutment bridge versus a conventional bridge, for use in future DOTD projects. This includes identifying limitations of the prototype semi-integral abutment bridge design.

METHODOLOGY

The performance and conditions of the prototype semi-integral abutment bridges and a selected set of representative conventional bridges were evaluated based on available information that included design and maintenance records, field evaluation and testing, conventional structural and geotechnical analyses, finite element analysis (FEA), and cost/benefit analysis.

Available Information

A representative set of four comparable conventional bridges was identified in consultation with LTRC and DOTD for inclusion in the study. Tulane and UNO compiled the available information pertaining to the six semi-integral bridges and the representative set of conventional bridges from DOTD offices. The information included construction drawings, soil information, and inspection and maintenance records. Specific information pertaining to each semi-integral bridge is summarized in table 3. All bridges have concrete decks and approach slabs. They also include concrete sleeper slabs with the exception of Bridge I-1. All adjacent roadways are paved with flexible (asphalt) pavement.

For a valid comparison between the two types of bridges, the selected conventional bridges were of similar age, design (span, width, capacity, etc.), soil conditions, average daily traffic, etc. In addition, the selected conventional bridges were within the general geographical area of the six semi-integral bridges to reduce variations in ambient conditions and to reduce travel time during field-testing. The main information pertaining to the four conventional bridges considered in the study is summarized in table 4.

Table 3
DOTD prototype semi-integral abutment bridges

Property*	**Bridge**					
Code	I-1	I-2	I-3	I-4	I-5	I-6
Name	Bayou Louis	Bushley Bayou	Unnamed Creek	Beaver Creek	Bayou Bourbeaux	Whiskey Chitto Creek & Relief
SP No.	39-04-31	041-01-0030	129-02-0021	129-02-0021	835-10-0010	139-04-0014
ST No.	581303904031	581304101081	082212902079	082212902133	083583510023	070613904014
Year Built	1989	1998	1999	1999	1996	1996
Parish	Catahoula	Catahoula	Grant	Grant	Natchitoches	Beauregard
District	58	58	8	8	8	7
Highway	LA 8	LA 124	LA 122	LA 122	LA 490	LA 113
Total Length, feet-inches (m)	595-00 (181.5)	725-00 (221.0)	75-06 (23.0)	75-06 (23.0)	215-00 (65.5)	565-00 (172.2)
Spans	6	9	1	1	3	8
Girder Type	IV	III	III	III	III	III
Wall Thickness (t_3) inch (mm)	18 (457)	18 (457)	18 (457)	18 (457)	18 (457)	17 (432)
Deck Slab Thick. (t_2), inch (mm)	7 (178)	7.5 (191)	7.5 (191)	7.5 (191)	7.5 (191)	7.5 (191)
Haunch Depth (t_4), inch (mm)	14 (355)	18 (457)	18 (457)	18 (457)	18 (457)	18 (457)
Gap Width (G), inch (mm)	6 (152)	6 (152)	6 (152)	6 (152)	6 (152)	6 (152)
Hunch Angle β°	45	45	45	45	45	45
Length (a), feet (m)	36 (11.0)	34 (10. 4)	34 (10. 4)	34 (10. 4)	34 (10. 4)	34 (10. 4)
Embank. Height (H), feet (m)	5-07 (1.7)	3-00 (0.9)	4-06 (1.4)	4-06 (1.4)	3-08 (1.1)	3-08 (1.1)
Appr. Slab Length (A), feet (m)	40 (12.2)	40 (12.2)	40 (12.2)	40 (12.2)	40 (12.2)	40 (12.2)
Appr. Slab Width, feet-inches (m)	46-10 (14.3)	46-10 (14.3)	32-10 (10.0)	32-10 (10.0)	32-10 (10.0)	42-10 (13.1)
Appr. Slab Thick. (t_1), inch (mm)	10 (254)	12 (305)	12 (305)	12 (305)	12 (305)	12 (305)
Sleeper Slab Length, feet (m)	--	10 (3.1)	10 (3.1)	10 (3.1)	10 (3.1)	10 (3.1)

* Refer to Figure 7.

Table 4
Representative set of conventional bridges

Property	Bridge			
Code	C-1	C-2	C-3	C-4
Name	Little River	Big Creek	Nantaches Creek	Lena-Flatwoods
SP No.	041-01-23	040-03-0014	009-03-0022	455-05-0017
ST No.	58130410100221	08220400308471	08220090305981	08404550553001
Year Built	1978	1981	1983	1987
Parish	Catahoula	Grant	Grant	Rapides
District	58	8	8	8
Highway	LA 124	LA 8	US 71	I-49
Total Length, feet (m)	555 (169.2)	302 (92.1)	222 (67.7)	213 (64.9)
Spans	7	6	4	2
Approach. Slab Length (A), feet (m)	40 (12.2)	NA	40 (12.2)	40 (12.2)
Approach Slab Width, feet (m)	40/24 (12.2/7.3)	NA	40/24 (12.2/7.3)	39/27 (12.2/8.2)
Approach Slab Thick. (t_1), inch (mm)	10 (254)	NA	10 (254)	10 (254)
Sleeper Slab Length, m (ft)	NA	NA	NA	NA
Wall Thickness, inch (mm)	12 (305)	NA	12 (305)	12 (305)
Girder Type	III/IV	II	III	IV

Field Evaluation and Testing

In all, 10 trips were made to the prototype semi-integral abutment and representative conventional bridge sites for visual inspection and field-testing. Personnel from the local DOTD District offices participated in the fieldwork performed by Tulane and UNO. They provided expert advice and enforced safety procedures and traffic controls. The fieldwork included:

- The condition of various components of the semi-integral and representative conventional bridges, i.e., approach slabs, deck, roadway pavement, supports, abutments, embankments, etc. were visually inspected. The conditions of these structural elements were documented with sketches and photographs. Particular emphasis was given to the performance of the pavement, deck, and approach slabs of each bridge in terms of cracking, settlement, spalling, etc. Some of the photographs taken during the field inspections are included in Appendix A.
- Geodetic surveys were performed along the longitudinal direction of each of the six prototype semi-integral abutment bridges.
- For each semi-integral abutment bridge, 4-inch (102 mm) diameter inspection holes were drilled through the approach slabs on the roadway side directly over the vertical gap between the bridge backwall and the geosynthetic-reinforced embankment. The purpose of drilling the holes was to provide access into the gap space for inspection and measurement. DOTD personnel drilled the inspection holes using a truck-mounted rotary drill. It was originally planned to drill only one hole on the approach slab of the bridge. However, identification of the exact location of the gap was not always feasible and, occasionally, several attempts had to be made to drill the inspection hole, as shown in figure 6.

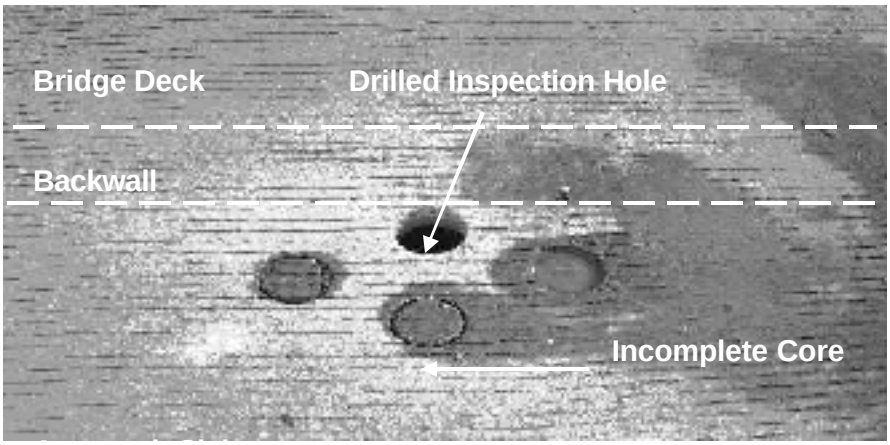

Figure 8
Inspection hole drilled in Bridge I-2

- DOTD personnel sealed the holes immediately after gap inspection was completed according to the procedure shown in figure 9. The procedure used to seal the access holes consisted of lowering a rectangular wood plate, 3 inches by 10 inches (76 mm by 354 mm) in plan, into the hole using a wire attached to a wood stick. The wood

plate was longer than the inspection hole diameter, but slightly smaller in width. In order to lower the wood plate below the bottom surface of the approach slab, it was inserted at an angle. When the plate reached the bottom of the hole, it was pulled by the wood stick so that it became directly flush with the bottom surface of the approach slab. The inspection hole was then filled with cement grout. The wire was subsequently cut at the top surface of the approach slab after the grout had hardened. In some cases, the holes were covered temporarily with a steel plug to maintain access for future inspections, as shown in figure 10. The plugs were subsequently removed and the holes were sealed according to the aforementioned procedure.

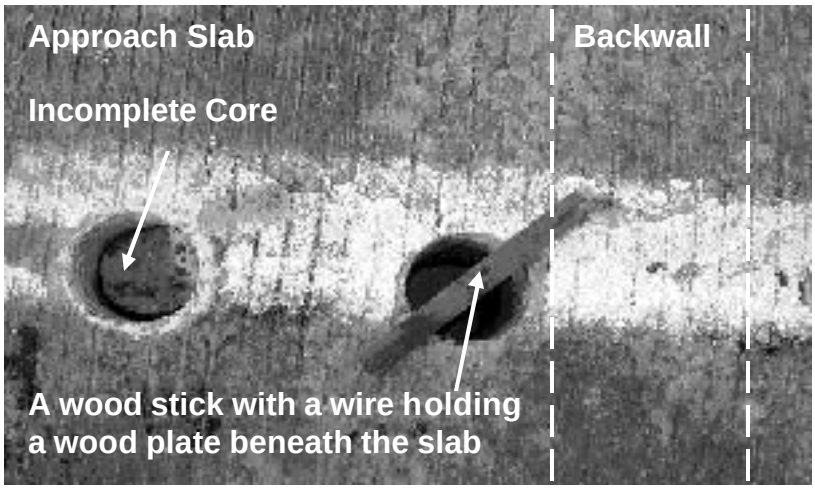

Figure 9
Sealing of inspection holes in Bridge I-5

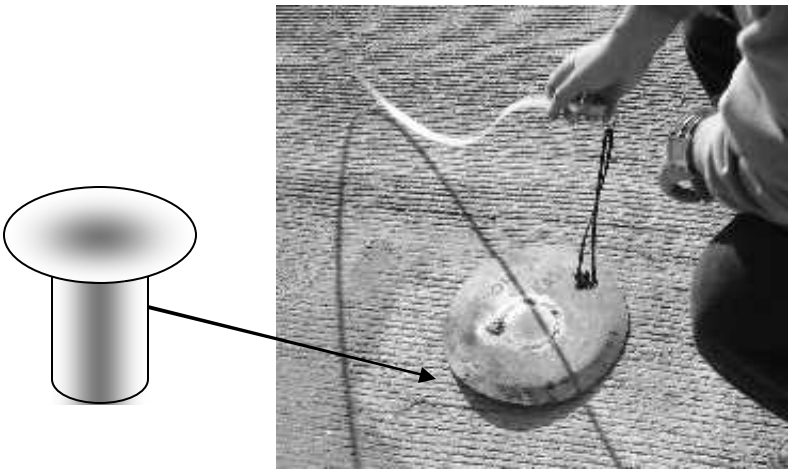

Figure 10
A temporary steel plug over an inspection hole in Bridge I-1

- A special measuring setup constructed at Tulane provided objective evaluation of the annular space dimensions (vertical gap). It was also used to lower a video camera to explore the conditions within the annular space. The width of the gap was measured at different depths from the approach slab surface using the setup shown in figure 11.
- The setup consisted of a wood frame bolted to an aluminum base plate, 30 inches square in plan and 0.5 inches thick (762 mm x 756 mm x 13 mm), with an opening in the middle, 12 inches square in plan (305 mm x 305 mm). A horizontal threaded rod that could be turned using a hand crank was attached to the frame. A vertical rod with extensions, each 3 feet (0.9 m) long and 0.75 inch (19 mm) in diameter, was attached to a mounting block that travels across the horizontal threaded rod over the opening in the base plate. The vertical rod could be lowered into the gap. The vertical rod was also designed to move laterally along the horizontal threaded rod to measure the width of the gap at any given depth. A scale was attached along the horizontal threaded rod to measure the distance the vertical rod travel within the hole. Two vertical scales were also attached along the wood frame, and tic marks made along the aluminum rods measured its penetration depth. Using these scales, it was possible to measure the variation of the gap size with depth at the inspection hole location. The ends of the vertical rods were threaded in a male/female configuration to simplify connecting.
- An aluminum adapter could also be attached to the threaded end of the rod to allow a video camera or sensors to be mounted. This setup could be easily transported, assembled in the field, and removed from one measurement location to the next. Since the feasible diameter of the drilled inspection holes was limited to 4 inches (102 mm) and part of the drilled hole could partially be over the embankment or backwall, the vertical rod did not occasionally travel to the other face of the annulus (backwall or embankment). In this case, feeling the conditions within the annulus space by hand was used to estimate the unmeasured distance and gap size. Figure 12 illustrates the use of the measuring setup over an inspection hole.
- A compact camera with infrared light sources (figure 13) and a baroscopic camera with a light source furnished by DOTD (figure 14) were used to inspect the conditions inside the annular space. In either case, the camera was lowered into the gap through the inspection hole and the conditions within the annulus space and the adjacent structures were recorded using a video tape recorder. When possible, a digital camera documented the gap conditions.

- Drilled concrete cores and samples of the geogrid, wood forms, steel reinforcement and backfill aggregate were collected from each site, as shown in figure 15.

One semi-integral bridge (I-1) was selected for more in-depth evaluation. This bridge was chosen for two reasons. First, it is the only bridge that has experienced problems at its joints with the adjacent roadway, and second, it is the only one with accessible weep holes along its backwalls, as shown in figure 16. A total of five weep holes on each backwall, 8 feet (2.4 m) apart, were used to monitor the bridge movement in reference to the face of the reinforced embankment. Local DOTD District personnel performed gap size measurements through each of the weep holes at a reasonable frequency. This change would reflect the change in the gap size with time and temperature.

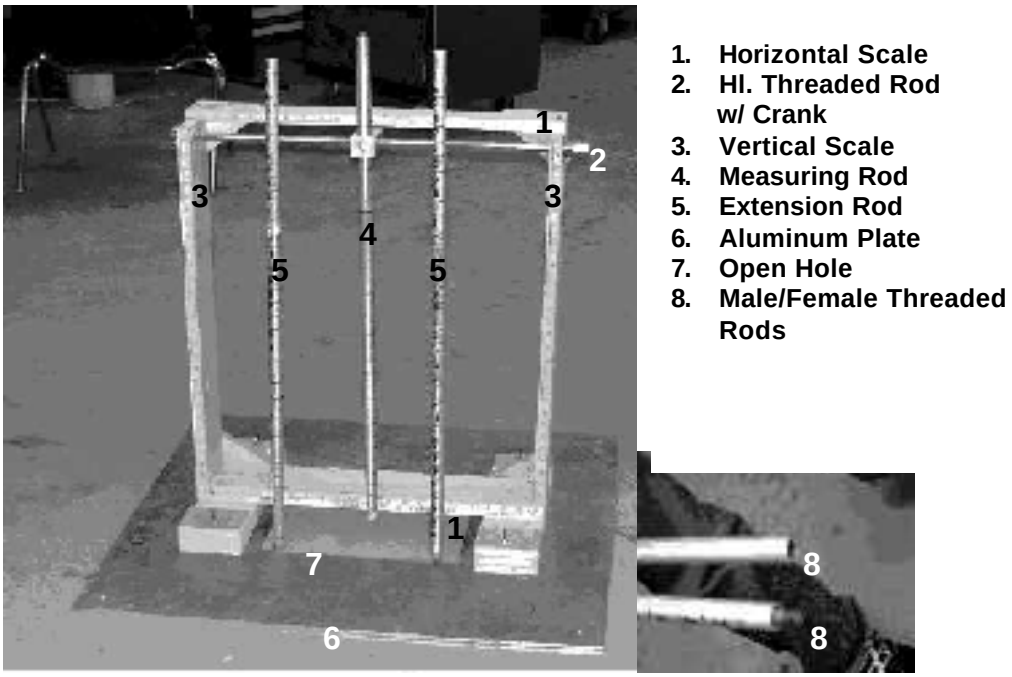

Figure 11
Gap measurement setup

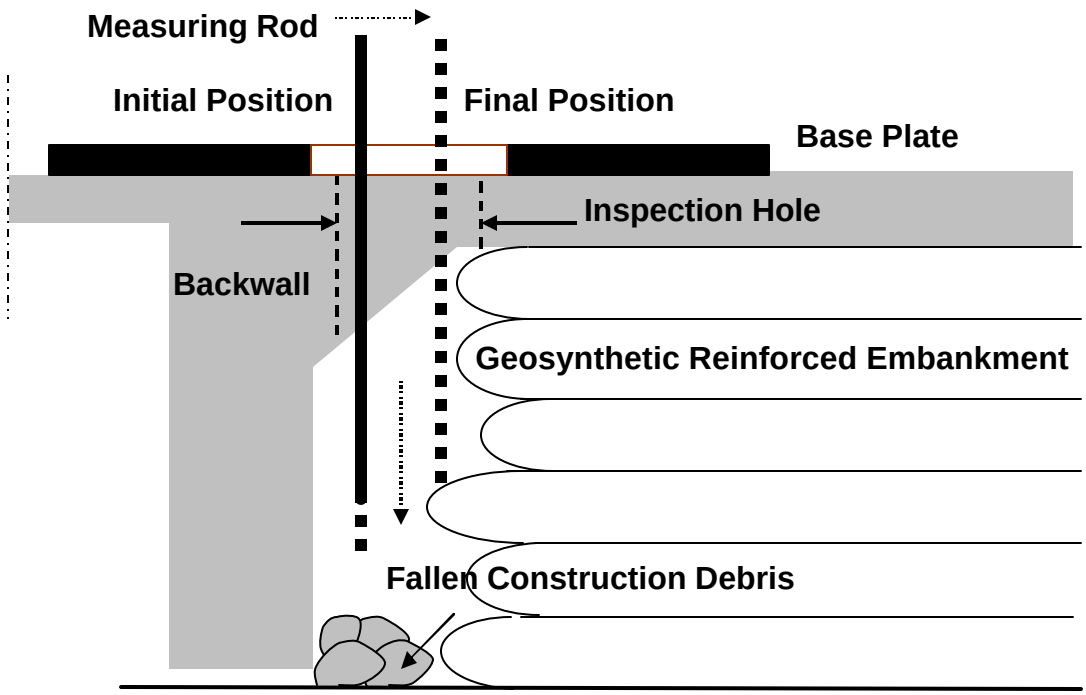

Figure 12
Gap size measurement through an inspection hole

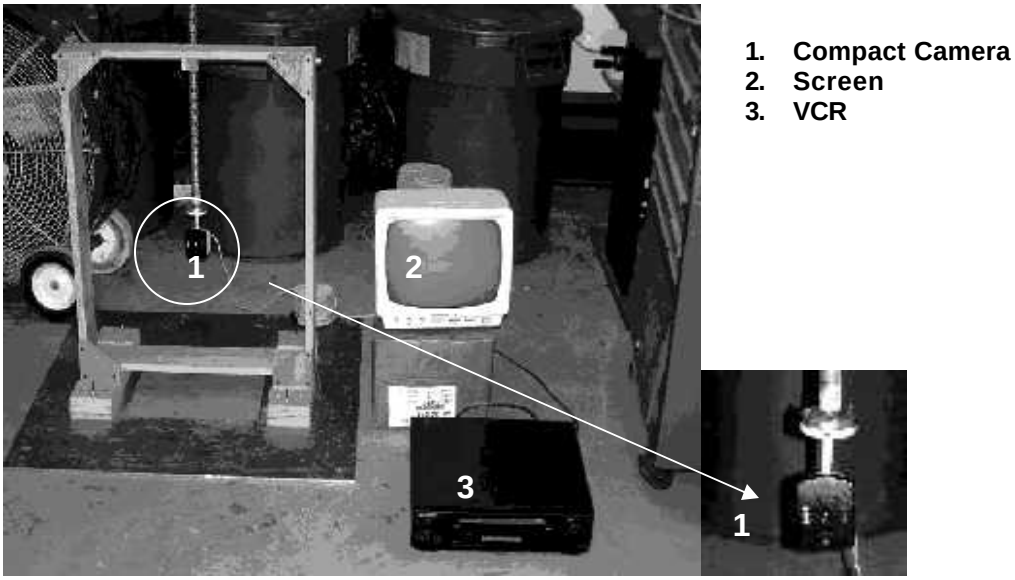

Figure 13
Compact camera attached to the measuring setup

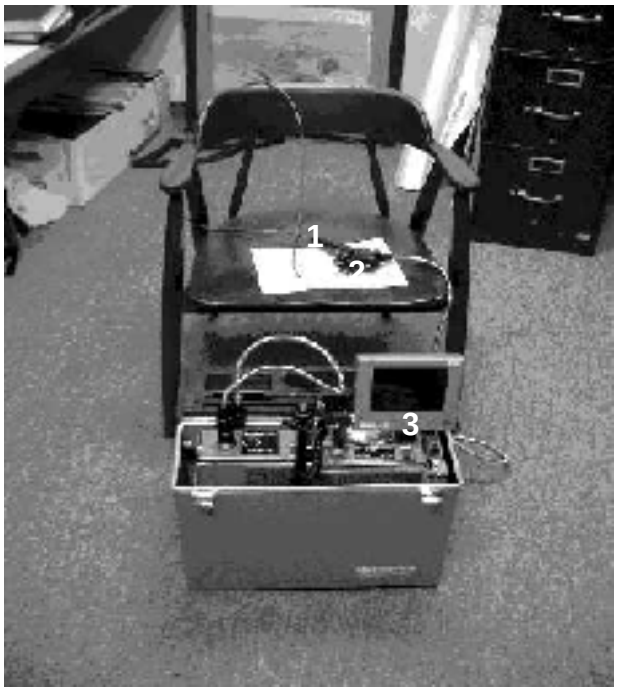

1. Camera
2. Joystick Control
3. Screen

Figure 14
DOTD's baroscope

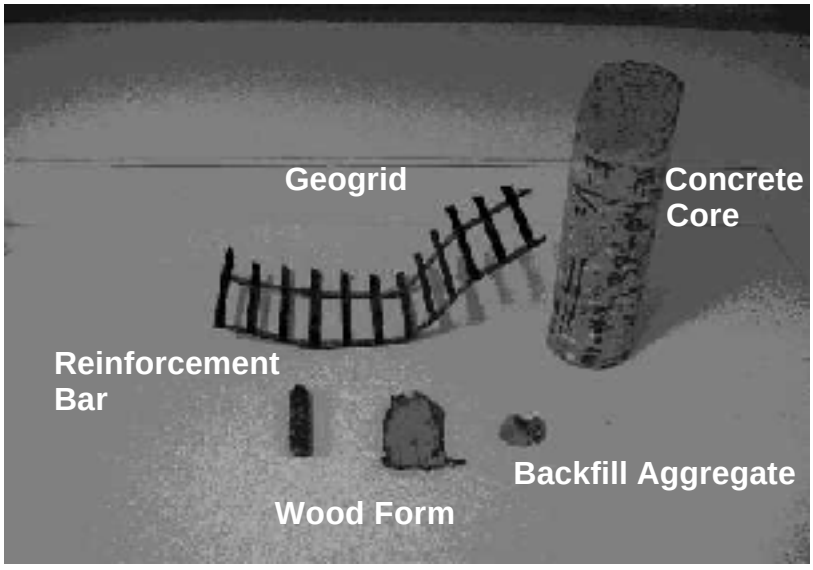

Figure 15
Samples collected from semi-integral bridge sites

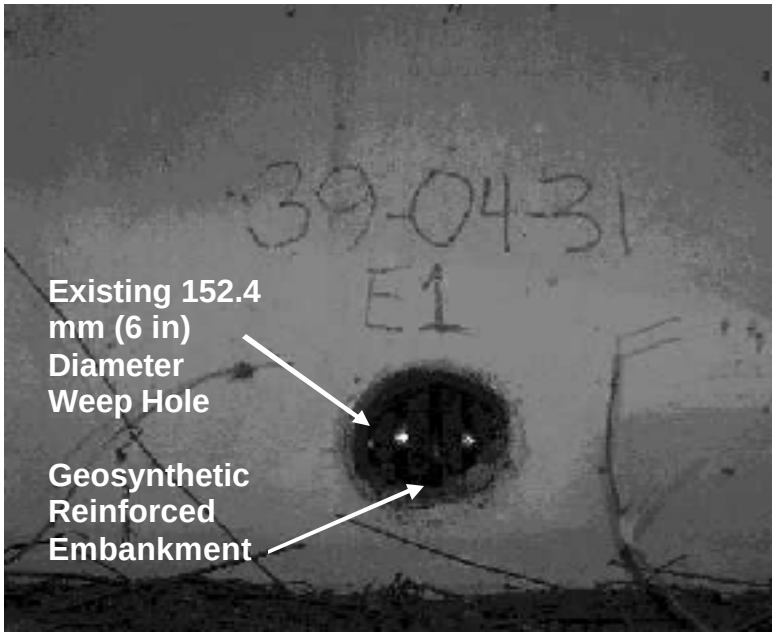

Figure 16
Weep hole on the east backwall of Bridge I-1

Local DOTD District personnel were present during the fieldwork performed by Tulane and UNO. Field inspections of the six prototype semi-integral abutment and the four conventional bridges were made to assess their performance and condition. In addition to visual inspections, field measurements, geodetic surveys, photographs and sketches were used to document the semi-integral bridge conditions. The purpose of the field inspections was to determine if any deficiencies or damage existed in the semi-integral abutment bridges. Results of the inspections were used to evaluate the existing design of the semi-integral abutment bridge and to develop recommendations for future designs. The results were also used to determine if deficiencies in the semi-integral abutment bridge are the result of secondary stresses.

For both groups of bridges, the principal elements of the superstructure were examined for any signs of cracking, movement, or settlement. This included the deck, abutments, girders, diaphragms, wingwalls, backwalls, and piers. All concrete elements were evaluated for cracking and spalling. Steel components were checked for cracking, corrosion and deformation. The crack size, length, direction and location were recorded for each structural component. The cause of each crack was subjectively evaluated so that the effectiveness of the DOTD prototype semi-integral abutment bridge design could be assessed. The embankment and other components of the bridge were also inspected and

documented. This inspection included the condition of the bearings, curbs, and expansion joints of the representative conventional bridges. The horizontal and vertical alignment and elevations of each structural element were also examined. More detailed information regarding elevations and movements of the bridge deck and approach slabs of the prototype semi-integral bridges were obtained through geodetic surveys. In addition, the bridge piers, roadway embankments, and canal banks were visually examined for erosion or scour. Any unusual movement or misalignment of the bridge structure or its various components, or any change in elevations of the structure, was also recorded.

Conventional Structural and Geotechnical Analyses

Conventional Structural Analysis

Bridge I-2 was selected for the conventional structural and geotechnical analyses. The bridge is a combination of 5 80-foot (24.4 m) long continuous and 4 80-foot (24.4 m) long continuous prestressed concrete girder spans, separated by an expansion dam. At each end of the bridge, there is a semi-integral abutment with 40-foot (12.2 m) long concrete approach slab. Type III precast, prestressed concrete girders are spaced 7-feet (2.1 m) to support a 7.5-inch (191 mm) thick concrete slab. The approach slabs are 12 inches (305 mm) thick. Bridge I-2 is the newest bridge with complete design records. It contains a finger joint in the middle span as well as saw-cut joints in the approach slab at a distance of 7.5 feet (2.3 m) from the backwall. Bridges I-3 through I-6 are relatively short bridges with fewer spans. More details regarding the six semi-integral bridges are listed in table 4.

The girder/backwall/approach slab system was analyzed using conventional methods. The abutments and piers were not analyzed because the abutments are semi-integral and not rigidly attached to the backwall. Therefore, forces do not transfer from the superstructure to the abutments due to the jointless bridge design. However, the superstructure itself is fixed at all pier locations. Some fixity of the superstructure to the piers is required to resist longitudinal forces along the bridge, similar to the requirement for a jointed bridge. Because the piers are flexible, the superstructure can still move to accommodate movements due to temperature variations.

Section properties were calculated for Type III prestressed girders, Type III girders with a composite slab and the approach slabs. Concrete strength was assumed to be 6,000 psi (41 MPa) for girders, and 4,200 psi 29 (MPa) for decks and approach slabs. These are the typical 28-day compressive strength values for type “P(m)” and type “AA” concrete [4]. For type “AA” concrete, this is the strength at which the contractor is paid 100 percent for his placement of concrete. Even if the contractor did not originally reach 100 percent of this

"goal" strength, it should be obtained after the bridge has been in place for several years. Simple span dead loads were calculated for the girders. Also, cantilever dead loads and simple span dead loads with soil pressure were calculated for the approach slabs. Ultimately, the approach slabs were analyzed as 7.5-feet (2.3 m) cantilever spans because any overstressing as a simple span would result in a fracture at the weak saw-cut joint and an essential behavior as a cantilever span. In addition, cantilever analysis resulted in higher moments on the backwall, a critical location for problems with jointless bridge design.

STAAD-III / ISDS (Structural Analysis and Design / Integrated Structural Design System) by Research Engineers, Inc., was used to develop influence line models for the five-span continuous girder spans, four-span continuous girder spans, and approach slab spans. As with many computer programs, STAAD-III was utilized for its timesaving advantage over developing influence lines by hand. Standard AASHTO HS-20 truck or lane loading was moved across the resulting influence lines to obtain maximum moments for each span [5]. Military loading was not reported for the structural analysis because the purpose of the structural analysis is to compare existing field conditions to calculated stress levels, not to design the bridge structure. Military loading is a possible future load the bridge structure may experience and not an active load on the structure. HS-20 truck loading controlled the live loading on the bridge structure. Both AASHTO live load distribution factors and live load impact were calculated for girder spans and approach slab spans. Distribution and impact factors were applied to live loads to obtain maximum moments for the girder spans and approach slab spans.

Conventional Geotechnical Analysis

Geotechnical analyses were also performed on Bridge I-2. Analyses were made using the loads computed from the conventional structural analyses. The geotechnical analyses were based on the soil borings and laboratory test data made at the time of the bridge construction. Three specific analyses were made to:

- Estimate long-term settlement of the bridge piers based on the calculated loads from the conventional structural analyses summarized in the previous section.
- Estimate approach slab embankment settlement, and
- Evaluate the DOTD geosynthetic-reinforced wall (embankment) used in the prototype integral abutment bridge design.

One undisturbed sample type soil test boring used in the analyses was drilled to a depth of 105 feet (32 m) by DOTD in 1991. Laboratory tests were performed by DOTD on

samples obtained from the boring. This testing consisted primarily of natural moisture content, unit weight, and unconfined compression. Triaxial Shear tests were performed on some of the more granular materials and Atterberg Limits tests were performed on selected cohesive samples. Results of these laboratory tests were shown on the boring log furnished by DOTD. The boring was used to plot the variations of moisture content, shear strength, wet density, and Liquid Limits with depth. This data was then used to develop the required parameters (C_c, OCR, e_o, etc.) for use in the geotechnical analyses. Some values were assumed when data was unavailable, such as a Liquid Limit or specific gravity.

Finite Element Analysis

Bridge I-1 was selected for the parametric study performed using the finite element method since more information is available relative to its design, construction and performance. Bridge I-1 includes six spans, each approximately 100 feet (30.5 m) long, followed by 40-feet (12.2 m) long approach slabs at each end. It does not include sleeper slabs. Bridge I-1 was thoroughly examined in the field during this study. More details regarding the six semi-integral bridges are listed earlier in table 3.

The finite element software package ANSYS Version 8 (ANSYS, Inc., 2004) was used to perform the parametric study. ANSYS provides an interpreted, Fortran 66-like, programming language called APDL (ANSYS Parametric Design Language), which is easy to use. However, it requires good understanding of both the ANSYS system and the theory of finite elements to produce meaningful results. APDL was employed to model the physical characteristics of the bridge and to investigate the problem. The required parameters were input into an ASCII file containing the pertinent APDL commands. When the file is executed, the APDL routine would use those commands to generate the finite element model (geometry, element types, material models, boundary conditions, loading system, and solution settings). The finite element model was calibrated using field measurements reported in an earlier section of this report and examined for convergence. Pre- and post-processors are also available in ANSYS to print and plot input and output data.

Three specific models were developed and used in this study. All three models were created using parameters defined in an APDL ANSYS format. Also, bridge components in all three models were created using gross section properties of the component. Cracked section properties were not considered. In Appendix B, a brief discussion of the validation and convergence of the FEM model used in this study, as well as the results of a preliminary detailed and thorough parametric study that accounts for the interface conditions, is presented. This model is proposed for future work on this type of bridges.

The first model, Model 1, was used for thermal analyses. This included all parameters under consideration except for the effect of the approach slab settlement and the effect of bridge skew. Because of bridge symmetry, this model depicts only one-fourth of the actual bridge (the bridge is a mirror image about its longitudinal axis and about a transverse axis along its mid-span). Therefore, a longitudinal strip of the bridge consisting of three girders, the deck, and the approach slab was considered in Model 1. A non-linear concrete material model was employed for the approach slab, deck, backwall, and girders. However, the cracking and crushing capabilities of the model were deactivated since the bridge was not loaded to failure. This particular model accelerated convergence of the computer analysis, considering the complexity of the model. The finite elements used to model the approach slab, deck, backwall, and girders were solid, cubic 3-D elements (ANSYS Solid65). This element is defined by eight nodes, each having three translational degrees of freedom in the nodal x, y, and z directions, as well as temperature as a fourth degree of freedom. The mesh employed for Model 1 consisted of 19,280 ANSYS Solid65 elements. The typical element size (length, height, or width) used in the model varied from 4 to 12 inches (100 to 305 mm). The default properties assigned to each component of the bridge are listed in table 5. These values were based on values obtained from the original design drawings or were assumed based on typical values of concrete [5].

Table 5
FEA material properties of the bridge components

Property	Girders	Approach Slab, Deck & Backwall
Compressive Strength of Concrete, f'_c	6,500 psi (45 MPa)	4,500 psi (31 MPa)
Unit Weight of Reinforced Concrete, w	150 pcf (24 kN/m^3)	150 pcf (24 kN/m^3)
Elastic Modulus, E_x	4.6x10^6 psi (3.2x10^{-4} MPa)	3.8x10^6 psi (2.6x10^{-4} MPa)
Poisson's Ratio, μ_{xy}	0.2	0.2
Thermal Expansion Coefficient, a_x	6 x 10^{-6} in/in°F (11 mm/mm°C)	6 x 10^{-6} in/in°F (11 mm/mm°C)

The selected compressive strength of concrete used in the model is higher than the actual design value specified in the bridge specifications. This increase accounts for the presence of reinforcing steel, assuming a smeared approach. Thickness of the approach slab and bridge deck depths was kept constant at 12 inches (305 mm) in order to simplify the model. The Type IV bridge girders were modeled as an "I" shaped section with rectangular top and bottom flanges with the depth of the section maintained as specified in the design

drawings. The depth of the top and bottom rectangular flanges was selected to yield the actual area of the flanges. It was found that ANSYS did not have the capability to accurately model pre-tensioned prestressed components (the girders) within a system. A finite element analysis using equivalent loads to represent the effects of prestressing was done, but this more accurately simulated in-place post-tensioning. The most accurate way to incorporate the effects of pre-tensioned prestressing of the girders was to manually calculate the stresses in the girders due to prestressing and to add these stresses to the FEA results of the parametric study (run without prestressing modeled). Mapped meshing was used whenever possible.

The approach slab of the actual bridge was cast over a geosynthetic-reinforced embankment. During the approach slab's construction, polyethylene sheet was placed over the top surface of the embankment. This relatively smooth interface reduced the interaction between the approach slab and the embankment. In the FEA model, the reinforced embankment was modeled as a series of roller supports at the bottom nodes of the elements representing the approach slab, excluding the nodes along the original vertical gap between the backwall and the vertical face of the geosynthetic-reinforced embankment. The girder bearing pads were also modeled as roller supports, with the exception of the bearing pad of the girder in the midspan of the bridge. This bearing pad was modeled as a hinge.

Model 2 was used to study the effect of approach slab settlement. This vertical downward settlement was simulated by manually inputting a downward vertical displacement at each roller support at the bottom surface of the approach slab elements. The number of roller supports at the approach slab's bottom surface for Model 1 was over 800. To reduce load input for this case, a second mesh was created. As this load case primarily induced bending, a 2-D model was created using plane stress elements. The approach slab nodal spacing was also increased, excluding those nodes close to the backwall, which is the most interesting location for this particular case. A linear elastic material model was used for all bridge components in this model. Actual approach slab and bridge deck depths were used. The cross-section properties input for Model 2 were for a longitudinal strip of the bridge similar to Model 1, but simplified to include a single girder with the appropriate effective width of the deck for the bridge elements. The same effective width was used for backwall and approach slab elements. Figure 17 shows a close up view of the mesh of the backwall area in Model 2 (the triangles indicate roller supports in the longitudinal direction).

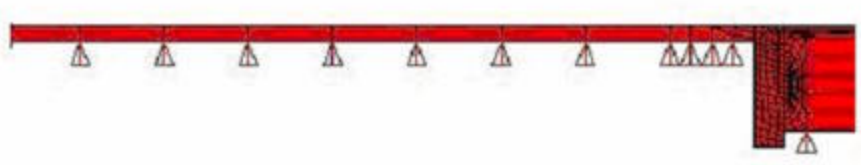

Figure 17
Partial Model 2 finite element mesh

Model 3 was used to examine the effect of the backwall skew. In this case, the full bridge including all six girders and all six spans was considered in the 3-D model. The approach slab, bridge deck, and backwall were all modeled as previously discussed in Model 1. The girders, however, were modeled as 3-D quadratic beam elements to ensure that the size of the model would not exceed the capabilities of the computer platform. Section properties of a Type IV girder were assigned to the corresponding beam elements. The section had to be offset to allow for a proper connection between the girder and deck. A linear elastic material model was used for the girder material in Model 3.

The coordinate systems used in Models 1, 2, and 3 are slightly different due to the difference in the geometry of the finite elements used in the three models. For all models, the y-axis is along the vertical direction. For Models 1 and 2, the z-axis is the longitudinal direction of the bridge and the x-axis is normal to the z-axis (transverse direction). For Model 3, the x-axis is the longitudinal direction of the bridge and the z-axis is normal to the x-axis (transverse direction). More information regarding the development of the finite element model and its verification and convergence is given in Appendix B. The parameters considered in the FEA study included:

- Uniform temperature increase assuming roller supports,
- Uniform temperature increase assuming hinge supports,
- Temperature gradient,
- Approach slab settlement, and
- Bridge skew.

The value of each parameter was varied in turn, while all other parameters were held at their default values. The value of each parameter had numerous effects on the resulting stresses and displacements in the different components of the bridge system.

DISCUSSION OF RESULTS

Existing Bridge Records

Tables 6 and 7 contain a summary of bridge inspection ratings obtained from the DOTD maintenance files. The DOTD inspection records indicated that the total overall structure and bearings ratings of the prototype semi-integral bridges are better than those of the comparable conventional bridges. The inspections also revealed some concerns with the deck joints and serious problems with the joint seals of the comparable conventional bridges. It should be noted that the primary advantage of the integral or semi-integral bridge design is the elimination of joints. Design and performance records of the various bridges were evaluated in view, of actual site conditions observed during site visits by the research team. The quality of the bridges, rideability was assessed based on their maintenance records as well as field inspections and in-situ geodetic surveys performed only on the semi-integral bridges. Fieldwork was performed over a period of about five months. Several trips to the test sites were made.

Because of its long span, bridge I-2 is the only semi-integral bridge with a finger joint between two continuous spans. The finger joint, though not typical for DOTD bridge design, has had no negative effect on the overall semi-integral bridge design. The district office has reported that the finger joint is performing adequately and it opens and closes in response to temperature variation. Bridge I-2 is also the only semi-integral bridge with a saw-cut joint in the approach slab. This saw-cut joint is located 7.5-feet (2.3 m) from the face of the backwall. The purpose of this saw-cut joint is to allow the 40-foot (12.2 m) long approach slab to act as a 7.5-foot (2.3 m) cantilever span, assuming soil support is lost beneath the approach slab due to subsoil settlement.

Table 6
Conventional bridges' inspection ratings

Bridge					Rating				
Code	**Name**	**SP No.**	**Year Built**	**Insp. Date**	**Total**	**Overall Structure**	**Deck Joints**	**Joint Seals**	**Bearings**
C-1	Little River	041-01-23	1978	6/19/99	8	8	7	0	8
C-2	Big Creek	040-03-0014	1981	8/9/00	6	7	7	6	7
C-3	Nantaches	009-03-0022	1983	7/27/00	6	7	7	6	7
C-4	Lena-Flatwoods	455-05-0017	1987	11/30/00	7	8	7	3	8
Average Rating					6.75	7.50	7.00	3.75	7.50
Best Rating					8	8	7	6	8
Lowest Rating					6	7	7	0	7

Table 7
Semi-integral bridges' inspection ratings

Bridge					Rating				
Code	**Name**	**SP No.**	**Year Built**	**Insp. Date**	**Total**	**Overall Structure**	**Deck Joints**	**Joint Seals**	**Bearings**
I-1	Bayou Louis	39-04-31	1989	6/12/97	8	8	-	-	8
I-2	Bushley Bayou	041-01-0030	1998	11/9/98	9	9	-	-	9
I-3	Unnamed Creek	129-02-0021	1999	NA	NA	NA	NA	NA	NA
I-4	Beaver Creek	129-02-0021	1999	NA	NA	NA	NA	NA	NA
I-5	Bayou Boubeaux	835-10-0010	1996	8/27/98	9	9	-	-	9
I-6	Whiskey Chitto Creek & Relief	139-04-0014	1996	10/4/00	8	8	-	-	9
Average Rating					8.50	8.50	-	-	8.75
Best Rating					9	9	-	-	9
Lowest Rating					8	8	-	-	8

Results of Bridge Inspections

Due to space limitations, the only detailed discussion presented herein relates to the prototype semi-integral abutment Bridge I-1. Results of the fieldwork performed at the remaining semi-integral abutment and conventional bridge sites are briefly discussed herein and only special observations concerning their performance are given. The following conclusions are based on the review of design and maintenance records and results of the field inspections for both bridge types:

- All six semi-integral abutment and four representative conventional bridges examined in this study were found to be in relatively good condition regardless of their age, length, location, etc.
- The available maintenance records do not indicate any unusual or excessive repairs made to any of the ten bridges.
- Rideability of all ten bridges was rated as good to very good, with the exception of semi-integral Bridge I-1. A 1- to 1½-inch (25 to 40 mm) bump exists on both ends at the joint between the approach slab and roadway.

From a structural viewpoint, all ten bridges could be ranked as very good to excellent. On a scale of 9, where 9 is excellent and 0 is poor, they would rank as an 8 or 9. Specifically:

- The principal elements of the superstructure in all bridges inspected in this study, including the deck, abutments, girders, diaphragms, wingwalls, backwalls and piers, are generally in good condition.
- None of the bridges has exhibited significant movement or settlement, with the exception of Bridge I-1. Bridge I-1 has moved longitudinally more to one side and one end than the others. This movement is most likely due to the bridge moving into the direction of least resistance. No measurable differences, unusual movement, or misalignment were observed in the horizontal and vertical alignment and elevations of the various structural elements in all ten bridges.
- The size, length, direction, and location of any visible cracks were recorded for each structure. In the decks of the various bridges with no consistent pattern or magnitude, few longitudinal cracks were observed. Mostly transverse surface cracks were apparent. Specifically, cracks were observed along the backwalls of semi-integral Bridge I-4, the wingwalls of Bridge I-3, and in the approach slabs of all bridges. Some minor cracks were also observed in all bridge decks. A small crack was detected over the bearings in Bridge C-3. Existing visible cracks were

predominantly surface or hair cracks, and none of them extended partially or completely through any of the concrete members.

- No spalling was detected in the various concrete elements of all ten bridges.
- No cracks or significant deformation were visible in the steel components of the ten bridges. Some surface corrosion was observed in some of the bearings, bolts, and slotted angles of the various bridges, but it had no definite correlation with relative age or location. In addition, a few nuts were missing from the fastening bolts of the bearings in some bridges.
- The embankments, piers, and canal banks did not indicate unusual erosion or scour in any of the inspected bridges. Some debris was found along the banks under the bridges due to flash floods. According to DOTD, some loss of support was observed near the abutments of Bridge C-2 that required mud jacking.
- The bearings and curbs of the representative conventional bridges were all in good condition. The expansion joints in most bridges contained loose debris, fallen fillers, and some gaps of less than ¾ inch (19 mm) wide.

Specific Observations Regarding Conventional Bridges

- In all four conventional bridges, rubber seal fillers along the expansion joints were either partially or fully loose, particularly in Bridge C-3.
- Several transverse and few longitudinal cracks were observed in the bridge decks, particularly in the approach slabs, as shown in figure 18.
- A camber was observed in the girders of Bridge C-1.
- In terms of rideability, all four bridges had a small bump at the interfaces between the approach slab and bridge deck and between the approach slab and roadway. The remaining joints within the bridge spans were acceptable.

Figure 18
A crack across the approach slab of Bridge C-1

Specific Observations Regarding Semi-Integral Abutment Bridges

- All semi-integral abutment bridges were constructed according to the design drawings.
- Performance of the various structural elements was consistent with the designs and ages of the structures. The bridges built in the 1990s appeared to be in better overall condition than the first bridge built in 1986 (I-1).
- In all semi-integral abutment bridges, the annular spaces (gap) between the backwalls and the geosynthetic-reinforced embankments were constructed as specified in the original design drawings and they appeared to be functioning satisfactorily. The gaps in Bridges I-3 and, I-4 were filled with gravel according to the design drawings.
- The size of the gaps varied with the depth and location of the six bridges, as will be discussed. In addition, some debris (concrete, gravel, geogrid, etc.) had fallen to the bottom of the annular space at some random locations, most likely during bridge construction. The amount of debris was insignificant and did not exhibit a specific pattern.
- Horizontal gaps between the surfaces of geosynthetic-reinforced embankments and the bottoms of the approach slabs were noted at some of the inspection hole locations.

Typically, these gaps were 1 inch (25 mm) or less and extended over only a small distance from the backwall. However, all inspection holes were drilled near the backwall. Therefore, the exact extent of the gaps along the approach slabs cannot be verified. Based on the conditions and location, it is hypothesized that the gaps were due to subsoil settlement.

- In all bridges, wood boards underlain by a plastic sheet were found under the approach slab and the 45 degrees haunch at the backwall. The geotextile and geogrids used to construct the reinforced embankment were generally intact, except for few minor locations where they were locally cut or damaged.
- While all inspections of the semi-integral abutment bridges were made within a short period and under similar ambient conditions, significant differences were observed in the size of the vertical gaps across these bridges. The gap sizes varied from 0.75 to 5 inches (20 to 127 mm), with an average gap of 2 inches (51 mm). The design drawings indicated a design gap size of 6 inches (152 mm) for all 6 bridges. It should be noted that based on the design calculations only a gap on the order of ¾ to 1 inch (19 to 25 mm) is needed to accommodate the anticipated movements of the geosynthetic wall face. However, a 6 inch (152 mm) gap was specified in the drawings for all 6 prototype bridges to account for construction conditions.

Bridge I-1 (SP 39-04-310)

Bridge I-1 is the first semi-integral bridge built in Louisiana and is the only semi-integral bridge in the group that does not have a sleeper slab between the approach slab and roadway. Figure 19 shows a plan view of the locations where a geodetic survey was performed on the bridge. Points A were marked on the shoulders along the approach slab at a constant spacing of 8.3 feet (2.54 m), starting from the interfaces with the bridge deck and roadway. Additional points, R and B, were also marked on the edges of the roadway and bridge deck, respectively. As shown in figure20, the elevations at the joints between the approach slab and roadway did not differ greatly. Differences of 2.88 inches (73 mm) and 3.2 inches (81 mm) existed at the bridge/approach slab interface on either end. Field inspections and the results of the geodetic surveys revealed that the approach slab offers a smooth transfer between the bridge deck and roadway. No appreciable difference in the approach slab's grade reflected differential settlements in the underlying roadway embankment.

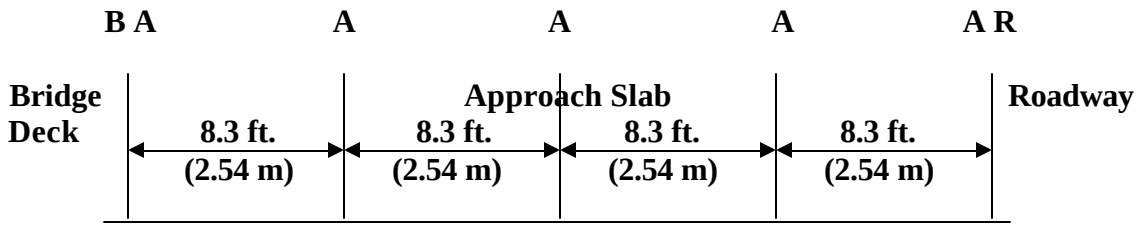

Figure 19
Locations of geodetic survey points

The vertical gaps on both ends of the bridge were examined through the 4-inch (102 mm) diameter inspection holes drilled in the approach slab. The gap measurements indicated that an annular space existed on both ends as specified in the design drawings. However, the gap size was generally larger on the east end of the bridge than on the west end. The gap size varied between 1.6 and 4.6 inches (45 and 117 mm), as shown in figure 21. The gap was about 1.6 inches (41 mm) wide at a depth of 11 inches (0.29 m) on the west end. The size of the gap increased to 3 inches (76 mm) at a depth of 38 inches (0.97 m). The gap size decreased below this depth, it was 2.1 inches (53 mm) at a depth of 72 inches (1.83 m). On the east end, the gap was 3.5 inches (89 mm) at the 37 inch (0.94 m) depth, and then it increase to 4.6 inches (117 mm) at a depth of 72 inches (1.83 m).

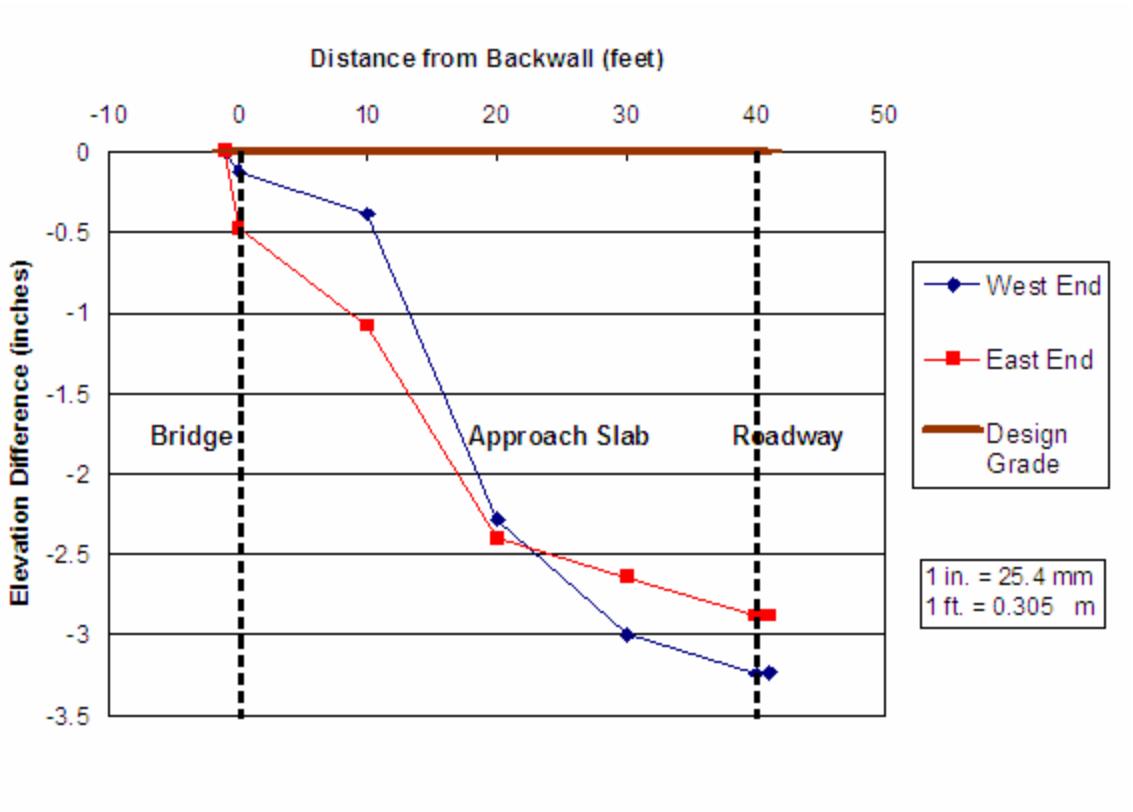

Figure 20
Longitudinal profile along Bridge I-1

In this bridge, the change in gap size with temperature and time was also monitored by measurements made through the existing weep holes along the backwalls on each side of the bridge. A sketch of the measurement procedure is shown on figure 22. Each time a measurement was taken by DOTD personnel, the ambient temperature at the bridge surface was also recorded. The average daily ambient temperature was also recorded at the bridge location. An effort was made to take these measurements as often as possible. Seven readings were taken by DOTD in a four-week span. It should be noted that measuring the gap space through the weep hole is subject to human judgment and possible associated errors. The measuring scale used should be entered at the same exact location each time a measurement is made, but this is not possible with different personnel taking the measurements. For example, a 0.5-inch (13 mm) change at the measurement location could result from personnel touching the geogrid face or penetrating into the actual soil surface within the embankment. A geogrid could be also damaged or cut at a given location, which could result in 1-inch (25 mm) error. In figure 23 the view of the gap through the weep hole of Bridge I-1 indicates a cut in the geogrid. This was the only bridge with a cut on the geogrid.

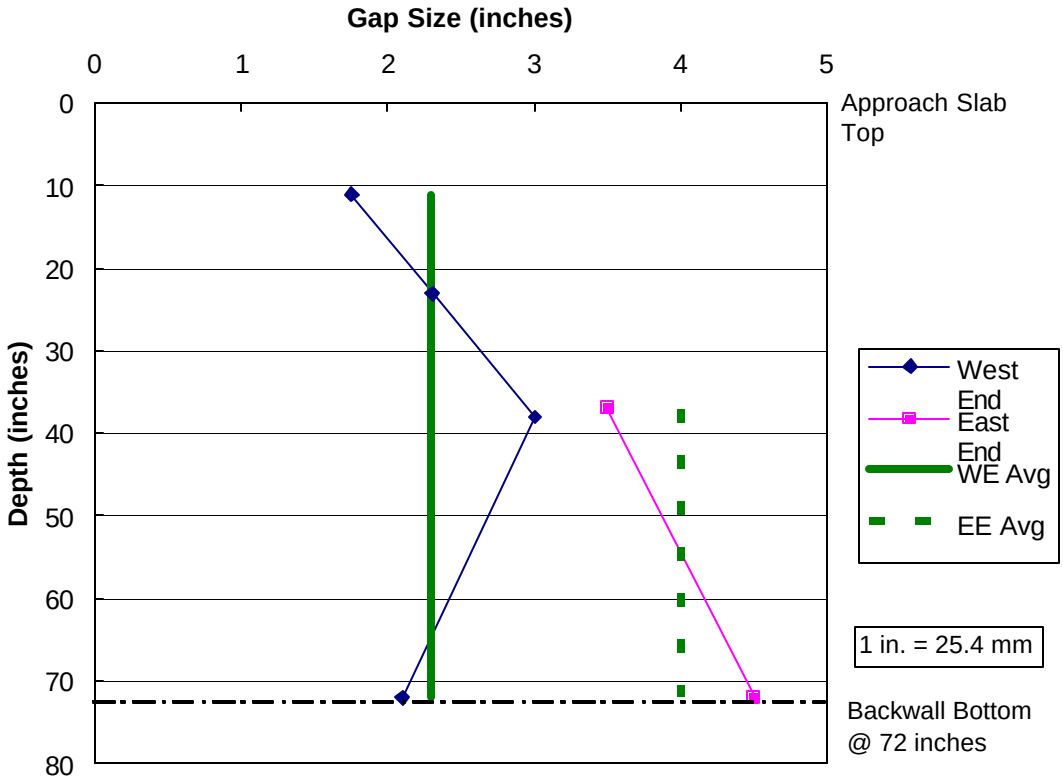

Figure 21
Variation of gap size in Bridge I-1

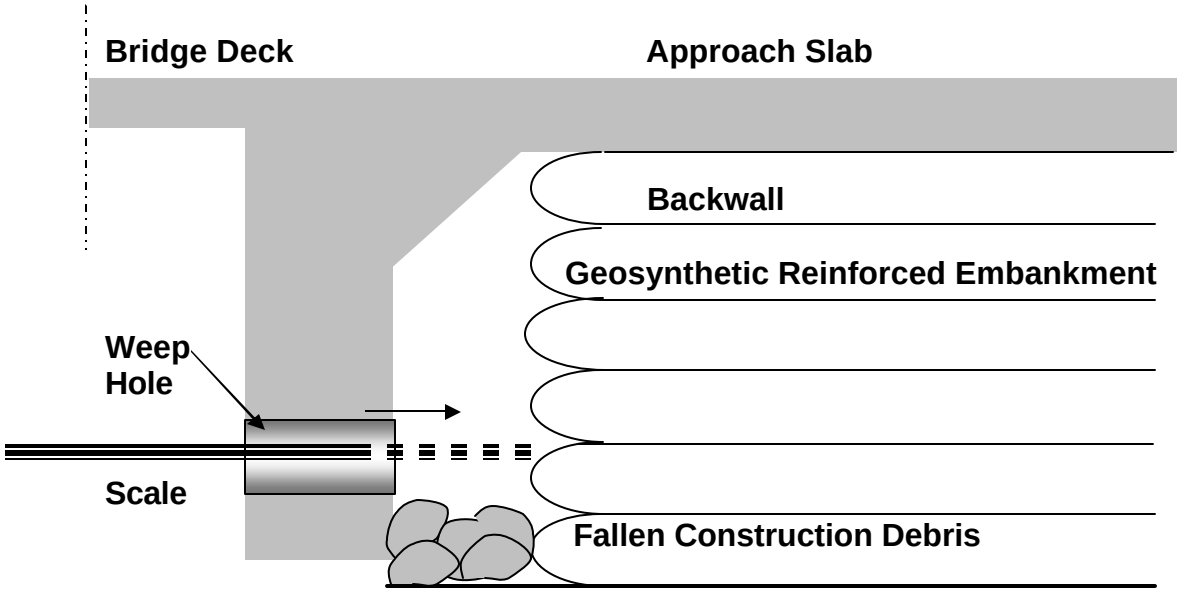

Figure 22
Weep hole measurement procedure

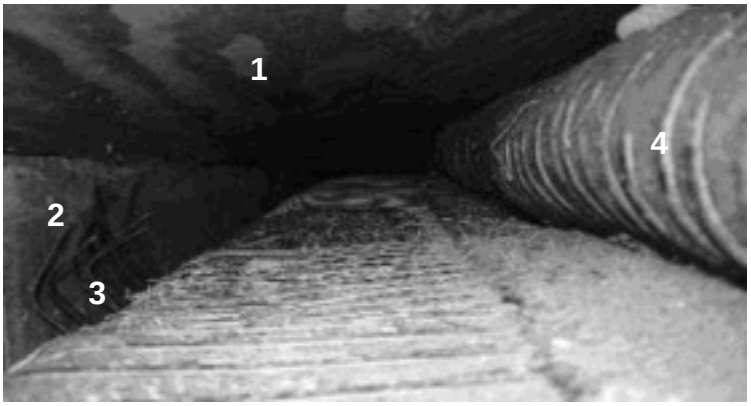

1. Wood Form **2. Backwall** **3. Cut Geogrid**
4. Geosynthetic Reinforced Embankment

Figure 23
A view through the annular space in Bridge I-1

Another attempt was made to measure the variation in the size of the joints between Bridge I-1's approach slab and the roadway pavement. As previously discussed, this bridge has experienced significant movement at these joints due to seasonal variations in temperature that required multiple asphalt overlays and other more frequent repairs. Two readings were taken, but measurements were discontinued as the district proceeded with repair work of these joints.

Figures 24 and 25 show the change in the gap size with time for both the east (E) and west (W) walls. This change is depicted through the measurements made through the weep holes across the backwalls on Bridge I-1. These figures indicate a variation in the gap size with distance across the backwall. Weep hole E1 is located on the north side of the east wall and weep hole E5 is located on its south side. The same is true for weep holes W1 and W5. For example, on April 17, 2003, the east wall gap was 7 inches (178 mm) wide near the edge of the backwall (shoulder) and 7.3 inches (185 mm) wide at centerline of the bridge. The figures also indicate the minimum gap size is 4 inches (102 mm) and 3 inches (76 mm) and maximum gap size is 14.5 inches (368 mm) and 14 inches (356 mm) along the east and west backwalls, respectively. The average gap size is 8.2 and 8.8 inches (208 mm and 223 mm) across the east and west walls, respectively. While these readings differ from those made at the inspection holes, they are all within the same order of magnitude, considering that they were made at different locations and depths.

Figures 26 and 27 show the change in the gap size with the ambient temperature recorded at the time of measurement. These temperatures may not accurately represent the actual ambient conditions since they were taken over the bridge at the time of the reading and may not represent the extreme conditions during a given day or a given month. Other conditions such as humidity and rain could have also affected the measurements.

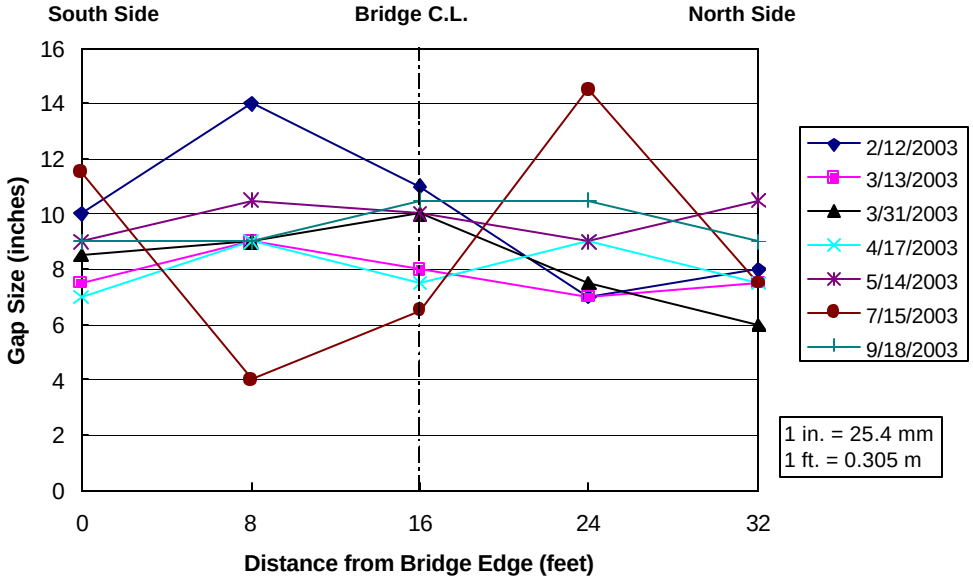

Figure 24
Variation of gap size across the east wall of Bridge I-1

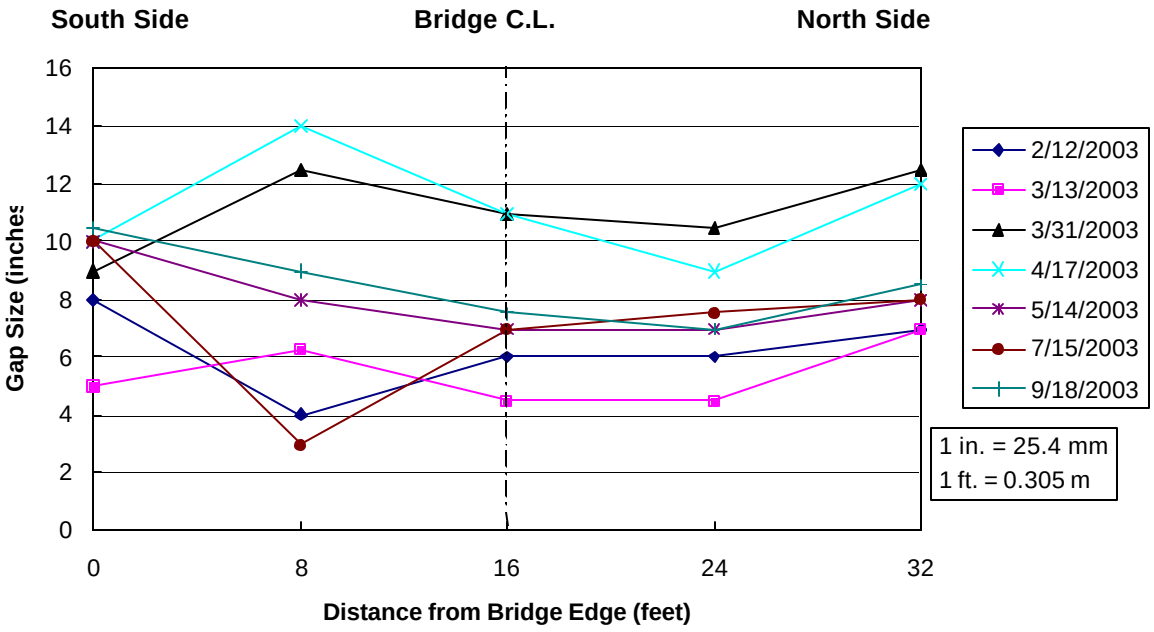

Figure 25
Variation of gap size across the west wall of Bridge I-1

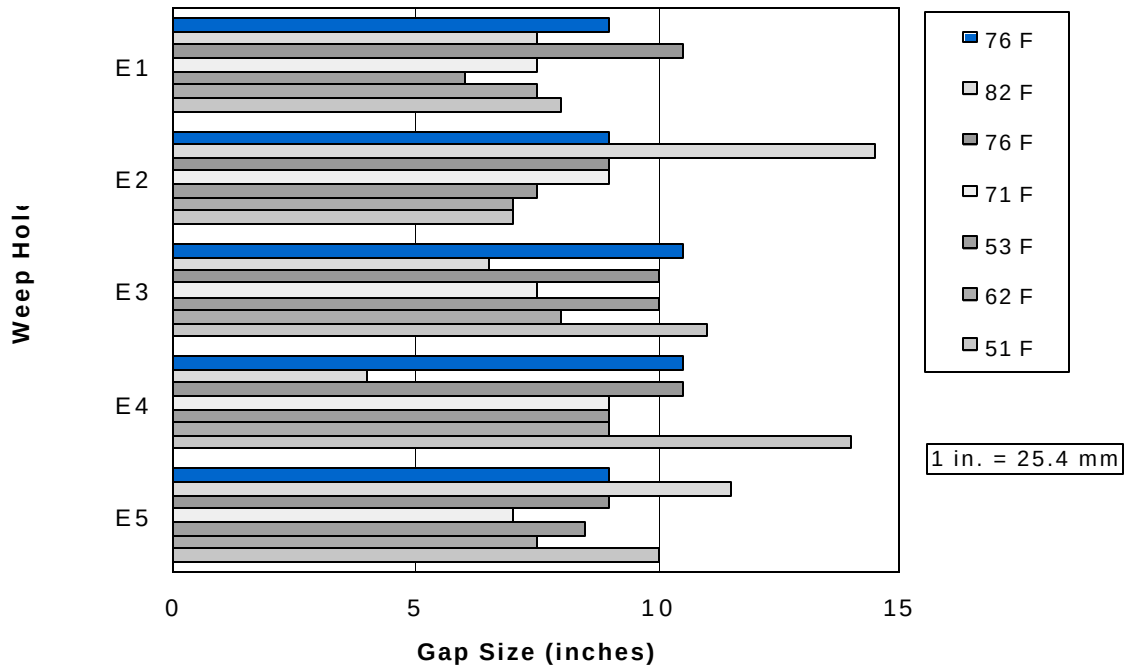

Figure 26
Variation of gap size (east wall) with temperature in Bridge I-1

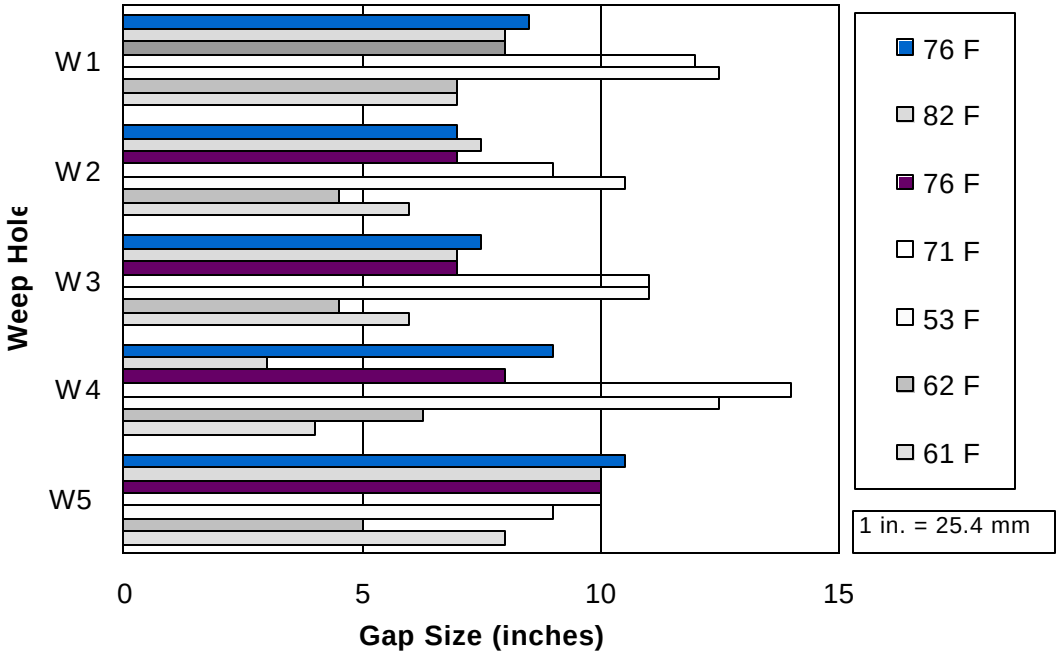

Figure 27
Variation of gap size (west wall) with temperature in Bridge I-1

Figure 28 and 29 show the change in the gap size using a 10-day average temperature. Some inconsistencies in these readings could be attributed to human errors, as previously discussed. After the linear average was determined, a best-fit line was drawn to show the trend. The theoretical trend was also calculated and plotted in the figure. The theoretical trend is based on a $6x10^{-6}$ inch/inch°F (11 mm/mm°C) thermal expansion coefficient for concrete. The linear average is the line connecting the average field measurements while omitting outliers (inconsistent data). Both graphs clearly demonstrate that gap size increases as temperature increases. From the average line, expansion rates of 1.54 and 2.55 inch/°F were determined for the east and west walls, respectively, whereas the theoretical rate was 0.98 inch/°F. Table 8 illustrates the effect of temperature on the long-term size of an original 6-inch (152 mm) gap.

Table 8
Effect of construction temperature on gap size

Extreme Temperature Difference	Long-Term Gap Size inch (mm)	
	Theoretical	Average
Construction at 32°F (0°C) and Highest Service Temperature is 86°F (30°C)	4.9 (123)	3.0 (76)
Construction at 86°F (30°C) and Lowest Service Temperature is 32°F (0°C)	7.2 (183)	9.0 (229)

Occasionally, measurements of the gap sizes through the drilled holes did not agree with those made through the weep holes. Deviations could be attributed to human errors, poor visibility inside the gap, tight access space, and variations in measurement location both with depth and along the backwall. For example, in the case of Bridge I-1, the measurement was made near weep hole W4, 8 feet (2.4 m) away from the edge of the wall. However, the inspection hole in the approach slab was made at a different location. The smallest gap measured through a weep hole was 4 inches (102 mm), whereas a minimum gap of 1.75 inches (45 mm) was measured through the inspection holes drilled through the approach slab.

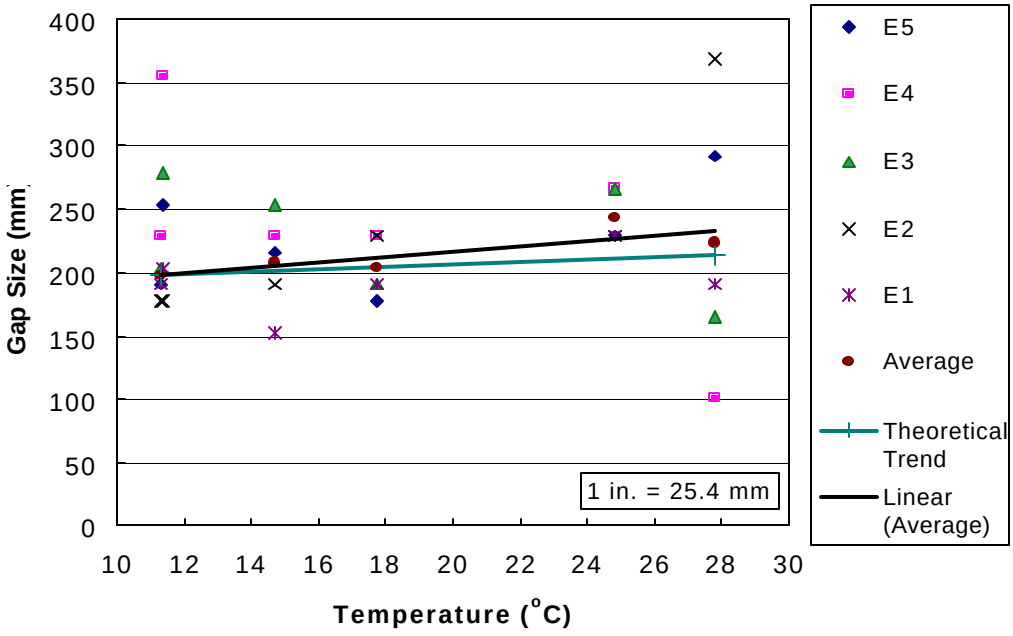

Figure 28
Variation in gap size (east wall) versus 10-day average temperature

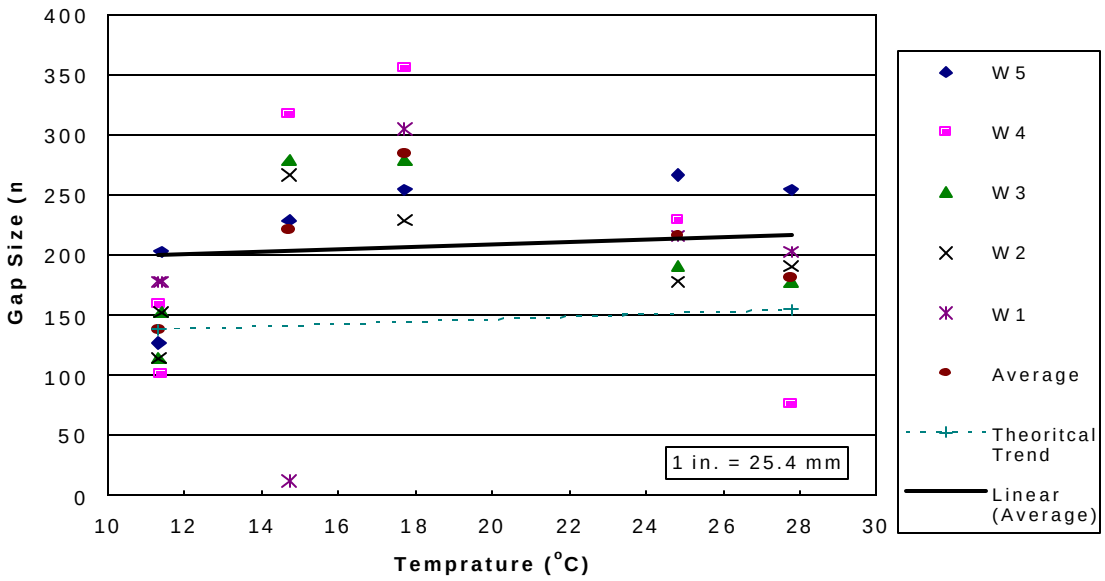

Figure 29
Variation in gap size (west wall) versus 10-day average temperature

Bridge I-2 (SP 41-01-0030)

This 725 feet (221 m) long bridge is the longest integral bridge built to date in Louisiana. Geodetic survey results showed differences between the edge of the bridge and the sleeper slab of about 1.73 inches (44 mm) on the northeast (NE) end and 2 inches (51 mm) on the southwest (SW) end, as shown in figure 30. On this approach slab and at about 30 feet (9.14 m) from the bridge deck, the southwest end exhibits a relatively high elevation difference from the deck of 3.7 in (94 mm). This difference decreases significantly to about 2 inches (51 mm) at the sleeper slab joint on the northeast end. According to the grade profile, it is clear that the approach slab did not have any significant settlement on the first 30 feet (9 m). However, a difference of 3.3 inches (85 mm) was observed at the approach slab roadway interface. This difference could be the result of either a construction error or a local high grade at the survey point.

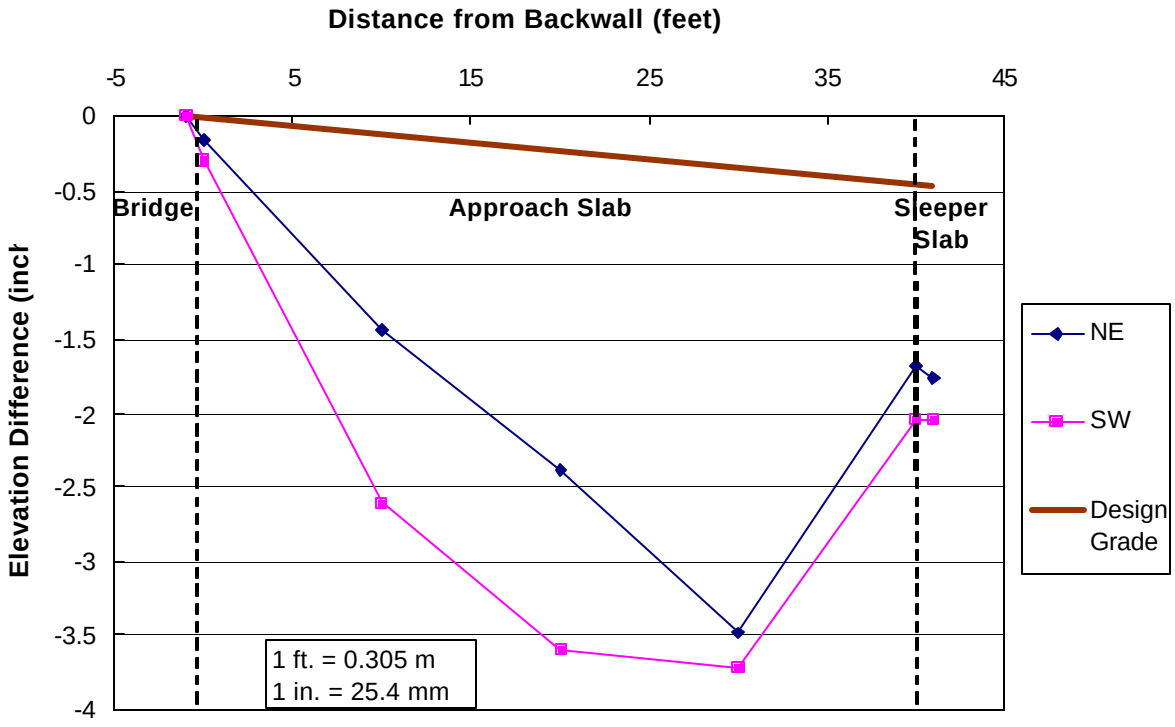

Figure 30
Longitudinal profile along Bridge I-2

Two attempts were made to drill inspection holes through the approach slabs. In the first attempt, drilling was only possible through half of the approach slab thickness. In the second attempt, the drill bit broke and no additional bits were available. However, the conditions inside the gap on the northeast end of the bridge were explored through an existing hole at the bridge on the embankment side. One measurement was made through

this hole at the top of the backwall, indicating a gap size of about 6 inches (153 mm), which is consistent with the design value.

Bridge I-2 B is the only semi-integral bridge with a finger joint between two continuous spans due to its long length. The finger joint, though not typical of DOTD bridge design, has had no negative effect on the overall semi-integral bridge design. The district office has reported that the opening of the finger joint has varied over time with large movements and that it is performing adequately. Bridge I-2 is also the only semi-integral bridge with a saw-cut joint in the approach slab. This saw-cut joint is located 7.5 feet (2.3 m) from the face of the backwall. It is designed to crack when the approach slab loses substantial soil support due to settlement of the roadway embankment. If the saw joint does crack, it would yield a 7.5 foot (2.3 m) cantilever span, which should provide a gradual transition between the bridge and the remainder of the approach slab. While the field inspection show that there was a small vertical gap between the approach slab and the embankment, the geodetic survey and visual inspection indicated that the saw cut joint had not cracked.

Bridges I-3 and I-4 (SP 129-02-0021)

There are two bridges listed as SP 129-02-0021. The approach and sleeper slabs on both bridges have performed relatively well with respect to rideability. However, Bridge I-4 appears to offer a smoother transition between the bridge and roadway. Results of the geodetic survey performed on Bridge I-3 are shown in figure 31. The results show an elevation difference between the edge of the bridge and the roadway on both ends of about 0.1 inch (2.5 mm). Bridge I-4, shown in figure 32, has between 0.26 and 0.36 inch (7 and 9 mm) difference in elevation. There was no change in the grade shown on the design drawings.

No gap measurements were made for these two bridges since the annular space on both ends of the bridge was filled with granular fill as specified in the design drawings. There are no records available that indicate how this backfill was placed and its degree of compaction. However, the records do indicate that the same contractor built both bridges. Based on retrieved samples from the inspection holes, the gap was filled with gravel and crushed stone. The same backfill material was also used to construct the front segments of the upper and bottom lifts of the geosynthetic-reinforced embankment near the backwall. No information was available on the reason for why gravel was placed within the gap space of these two bridges. Visual inspection, maintenance records, and observed performance of this bridge do not indicate any problems since their construction.

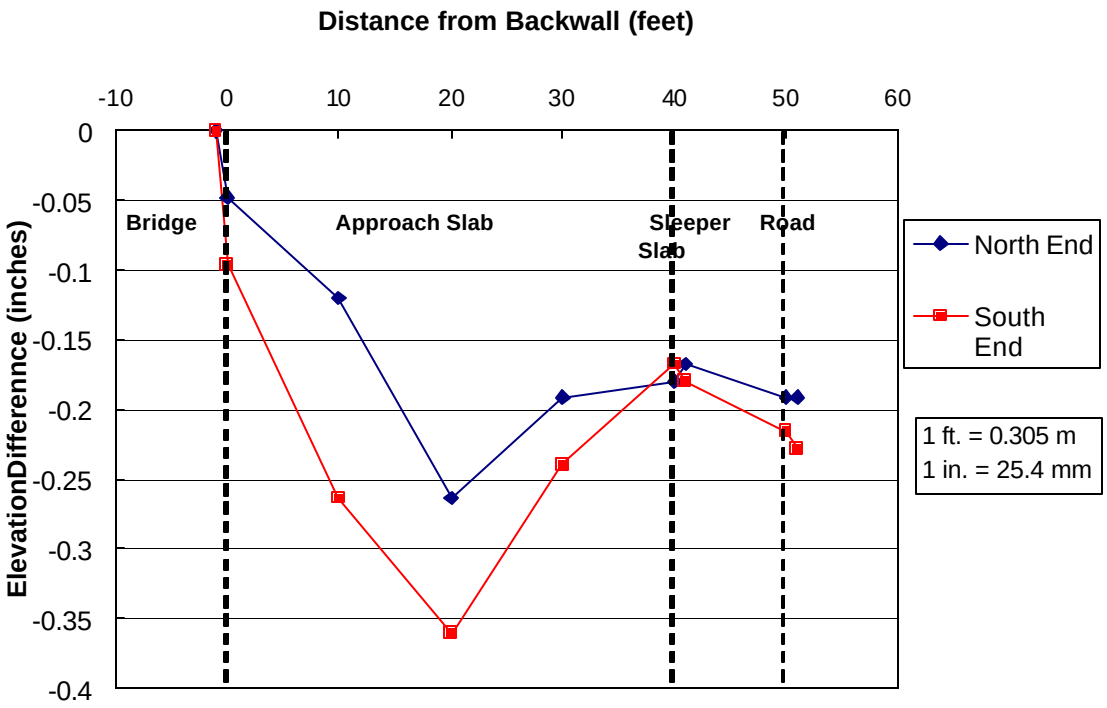

Figure 31
Longitudinal profile along Bridge I-3

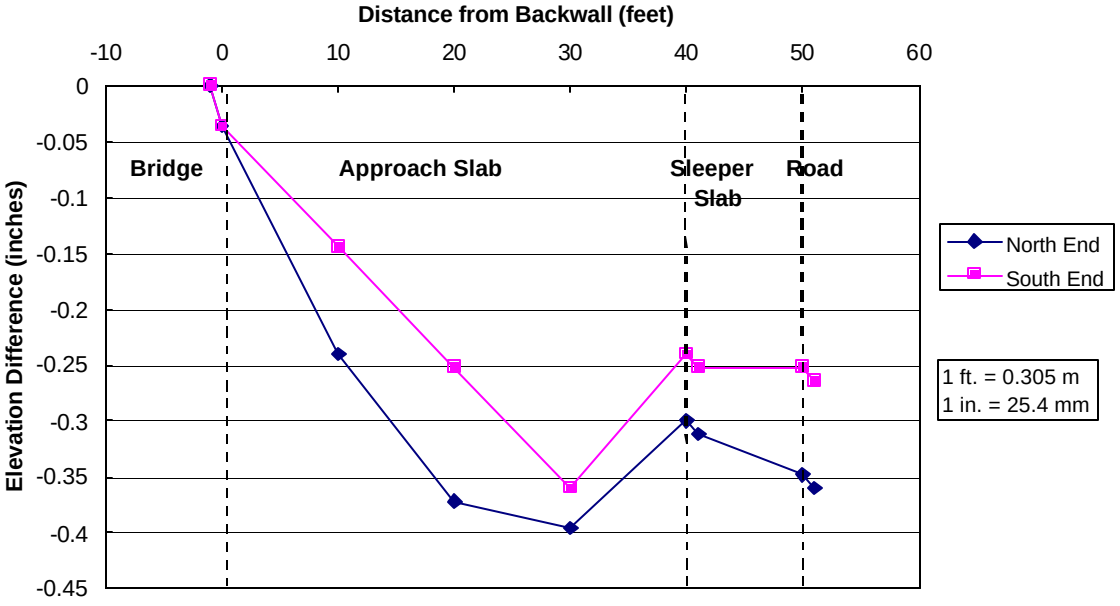

Figure 32
Longitudinal profile along Bridge I-4

Bridge I-5 (SP 835-104-0010)

Results of the geodetic survey performed on this bridge are shown in figure 33. As indicated by the shape of the longitudinal elevation profile, the approach slab offers a gradual transition between the bridge and the sleeper slab. On the southeast (SE) end of the bridge, a difference in elevation of less than about 1.8 inches (46 mm) exists between the bridge deck and the roadway, whereas the difference on the northwest (NW) end is about 2 inches (51 mm). The 10 feet (3.05 m) long sleeper slab offers a good transition between the approach slab and the roadway. At both joints with the sleeper slabs, the difference between the southeast end and the northwest end is less than 0.25 inches (6 mm). There was no change in the grade shown on the design drawings.

The gap size was also measured on both ends of Bridge I-5 through inspection holes drilled through the approach slab. The gap size varied between 4 and 5.1 inches (102 and 130 mm) on the southeast end and between 2 and 2.5 inches (51 and 64 mm) on the northwest end, as shown in figure 34. Interestingly, both gaps shared a similar configuration. They were larger near the top and bottom of the backwall and smaller around the middle depth. It was also evident that the gap was wider on the southeast end. The deepest gap depth reachable from the inspection hole was 49 inches (1.25 m) on the northwest end. Fallen debris from bridge construction was encountered below this depth, preventing any further penetration by the measuring setup. An attempt to identify the nature of the debris was impossible due to dark conditions inside the hole, the small diameter of the inspection hole, and the depth of the debris. However, based on inspection of other bridges, it is likely that the debris consisted mainly of fallen concrete, wood from construction forms, and gravel. Fallen concrete is particularly incompressible, and it may result in some problems if it extends laterally and/or to some depth. However, this does not appear to be the case in any of the inspected bridges.

Bridge I-6 (SP 139-04-0014)

Figure 35 indicates a difference in relative elevation of about 0.48 to 0.62 inch (12 to 16 mm) between the end of the bridge and edge of the sleeper slab. At the middle of the approach slab, the maximum difference in elevation is about 0.7 inch (18 mm). The design grade profile was not available on the design plans. The width of the gap between the backwall and the geosynthetic-reinforced embankment was measured on the southeast end of the bridge. The gap size varied between 4 and 6 inches (102 and 152 mm), as shown in figure 36. The figure shows that the gap size decreases with depth.

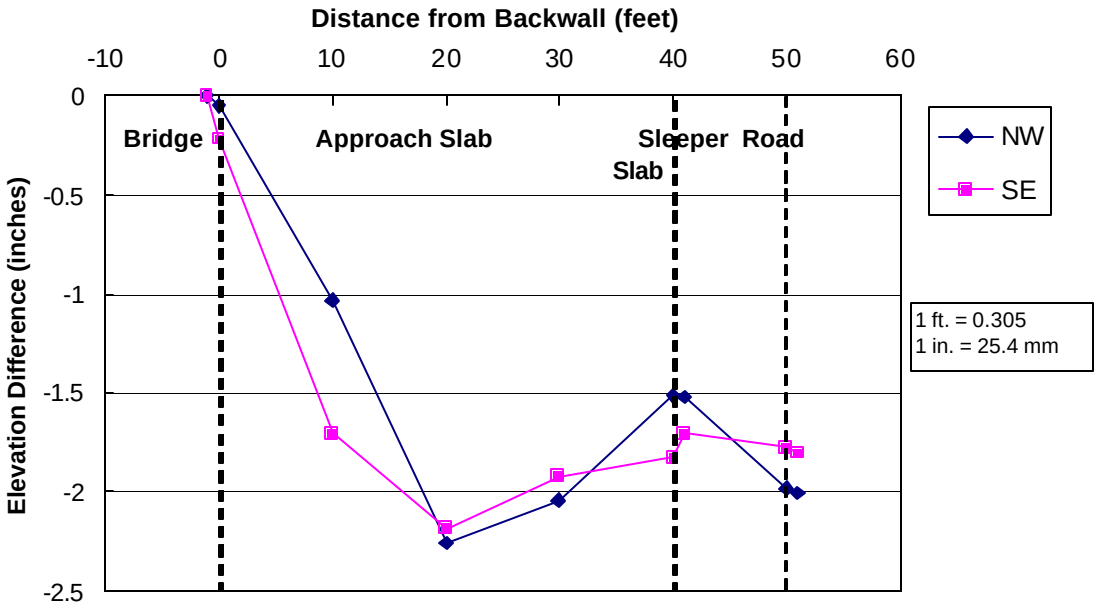

Figure 33
Longitudinal profile along Bridge I-5

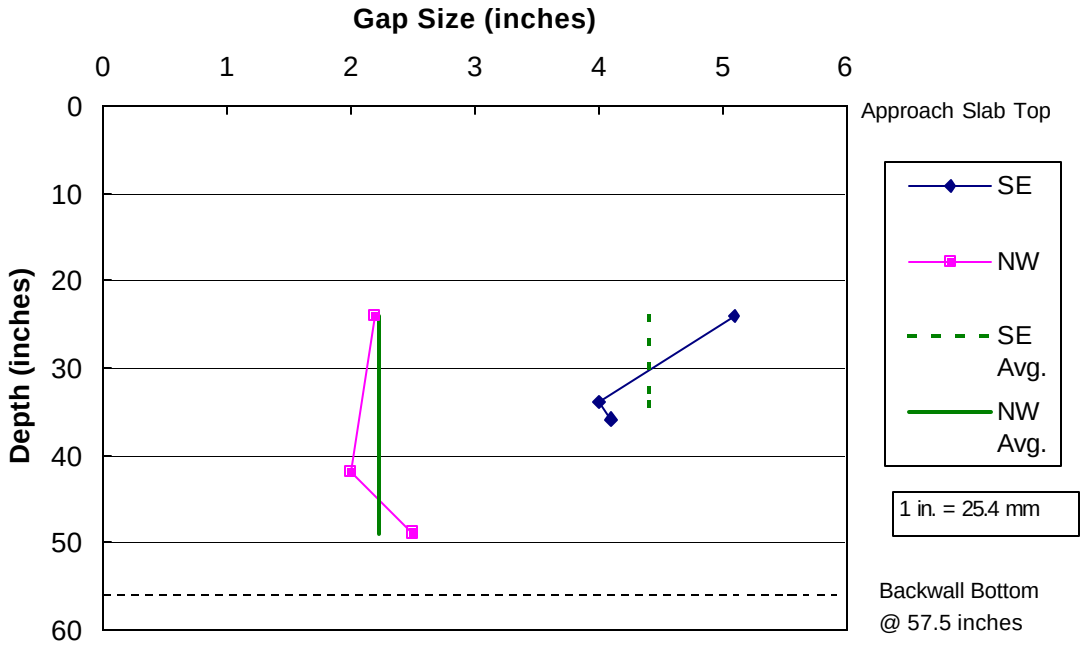

Figure 34
Variation in gap size of Bridge I-5

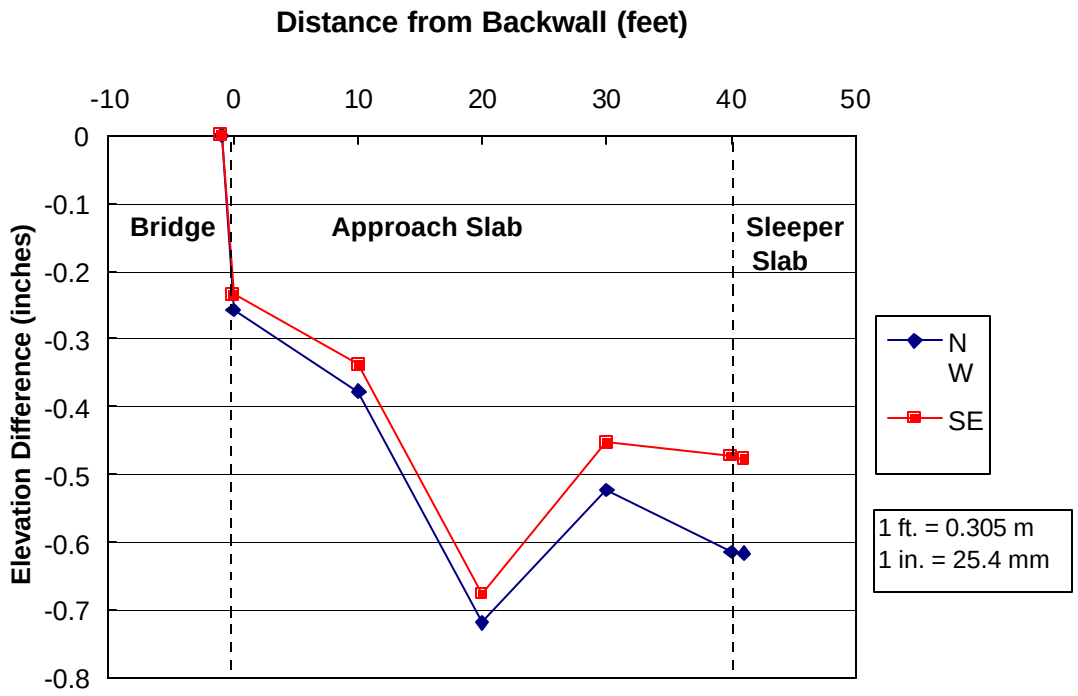

Figure 35
Longitudinal profile along Bridge I-6

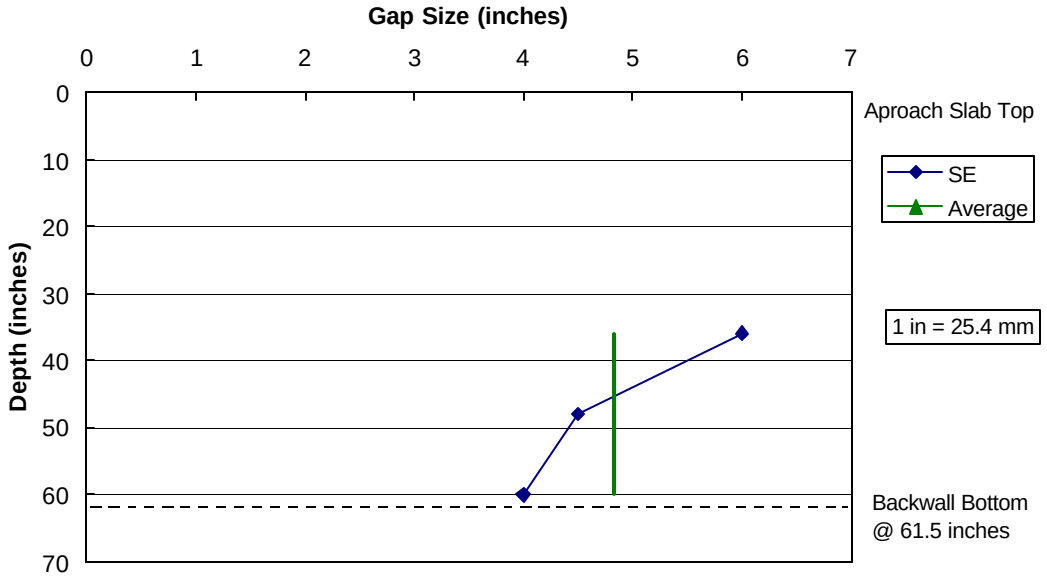

Figure 36
Variation of gap size in Bridge I-6

Comparison of all Six Semi-Integral Abutment Bridges

Figure 37, compares all the profiles (relative elevations) along the bridge deck, approach slab, and sleeper slab of all the semi-integral abutment bridges examined in this study. The figure indicates that bridges I-1 and I-2 had the largest elevation differences. With the exception of Bridge I-1, all of the approach slabs had the maximum grade difference near their midspan. In Bridge I-1, the grade difference increased with distance away from the backwall. The midspan dip observed in most of the approach slabs was relatively mild and should not be of concern. Figure 37 shows that for all bridges, the dip is less than 1 inch (25 mm), with the exception of Bridge I-2 is dip of about 1 ½ inches (38 mm). No cracks were found in the midspan area of any of the approach slabs after a through check. Therefore, the difference in elevation or grade (dip) at midspan was not likely due to deflection of the approach slab resulting from embankment settlement. It could have been due to local low and high points on the structure surface where the geodetic survey was performed, human error, or construction differences. Some lateral movements have had probably occurred in the wall face of the embankment following removal of the construction forms.

Figure 38 shows the variations in the gap width with depth, as measured through the inspection holes drilled through the approach slabs of three of the semi-integral bridges. As previously discussed, the gap profile for each bridge was different, which could be attributed to the difference in construction, as there is no specific pattern that could be associated with service conditions. However, the smallest gap measured in all bridges through the inspection access holes was at least 1.75 inches (45 mm) in Bridge I-1 and the largest gap of 6 inches (152 mm) was also measured in Bridge I-6.

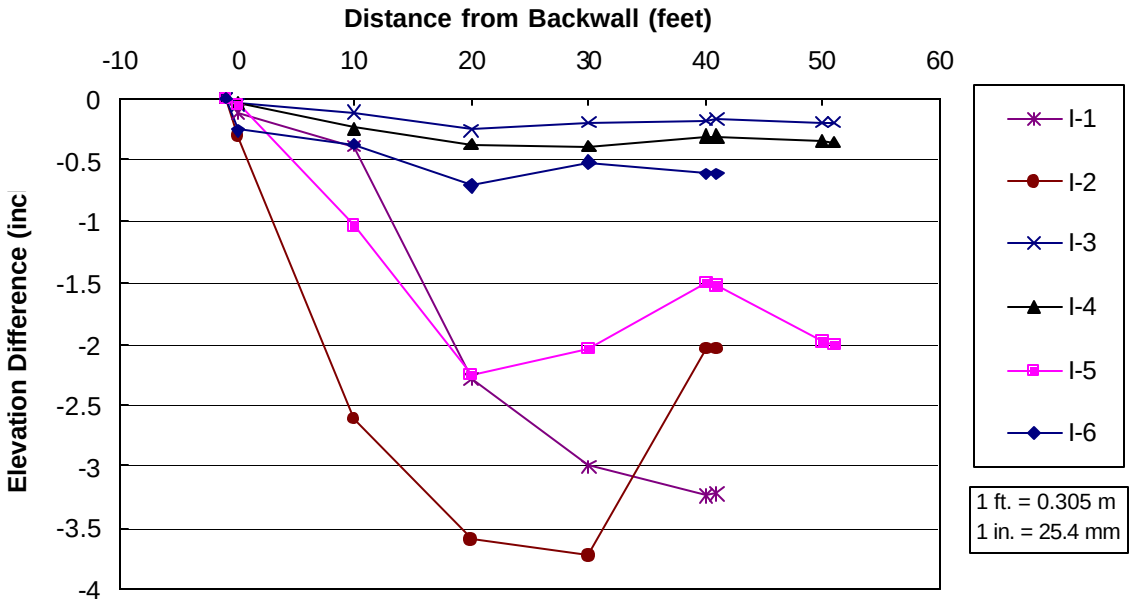

.

Figure 37
Longitudinal profiles along all semi-integral bridges

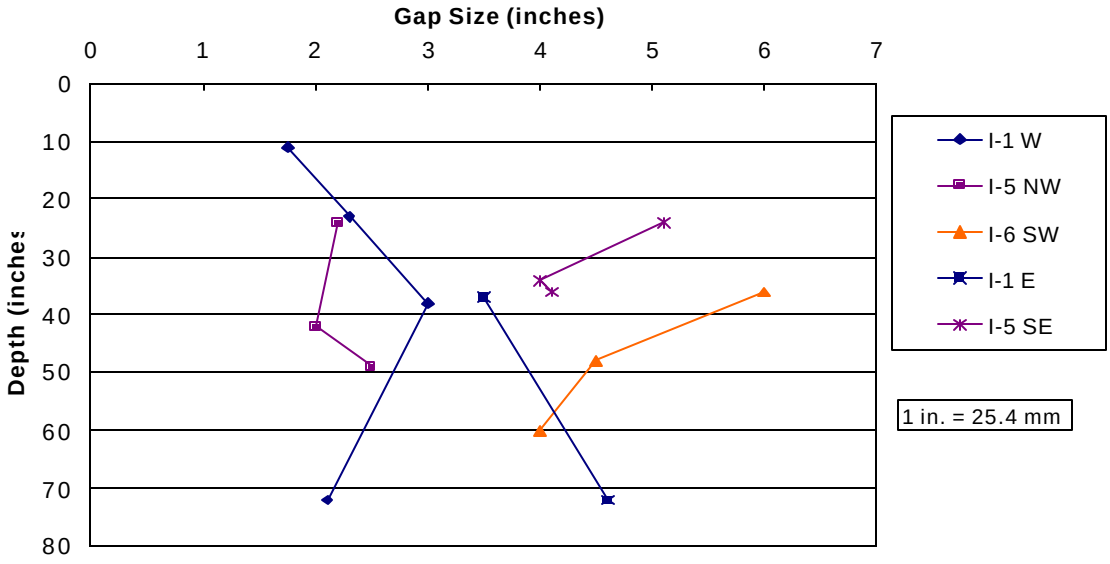

Figure 38
Measured annular space in existing prototype semi-integral bridges

Conventional Structural and Geotechnical Analyses

In general, results of any analytical analysis depend on the theory, formulas and equations, analysis software, design assumptions, applicable specifications, interpretation of data and personal judgment considered by the designer. Therefore, the results of any given analysis may differ from one agency to another, and the results of the analyses included in this report may differ slightly from those performed by DOTD. However, both results should ultimately fall within an acceptable range and be of similar relative magnitude. Accordingly, the results and conclusions should be independent of the analysis type.

Conventional Structural Analysis

A conventional structural analysis was performed on the Bushley Bayou Bridge (I-2) in Catahoula Parish. Figure 39 is an elevation view of the DOTD semi-integral bridge configuration used for the conventional analysis.

Temperature movement for the 5-span continuous structure with an approach slab was calculated to be about 2.22 inches (57 mm) for a temperature increase of 70 ^{o}F (39 ^{o}C). The expansion dam and joint at the end of the approach slab are sufficient to withstand this amount of movement. Therefore, based on closed-form solution type analysis, temperature variation within the range analyzed should not cause distress in the bridge structure. In field inspections, no signs of distress due to temperature movement were observed.

For the conventional analysis of the bridge girders/slab spans, simple span dead loads were calculated. Influence lines were developed and standard AASHTO HS-20 truck or lane loading was moved along the influence lines to obtain maximum live load moments. For Type III prestressed girders, final prestress strand force losses were determined and final prestress strand forces were calculated for girder centerline and end strand patterns [1]. Final prestress losses for the 0.5 inch (13 mm) low-relaxation strands were estimated at 45,000 psi (310 MPa). Final prestress forces were calculated as 674.8 kips (3,000 kN) at the centerline girder span and 482 kips (2,144 kN) at the girder ends. Final stresses were calculated at the top and bottom of the girder and top of the slab for positive moments at centerline girder spans. They were also calculated at the same location for negative moments at the piers. Allowable stresses were calculated at these same locations. Approach slabs were analyzed using the Strength Design Method [5]. Dead loads, live loads, impact, and lane distribution factors were added, with appropriate load factors for a 1-foot (305 mm) width of slab. The allowable moment was calculated for the approach slab and compared to the actual loads. Tables 10 and 11 show actual forces and allowable forces for the Type III girders and

approach slabs of Bridge I-2, which were obtained from the foregoing conventional structural analysis. In these tables, the moment is calculated at the approach slab/backwall connection.

Table 9
Comparisons of stresses in Type III, prestressed girder/slab spans

	Calculated Stress psi (MPa)*	Allowable Stress psi (MPa)*
Centerline Span:		
Girder Top	-2,103 (-14.5)	-3,600 (-24.8)
Girder Bottom	+20 (+0.1)	+465 (+3.2)
Slab Top	-310 (-2.1)	-2,520 (-17.4)
End of Span (Pier):		
Girder Top	+468 (+3.2)**	+465 (+3.2)**
Girder Bottom	-969 (-6.7)	-3,600 (-24.8)
Slab Top	+429 (+3.0)	+465 (+3.2)

* (+) Tension (-) Compression

** For all purposes of comparison and considering the approximations within the calculations, these values may be considered essentially equal.

Table 10
Moment comparison for approach slab spans

Calculated Moment ft-k (kN-m)	Allowable Moment ft-k (kN-m)
55.4 (75)	65.8 (89)

As shown in Tables 9 and 10, all of the actual design loads are at or below the calculated allowable values. Based on the results of the conventional structural analyses, the approach slab/backwall connection of the semi-integral bridge is not overstressed; thus, the bridge design is satisfactory. This conclusion is supported by the field examination of this bridge, which indicated no signs of distress in the superstructure or approach slabs. A typical STADD-III input file is provided in Appendix C. Other input and output files are furnished on the project CD-ROM.

It should be noted that the foregoing conventional structural analysis was performed using only the HS-20 or lane loading. Alternate load case was not considered in the analysis. The purpose of the conventional structural analysis was not to re-design or check the actual DOTD design of the bridge, but to assess the overall design of the spans and to verify the observed field performance. The alternate loading conditions need to be considered in a formal design in addition to the HS-20 and lane loading to check for any unusual or non-standard vehicle configurations.

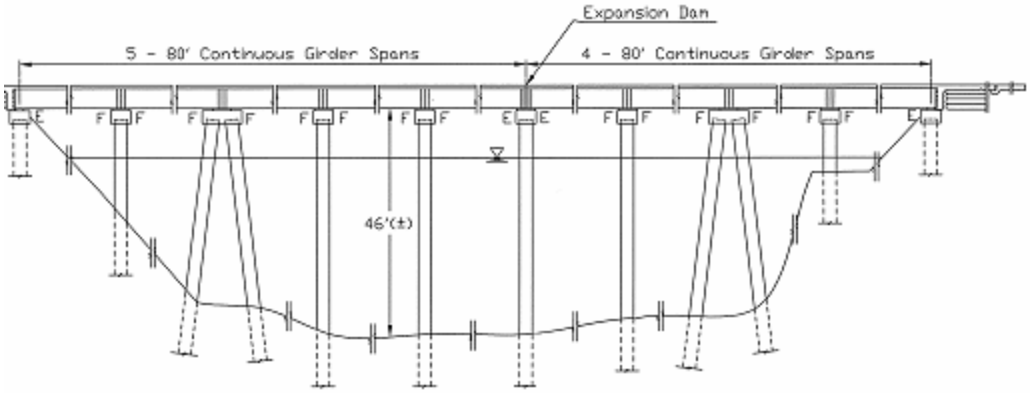

Figure 39
Semi-integral Bridge I-2 configuration used for conventional analysis

Geotechnical Analysis

A review of the soil boring and laboratory test data indicated that the near surface soils at this site of Bridge I-2 consisted predominantly of pre-compressed cohesive soils of a medium to very stiff consistency. The unconfined compressive strength of the subsoils varied between about 1,600 to 4,500 psf (160 to 450 kN/m^2). Some granular strata were also interbedded between the 34- and 58-feet (10.4 and 17.7 m) depths at the boring location. The moisture content of most soils varied between 20 and 30 percent. Some soil samples at about the 28- and 45-feet (8.53 and 13.72 m) depths had a relatively higher moisture content between 40 and 60 percent. Most of the soils at the boring location were generally classified as CL according to the USCS/ASTM, and A-6 according to AASHTO soil classification systems [5], [6]. The soils with higher moisture contents were classified as CH or A-7-6.

Settlement analysis of the pile-supported bridge piers was made using the soil boring made at the site and the structural loads on the abutment calculated by the conventional structural analysis. The design drawings indicated that each bridge abutment is supported on a single row of 5 piles that are 90 feet (27.4 m) long and spaced at 10.13 feet (3 m) on centers. Results of the analyses indicated that long-term settlement of the pile-supported pier should be approximately 0.2 to 0.5 inch (5 to 13 mm). Field inspections and a review of Bridge I-2 available maintenance records indicated that its piers have performed satisfactorily. The piers did not experience any measurable settlement, lateral movement, or rotation. These results were expected considering the precompressed character of the

cohesive subsoils encountered at this bridge site. This analysis confirmed that the piers are in good condition, performing as expected, and that future pier settlement should not be of concern.

Settlement analysis of the embankment underlying the approach slab was also performed. The embankment configuration and dimensions were obtained from the DOTD design drawings, which showed that the embankment is 3 feet (0.91 m) high and 46.8 feet (14.3 m) wide. It was constructed of non-plastic granular fill. The first 10 feet (3.1 m) of the top lift and the first 3 feet (0.91 m) of the bottom lift surrounding the 4-inch (102 mm) diameter perforated pipe were filled with gravel/crushed stone fill. The analysis included calculation of the expected settlement of the embankment from the self-weight of the 12-inch (105 mm) thick approach slab and the underlying embankment. The calculated long-term settlement was approximately 0.5 to 1 inch (13 to 25 mm). Field measurements indicated a 1- to 2-inch (25 to 51 mm) difference in grade at the edge of the approach slab. A higher grade difference of about 3 inches (76 mm) was measured around 10 feet (3.1 m) from the edge. As previously discussed, this variation could be due to high or low local points on the approach slab due to a construction or survey error.

Bridge I-2 and the other five integral abutment bridges are all replacement structures. Accordingly, most of the primary consolidation settlement has occurred under the loads of the original structures. While no detailed analyses were performed on the other semi-integral and conventional bridges examined in this study, similar settlement should be expected since they were all built in areas of relatively similar subsoil conditions. The measured difference in grade of the approach slabs in Bridges I-3, I-4, and I-6 was generally less than 0.5 inch (13 mm).

The design and stability of the geosynthetic-reinforced wall (embankment) of Bridge I-2 was also examined. DOTD design drawings provided the embankment configuration and dimensions. However, in the absence of design calculations and construction records, some assumptions were made relative to the type and properties of the geosynthetic materials used in construction. The analysis included calculation of the safety factors against sliding, overturning, and bearing capacity for the geosynthetic wall face of the embankment. In addition, the analysis examined the adequacy of the reinforcement spacing and the selected anchorage length.

The analyses were performed according to the procedures specified by FHWA for design of wrap-around facings and geosynthetic-reinforced MSE walls [7]. The Tensar Corporation's software package MesaPro (Tensar 1998) was used for the analyses [8]. The

analysis assumed that a granular backfill with a 30-degree angle of internal friction (ϕ) and a unit weight (γ) of 120 pcf (18.9 kN/m^3) was used for construction of the embankment. This assumption was consistent with the prototype bridge design used by DOTD. A pre-compressed natural soil (subgrade) with undrained cohesion (C_u) of 1,000 psf (100 kN/m^2) and a unit weight (γ) of 120 pcf (18.9 kN/m^3) was considered in the analysis. For the purpose of comparison, additional analysis was made considering other possible consistencies for the natural soil subgrade. Results of these analyses are summarized in table 11. Specifications of the geogrid used in the MesaPro analysis are given in Appendix D [8].

Table 11
Adequacy of reinforced embankment over different soil subgrade

Subgrade Consistency	Properties	Safety Factors of Wall
Very soft to soft	C_u = 250 psf (12 kN/m^2) γ = 90 pcf (14.2 kN/m^3)	Unsatisfactory for bearing capacity
Medium stiff to stiff	C_u = 500 psf (24 kN/m^2) γ = 100 pcf (15.7 kN/m^3)	Satisfactory
Stiff to very stiff	C_u = 1,000 psf (48 kN/m^2) γ = 120 pcf (18.9 kN/m^3)	Satisfactory

Results of the analyses indicated that the present design of the geosynthetic-reinforced embankment is satisfactory and on the conservative side for fair to good (medium stiff to stiff) soil subgrade conditions. This is due to the relatively small height of the embankment and the precompressed subsoils. This conservative design was necessary to create an annular space (gap) between the embankment face and the backwall. In view of the satisfactory conditions of the annular space observed in the field in all of the six prototype semi-integral abutment bridges, the current DOTD design is adequate and should not be modified for fair to good soil subgrade.

Finite Element Analysis (FEA)

Finite element analysis was performed to investigate limitations of the present DOTD semi-integral abutment bridge design. This analysis was based on design information compiled from DOTD design drawings and records. A parametric study used the finite element analysis (FEA) to examine the effect of various design parameters on the performance of the prototype semi-integral bridge. Data obtained from the field

measurements and inspections along with weather records were used to calibrate the finite element models or to perform the parametric study.

Due to space limitations, only those effects deemed most important will be reported herein. The ANSYS [9] output files can be made available should more information be desired later. Of particular interest was the response of the concrete backwall, particularly the connections of both the approach slab and bridge deck with the backwall. This is due to the unique DOTD prototype design (inclusion of a geosynthetic-reinforced embankment and gap) and DOTD interest in its performance. In addition, some transverse hair cracks were observed along the backwall in some of the bridges during the field inspections, as reported earlier in this study. Although field inspections of the girders showed no cause for concern, stresses at the bottom of the interior girder at midspan are also reported since they represent maximum values. Figure 40 shows locations of the specific nodes where results of the FEA results are reported.

As temperature was varied while assuming either roller supports or hinge supports at the boundaries the following data were reported: the longitudinal displacement ($?_z$) at end of the approach slab (Node A); the stresses at top of the deck at the girder/backwall connection (Node B), bottom of the approach slab at the vertical gap (Node C**), and bottom of the approach slab at the vertical gap (Node D); and the change in s_{zz} at top of the girder at the centerline of bearing (Node E) and at the bottom of the girder at midspan (Node F). For the study of temperature gradient effects, the stresses at the bottom of the approach slab at the vertical gap (Node C), top of the approach slab at the vertical gap (Node G), and top of the deck at the girder/backwall connection (Node B) were examined. As approach slab settlement was varied, the stresses at the top of the approach slab at the vertical gap (Node G), bottom of the approach slab at the vertical gap (Node D), and top of the deck at the girder/backwall connection (Node B) were examined. To study bridge skew, the total transverse reaction at the bottom surface of the abutment as well as the stresses in the slab near the top of the girder at the centerline of the bearing (Node H) were reported. All of these nodes were located along the longitudinal centerline of the interior girder (z-axis) except for the nodes marked with "**". These nodes were located midway between the girders in the transverse direction (x-axis for Models 1 and 2).

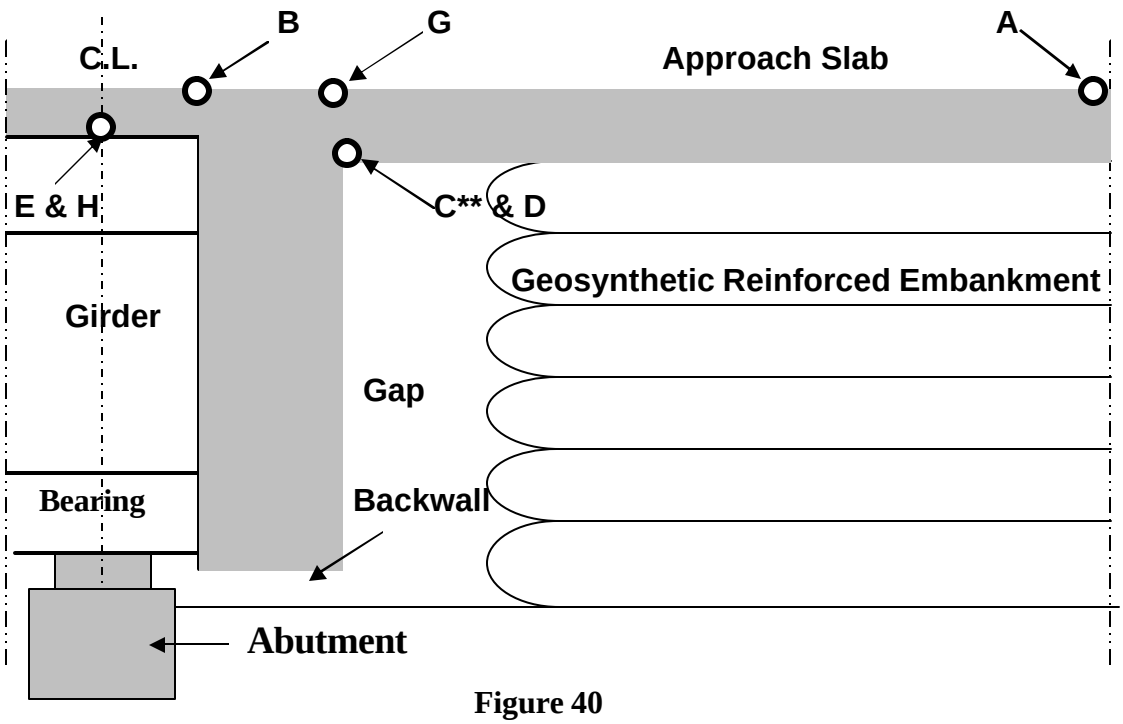

Figure 40
Locations of nodes in the reported FEA results

The results listed in this section include the effect of:

- Uniform temperature increase, assuming roller supports
- Uniform temperature increase, assuming hinge supports
- Temperature gradient
- Approach slab settlement
- Bridge skew

The results reported herein include the effects of self-weight of the structure. Allowable stresses are based on actual specified concrete design strength (for the deck, backwall and approach slab: f'_c = 4,200 psi (29 MPa); for the girders: f'_c = 6000 psi (41 MPa). For the deck, approach slab, and backwall, an allowable compressive stress of 2,520 psi (17 MPa) and a modulus of rupture of 486 psi (3 MPa) were assumed. For the girders, an allowable compressive strength of 3,600 psi (25 MPa) and an allowable tensile strength of 468 psi (3 MPa) were assumed.

Effect of Uniform Temperature Increase with Roller Supports

Model 1 was used in this analysis. The uniform temperature case examined the response of the bridge as it experienced a uniform seasonal change in temperature. The bridge's self-weight was also considered in this model. The stresses in the prestressed concrete girders due to prestressing were manually calculated and incorporated into the FEA

results. A temperature difference of 100°F (56°C) was assumed to be the extreme seasonal variation in temperature for a structure in Bridge I-1's general area. The displacement at the end of the approach slab and the stresses due to the temperature variation were recorded at the sample nodal points previously discussed. Table 12 and figure 41 depict the effect of a uniform temperature change on the longitudinal displacement at the end of the approach slab. The field investigation revealed that Bridge I-1 did expand and contract longitudinally along the *z*-direction.

Table 12
Longitudinal displacement due to temperature increase (w/rollers)

Temperature Increase (DH), °F (°C)	**Dz at Node A, inches (mm)**
100 (56)	2.4 (61.5)
67 (37)	1.6 (40.6)
33 (18)	0.8 (20.3)
25 (14)	0.5 (12.3)
0 (0)	0.0 (0.0)

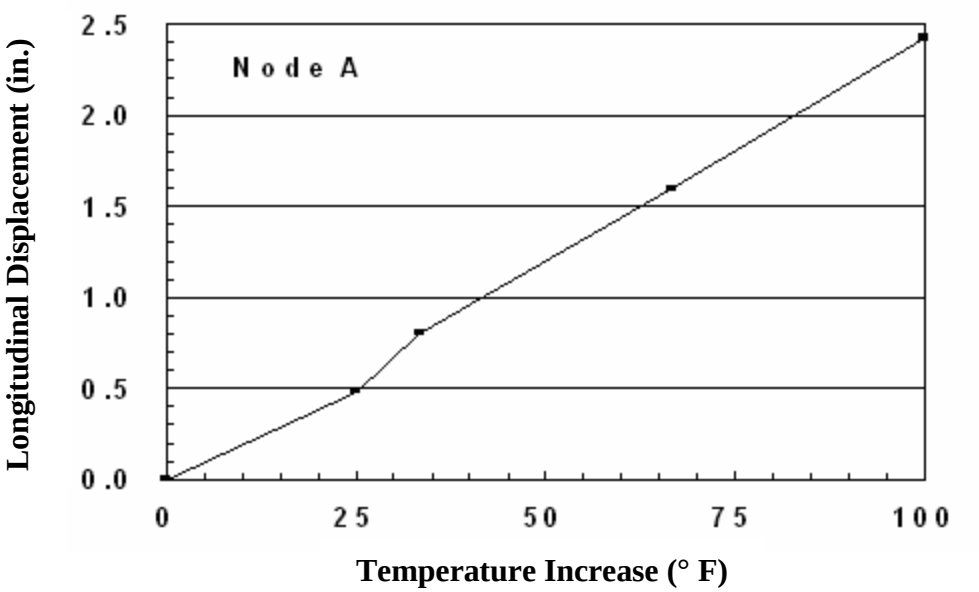

Figure 41
Longitudinal displacement due to temperature increase (w/rollers)

For the range of temperature variation considered in the analyses, the concrete stresses computed by the FEA were all within the allowable limits, as shown in tables 13, 14,

and figure 42, except for temperature increases in excess of 67 ^{o}F (37 ^{o}C). Temperature increases greater than 50 ^{o}F (28 ^{o}C) were not expected at the bridge site.

Table 13

Computed stresses due to temperature increase (w/rollers)

Node	Temperature Increase (ΔH), ^{o}F (^{o}C)	Computed Stresses, psi*					
		σ_{xx}	σ_{yy}	σ_{zz}	τ_{xy}	τ_{yz}	τ_{xz}
B	100 (56)	172	234	724	-13	-30	22
	67 (37)	113	153	472	-9	5	8
	33 (18)	56	74	228	-4	39	-4
	25 (14)	33	43	132	-2	52	-9
	0 (0)	-1	-5	-16	0	72	-17
C	100 (56)	9	723	-853	1	-60	11
	67 (37)	6	476	-584	0	-97	7
	33 (18)	3	235	-323	0	-132	4
	25 (14)	2	141	-220	0	-147	2
	0 (0)	1	-5	-62	0	-168	0
D	100 (56)	302	700	743	4	122	-2
	67 (37)	199	462	477	3	90	-1
	33 (18)	99	231	218	1	59	1
	25 (14)	60	140	116	1	47	2
	0 (0)	-1	-1	-41	0	28	3

* 1 psi = 145.93 MPa

Table 14

Longitudinal stress due to temperature increase (w/rollers)

Temperature Increase (ΔH), ^{o}F (^{o}C)	Computed Stress σ_{zz}, psi (MPa)	
	Node E	Node F
100 (56)	-148 (-1.0)	-774 (-5.3)
67 (37)	-131 (-0.9)	-753 (-5.2)
33 (18)	-114 (-0.8)	-732 (-5.0)
0 (0)	-97 (-0.7)	-711 (-4.9)

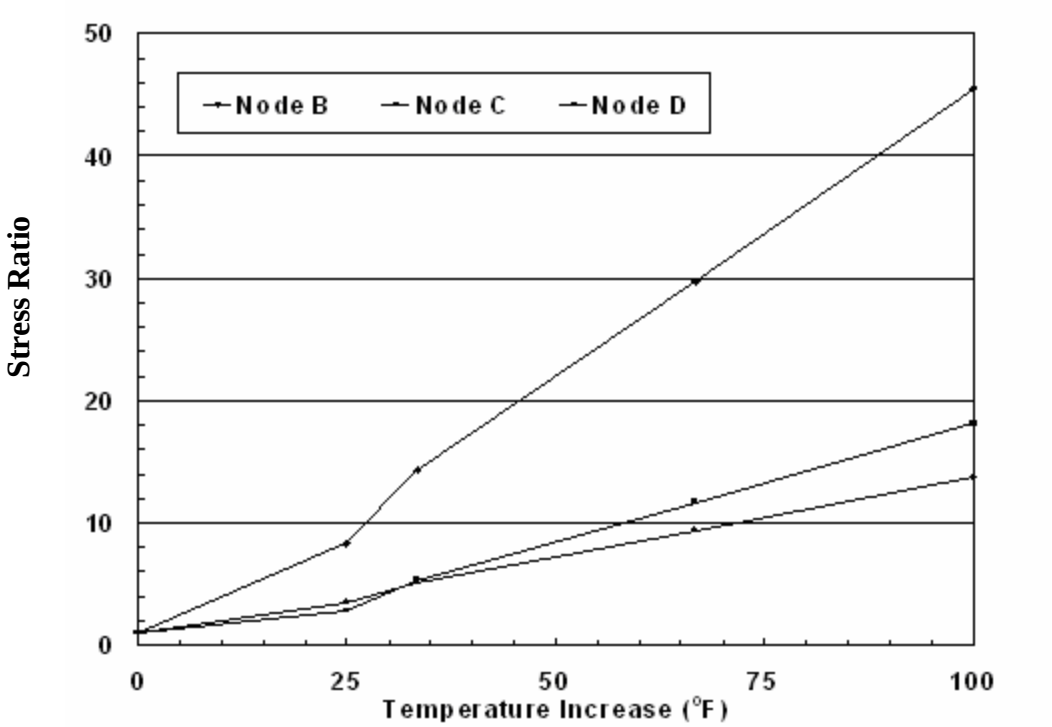

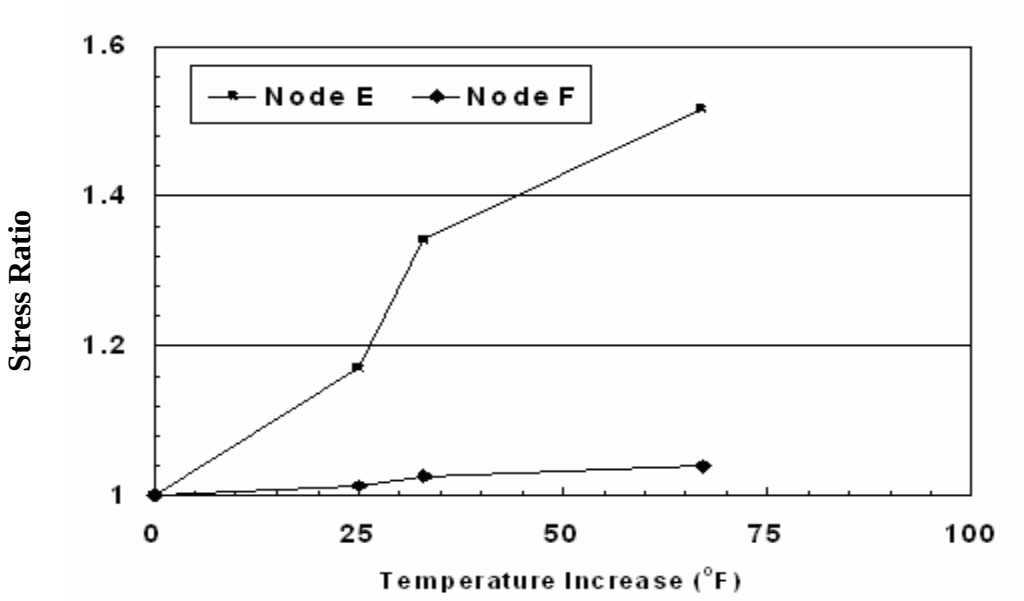

Stress Ratio = $\sigma_{zz}(\Delta T)/\sigma_{zz}$(Self Weight)

Figure 42
Effect of temperature increase on σ_{zz} (w/rollers)

As can be seen, there is a linear correlation between the overall temperature increase and the resulting stresses. The effect a specific overall temperature increase can be estimated using these tables and figures and then added to the stresses due to other loads at the zero stress condition (the reference design temperature). For example, the reference temperature for Bridge I-1 can be estimated as the temperature at the time of its construction, or 75°F (24 °C). For a design that accounts for a high temperature of 100 °F (38 °C), the stresses due to a temperature difference of 25 °F (14 °C) should be added to the zero stresses at the reference temperature.

Average ambient temperatures within the geographical area of the six prototype integral bridges are shown in table 15, which is based on 2002 data obtained from various weather web sites e.g., Weather Underground [10]. This information could be used to evaluate the effect of ambient conditions on the performance of a given bridge. For example, in a worst-case scenario, a maximum temperature change of 50°F (28°C) could be assumed for Bridge I-1 in DOTD district 58. Assuming the bridge was constructed at a reference temperature of 57°F (14°C), the expected maximum difference in temperature would then be 25°F (14°C).

Table 15
Average ambient temperature in 2002 at the integral bridge sites

DOTD District	Average Monthly Temperature °F												Temperature Range °F			
	J	F	M	A	M	J	J	A	S	O	N	D	Avg.	Max	Min	DT
07	52	54	61	66	75	81	82	82	79	70	61	54	36	50	20	31
08	48	52	61	66	73	81	82	82	79	68	57	52	34	50	16	34
58	46	52	57	66	73	81	82	82	77	66	57	48	34	50	14	36
DOTD District	**Average Monthly Temperature °C**												**Temperature Range °C**			
	J	F	M	A	M	J	J	A	S	O	N	D	Avg.	Max	Min	DT
07	11	12	16	19	24	27	28	28	26	21	16	12	20	28	11	17
08	9	11	16	19	23	27	28	28	26	20	14	11	19	28	9	19
58	8	11	14	19	23	27	28	28	25	19	14	9	19	28	8	20

Based on the FEA results, no overstresses corresponding to this maximum temperature range would be expected. Therefore, Bridge I-1 components would not be overstressed due to the most possible temperature increase. Using these tables and figures, it can be predicted that the longitudinal displacement of Bridge I-1 for a 50°F (28°C) increase in temperature would be on around 1.2 inches (31 mm). Thus, for all future semi-integral bridges, it is recommended that a sleeper slab be used at the far end of the approach slab with

a joint sized to allow for the anticipated thermal movement based on the maximum temperature difference, as was the case in the other five semi-integral bridges.

Effect of Uniform Temperature Increase with Hinge Supports

A second uniform temperature increase was also examined using Model 1, but with different boundary conditions. The DOTD semi-integral abutment bridges are cast integral with the backwall and approach slab, but not with the abutment substructure. Once the bond between the approach slab and the geosynthetic-reinforced embankment or the bond between the bottom of the girders and top of the bearing pads is broken, the bridge/backwall/approach slab system will displace longitudinally due to changes in thermal conditions, A fully integral abutment bridge would have greater constraint against longitudinal displacement. All bridge components, including the substructure, must be designed accordingly. All integral and semi-integral bridges behave as if they are fully constrained against longitudinal movement initially. Sometime during the first seasonal thermal cycle, the bond due to friction and adhesion at the structures boundaries (and the stiffness of the abutment's foundation, if fully integral) is overcome. For this case, a finite element model with rollers in the longitudinal direction would most closely simulate actual bridge behavior. The results of this case were given in the previous section, "Effect of uniform temperature increase with roller supports".

Model 1 was modified to simulate bridge behavior prior to longitudinal movement, before the adhesion and frictional bonds are overcome at the girder/bearing pad interface and at the bottom of the approach slabs. Roller supports were replaced with hinges that do not allow translation in the longitudinal direction. At this time, there is no reliable method available to estimate when longitudinal movement occurs and the actual magnitude of this movement or the adhesive and frictional forces that are overcome at the initiation of movement. The actual bridge longitudinal movement would be somewhere between the values reported in table 12 (with rollers) and table 16 (with hinges). In the future, a more advanced FEA parametric study could be done to focus on the soil/structure interaction at these interfaces.

This second case simulated the behavior of an integral abutment bridge with integral approach slabs before the interface bonds broke (boundary conditions with hinges). As expected, the longitudinal displacement of Node A at the end of the approach slab was significantly decreased, as shown in table 16 and figure 43. Also, as indicated in tables 17, 18, and figure 44, the stresses increased significantly when compared with those computed for the previous case "Effect of uniform temperature increase with roller supports". In many instances throughout the model, the concrete elements exhibited overstress failure. However, the DOTD prototype semi-integral bridges would not be subject to overstress at the higher

temperatures, since the actual bridge support conditions would more closely match those modeled with rollers sometime during the first thermal cycle that the bridges would experience.

Table 16
Longitudinal displacement due to temperature increase (w/hinges)

Temperature Increase (DT), ^{o}F (^{o}C)	**Dz at Node A, in (mm)**
100 (56)	0.6 (14.0)
67 (37)	0.4 (9.3)
33 (18)	0.2 (4.7)
25 (14)	0.1 (3.5)
0 (0)	0.0 (0.0)

Table 17
Computed stresses due to temperature increase (w/hinges)

Node	**Temperature Increase (DT), ^{o}F(^{o}C)**	**Computed Stresses, psi***					
		s_{xx}	s_{yy}	s_{zz}	t_{xy}	t_{yz}	t_{xz}
B	100 (56)	-646	-932	-1667	-78	481	63
	67 (37)	-383	-669	-972	-33	337	32
	33 (18)	-320	-606	-807	-22	302	24
	25 (14)	-127	-411	-300	12	195	0
C	100 (56)	-322	-433	-1406	-12	-261	22
	67 (37)	-159	-110	-781	-9	-88	10
	33 (18)	-119	-33	-630	-8	-46	7
	25 (14)	2	202	-158	-6	82	-2
D	100 (56)	-18	-1006	1236	-21	-169	63
	67 (37)	-74	-663	494	-22	7	33
	33 (18)	-87	-581	315	-22	50	26
	25 (14)	-131	-330	-244	-23	180	4

* 1 psi = 145.93 MPa

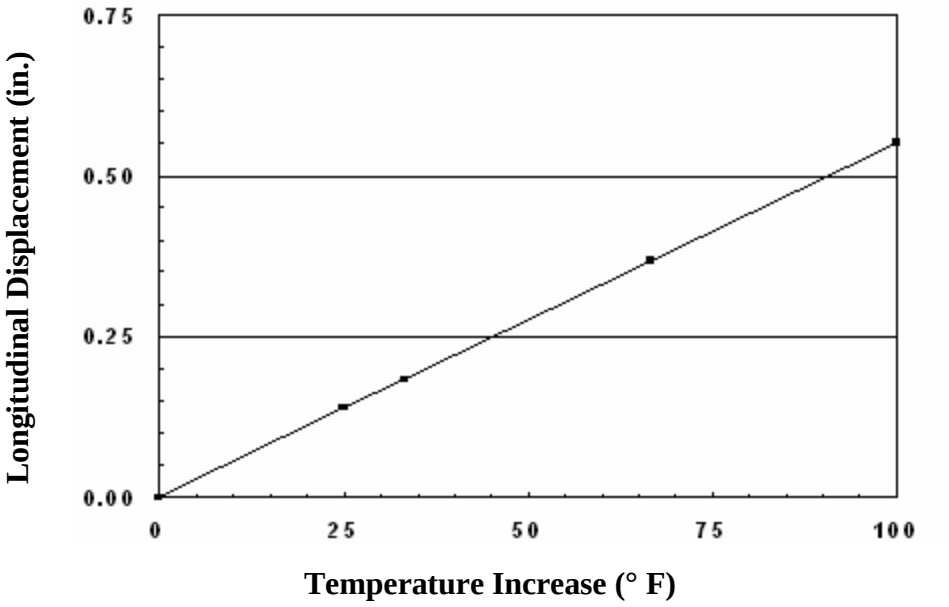

Figure 43
Longitudinal displacement due to temperature increase (w/hinges)

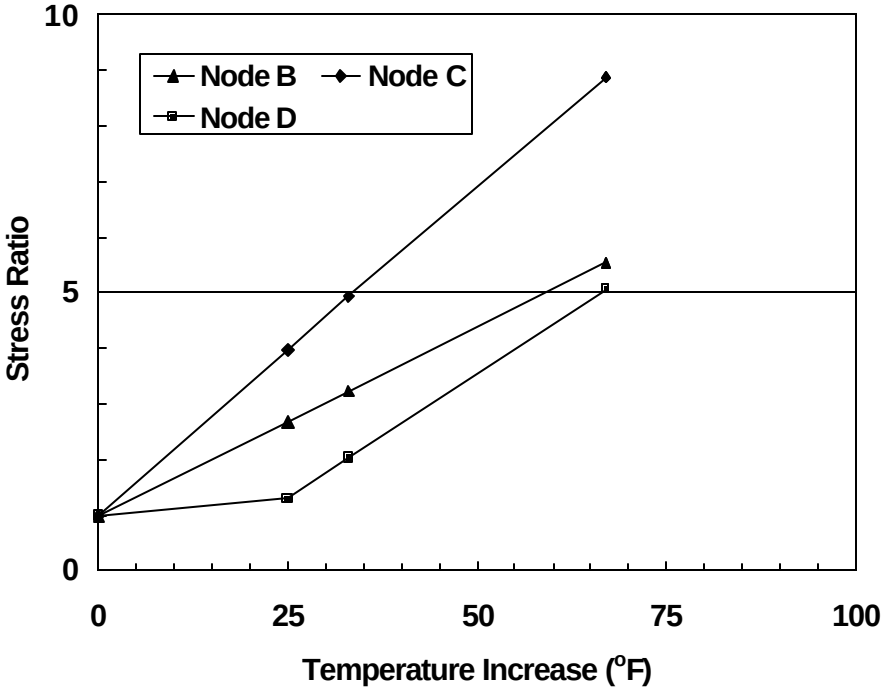

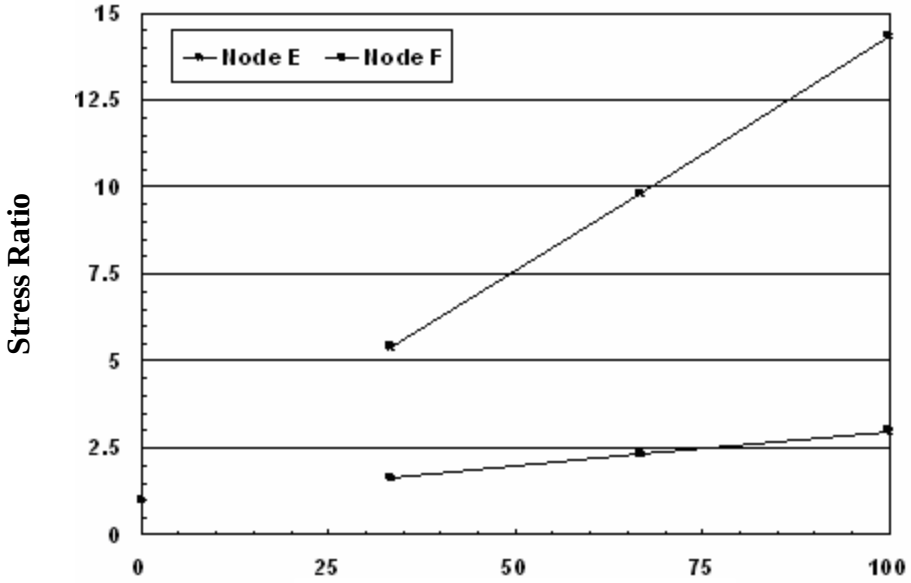

Stress Ratio = $\sigma_{zz}(\Delta T)/\sigma_{zz}$(Self Weight)

Figure 44
Effect of temperature increase on σ_{zz} (w/hinges)

Table 18
Longitudinal stress due to temperature increase (w/hinges)

Temperature Increase (DT), °F (°C)	Computed Stress s_{zz}, psi (MPa)	
	Node E	Node F
100 (56)	-1427 (-9.8)	-4078 (-28.1)
67 (37)	-975 (-6.7)	-2945 (-20.3)
33 (18)	-538 (-3.7)	-1845 (-12.7)
25 (14)	-100 (-0.7)	-745 (-5.1)

Effect of Temperature Gradient

A temperature gradient study was approximated by thermally loading the nodes of the mesh from a lower temperature at the bottom to a higher value at the top. This study simulated the variation in temperature through the depth of a bridge caused by the radiant heat of the sun. A temperature reference of 75°F (24°C) was used for all cases. The bridge was assumed to have been constructed at 75°F (24°C). At this reference temperature, thermal strains were zero at all points in the structure. The bridge was then loaded to the starting or initial temperature. The initial temperature is defined as the ambient temperature at the bottoms of all bridge components. The temperature was then increased as a linear function of depth until the top surfaces of the bridge components reached a temperature 20°F (11°C) greater than the bottom surface, which remained at the initial temperature. The "zero" temperature gradient stresses listed in table 19 and figure 45 were those due to gravity self-weight loads at the reference temperature (thermal stresses are zero in this case). Stresses at Node B, which was at the top of the bridge deck at the girder/backwall connection, increased linearly. The longitudinal stresses at Nodes C and G showed no correlation. The reference temperature, or the average temperature at which the bridge was constructed, is a major factor in the behavior of the structure as it undergoes a thermal gradient variation. Upon review of the FEA results, no overstressing was detected in any of the bridge components for the temperature gradient cases.

Table 19
Computed stresses due to temperature gradient

Node	Temperature Gradient, ^{o}F	Computed Stresses, psi					
		s_{xx}	s_{yy}	s_{zz}	t_{xy}	t_{yz}	t_{xz}
B	95 ? 115	132	30	490	12	-35	5
	85 ? 105	118	27	414	13	-23	-1
	75 ? 95	104	24	339	14	-12	-6
	35 ? 55	50	14	43	19	33	-27
	0	77	19	187	17	11	-17
C	95 ? 115	71	388	117	-3	98	4
	85 ? 105	28	285	13	-3	83	3
	75 ? 95	-14	182	-91	-3	68	2
	35 ? 55	-179	-219	-495	-2	9	-2
	0	-99	-23	-298	-2	38	0
G	95 ? 115	23	389	-56	-1	90	-9
	85 ? 105	22	287	44	-1	77	-10
	75 ? 95	20	184	143	-1	64	-10
	35 ? 55						
	0	18	-21	342	-1	38	-11

Node	Temperature Gradient, ^{o}C	Computed Stresses, MPa					
		s_{xx}	s_{yy}	s_{zz}	t_{xy}	t_{yz}	t_{xz}
B	35 ? 46	0.9	0.2	3.4	0.1	-0.2	0.0
	29 ? 41	0.8	0.2	2.9	0.1	-0.2	0.0
	24 ? 35	0.7	0.2	2.3	0.1	-0.1	0.0
	2 ? 13	0.3	0.1	0.3	0.1	0.2	-0.2
	0	0.5	0.1	1.3	0.1	0.1	-0.1
C	35 ? 46	0.5	2.7	0.8	0.0	0.7	0.0
	29 ? 41	0.2	2.0	0.1	0.0	0.6	0.0
	24 ? 35	-0.1	1.3	-0.6	0.0	0.5	0.0
	2 ? 13	-1.2	-1.5	-3.4	0.0	0.1	0.0
	0	-0.7	-0.2	-2.1	0.0	0.3	0.0
G	35 ? 46	0.2	2.7	-0.4	0.0	0.6	-0.1
	29 ? 41	0.1	2.0	0.3	0.0	0.5	-0.1
	24 ? 35	0.1	1.3	1.0	0.0	0.4	-0.1
	2 ? 13	NA	NA	NA	NA	NA	NA
	0	0.1	-0.1	2.4	0.0	0.3	-0.1

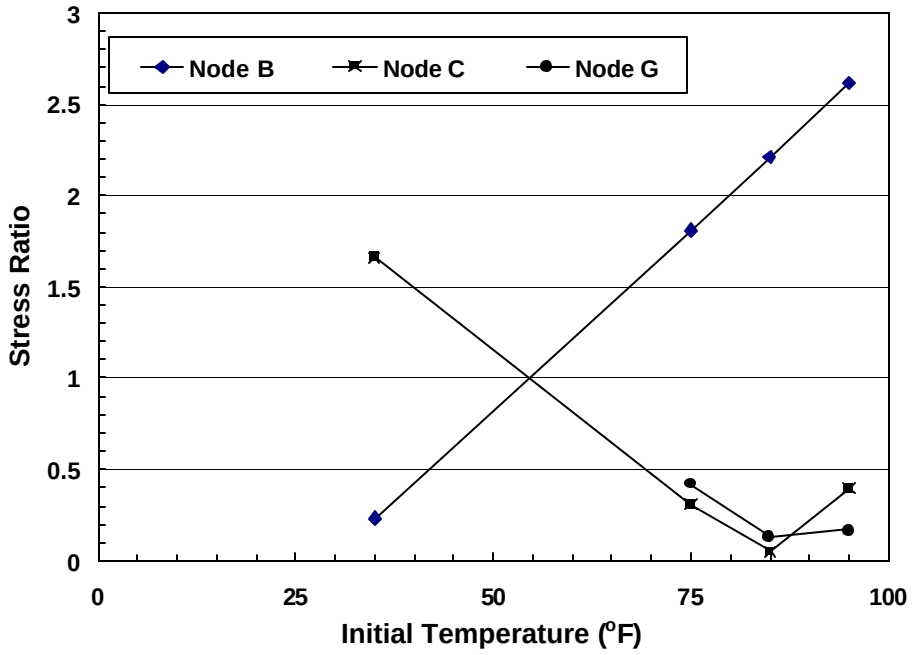

Stress Ratio = σ_{zz}(Temp. Gradient)/σ_{zz}(Self Weight)

Figure 45
Effect of 20°F (11°C) increase in temperature on σ_{zz}
[75°F (24°C) reference temperature]

Effect of Approach Slab Settlement

By imposing a vertical displacement along the bottom nodes of the approach slab, the settlement of the underlying earth embankment was simulated. Model 2 was used for this case with the boundary conditions of roller supports at the girder bearings and bottom of the approach slab. The zero settlement case represented the model being loaded with only its self-weight. A forced vertical downward displacement of the rollers supporting the approach slab was taken as the load in combination with self-weight. Three settlement cases were analyzed, along with the zero settlement case. A maximum downward settlement of the roller at the far end of the approach slab was assumed. The remaining rollers supporting the approach slab were displaced linearly with zero displacement applied at the connection of the approach slab to the backwall. The maximum displacement at the far end was varied from 1, 2, and 4 inches (25, 51 and 102 mm). Table 20 and figure 46 list the results of this case.

The stresses at Nodes B and G at the top surface of the backwall indicated that cracking has occurred in all cases with the exception of the zero settlement case. These results also show that Node D at the bottom of the approach slab where it connects to the

backwall is overstressed in compression. Calculations using the figures and tables for this loading case indicated that Node D could become overstressed in compression due to approximately 1.1 inches (30 mm) of far end settlement. Thus the section at this location, for these loadings, has cracked at the top surface. These analyses do not necessarily indicate a failure condition. The FEA did not explicitly take into account the presence of reinforcing steel or cracked section properties. The effect of reinforcing steel was handled using a smeared approach in the FEA model. This is standard practice in modeling structures of this scale. The haunch at the connection between the backwall and the approach slab was not included in the finite element model. Based on these results, settlement of the approach slab is the most important factor affecting the semi-integral abutment design and should, therefore, be accounted for in design of the structural components of the superstructure. A more detailed FEA of the abutment area would yield more conclusive results.

In addition, the field investigation revealed that there was an approximately 1-inch (25 mm) deep horizontal gap under the extreme edge of the embankment near the backwall. The access holes allowed for crude hand measurement of this horizontal gap. The extent of the separation with distance away from the backwall could not be determined since the access holes were only drilled near the backwall. This separation was not considered in the finite element model where full contact was assumed throughout the length of the approach slab.

In light of the observed settlement of the embankment supporting the approach slab, a weak joint (internal hinge) placed in the 40-foot (12 m) long approach slab approximately 10 feet (3 m) away from the backwall (1/4 of the slab length), is recommended in order to eliminate the potential for overstress at the top of the backwall due to approach slab settlement. This weak joint has been incorporated in the design of Bridge I-2 through a saw-cut joint.

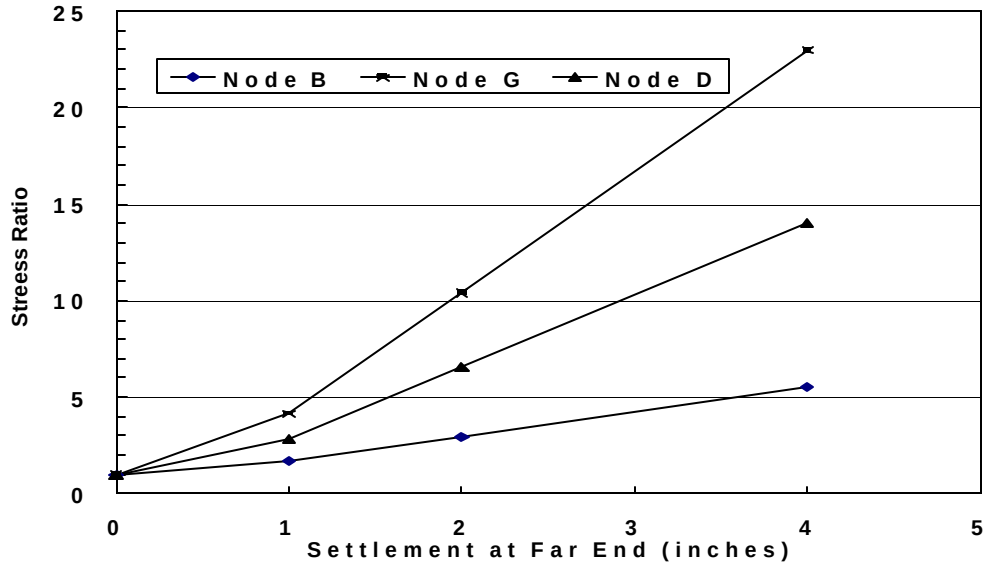

Stress Ratio = σ_{zz} (Settlement)/σ_{zz} (Self Weight)

Figure 46
Effect of approach slab settlement on σ_{zz}

Table 20
Computed stresses due to approach slab settlement

Settlement of Approach Slab at Far End, inches (mm)	Computed σ_{zz} Stresses, psi (MPa)		
	Node B	Node G	Node D
4 (102)	2,761 (19.0)	11,117 (76.7)	-9,445 (-65.1)
2 (51)	1,469 (10.1)	5,041 (34.8)	-4,433 (-30.6)
1 (25)	823 (5.7)	2,003 (13.8)	-1,927 (-13.3)
0 (0)	500 (3.4)	484 (3.3)	-674 (-4.6)

Effect of Skew

Model 3 with roller supports was used for the skew study. Reference is made to the coordinate system used for Model 3. As abutment rotation increased from 0 to 30 degrees, so did the transverse force transferred to the foundation by the connection of the girders to the pile cap. Table 21 and figure 47 show that this transverse force increased to 171 lbs (762 N) at a 30 degree skew. The results shown for Node H (located at the bottom of the deck at the

centerline of the girder bearing) in table 22 and figure 48 indicate a general increase in all stress components. The location of Node H might differ slightly for each skew case. The finite element mesh for all cases was automatically generated using the APDL (ANSYS Parametric Design Language) routine. In all previous cases, the mesh did not change when the value of the parameter under consideration changed temperature or settlement. However, for the skew case, the mesh generated for each skew angle was different. Therefore, the reported results may show a slight deviation. Upon review of this study's results, a skew of 30 degrees did not overstress any bridge component. However, this study did not include the combined effects of live load, wind, and/or temperature, which may become critical.

Table 21
Effect of skew on transverse reaction at abutment

Skew (Transverse Direction) (degrees)	SF Transverse, lbs (N)
30	171 (762)
20	105 (467)
10	64 (284)
0	0 (0)

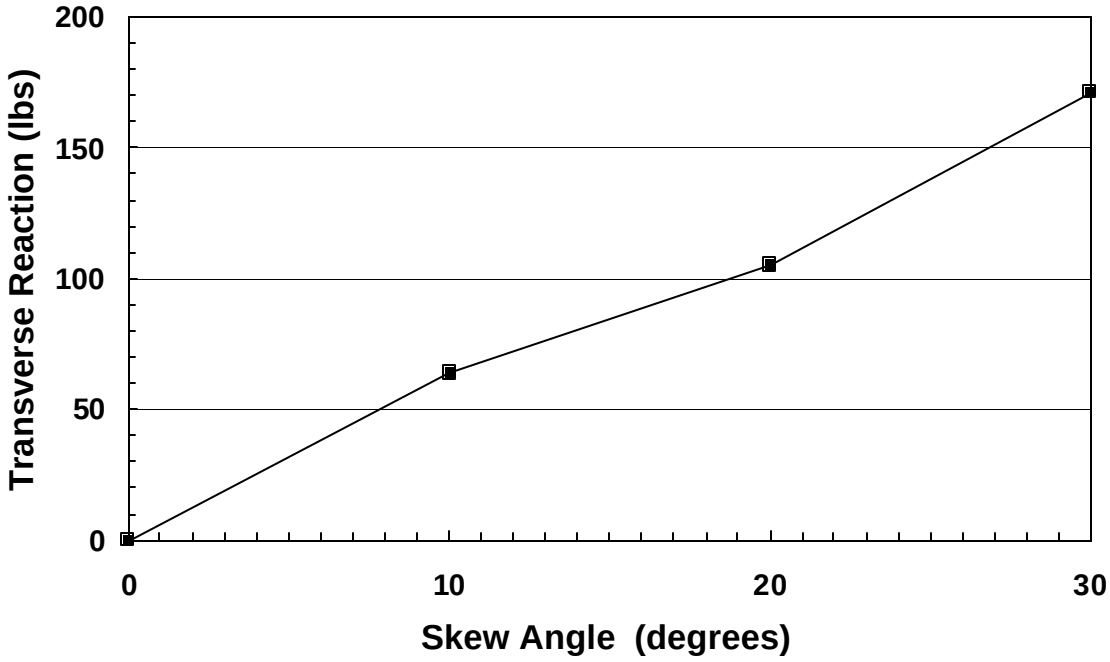

Figure 47
Effect of skew on transverse reaction

Table 22
Effect of skew on stresses at Node H

Skew Angle (degrees)	Resulting Stresses at Node H, psi (MPa)					
	σ_{xx}	σ_{yy}	σ_{zz}	τ_{xy}	τ_{yz}	τ_{xz}
25	246 (1.7)	-15 (-0.1)	66 (0.5)	6 (0.0)	0 (0.0)	-76 (-0.5)
20	254 (1.8)	-16 (-0.1)	54 (0.4)	5 (0.0)	0 (0.0)	-62 (-0.4)
15	229 (1.6)	-18 (-0.1)	39 (0.3)	13 (0.1)	-1 (0.0)	-38 (-0.3)
10	228 (1.6)	-19 (-0.1)	34 (0.2)	13 (0.1)	-1 (0.0)	-25 (-0.2)
5	227 (1.6)	-20 (-0.1)	30 (0.2)	14 (0.1)	0 (0.0)	-12 (-0.1)
0	195 (1.3)	-18 (-0.1)	21 (0.1)	14 (0.1)	0 (0.0)	1 (0.0)

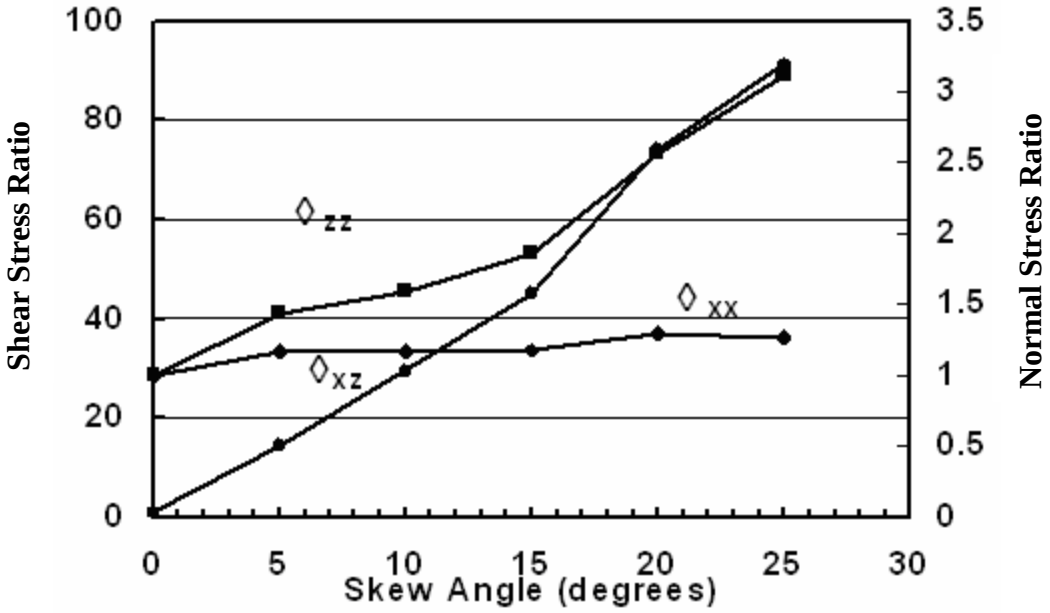

Shear Stress Ratio = τ_{xz}**(Skew)/** τ_{xz}**(Self Weight)**

Stress Ratio = σ_{xx}**(Skew)/** σ_{xx}**(Self Weight)**

Stress Ratio = σ_{zz}**(Skew)/** σ_{zz}**(Self Weight)**

Figure 48
Effect of skew on stress state of Node H

Cost/Benefit Analysis

A cost/benefit analysis was performed on the semi-integral Bridge I-2 in Catahoula Parish. The calculated cost was compared to that of a comparable conventional bridge of the same span lengths and dimensions. Costs of the various items used in the analysis were based on the actual cost data and present unit prices for DOTD 2003 projects.

Due to the semi-integral abutment design of Bridge I-2, most structural components were nearly identical for the semi-integral abutment and comparable conventional bridge designs. The difference in cost was mainly due to the requirement for preformed compression joints and depth requirements for the approach slabs. For the conventional bridge configuration, compression joints were located at each abutment and all piers, similar to the four comparable conventional bridges. Thickness of the approach slabs used for the conventional bridge was the same as the approach slab thickness for the four comparable conventional bridges. Table 23 shows the various items in the semi-integral abutment bridge and the comparable conventional bridge and compares the costs of the semi-integral abutment bridge items, and the comparable conventional bridge items.

The difference in cost between the existing Bridge I-2 and the comparable conventional bridge of similar dimensions and spans was approximately $28,311, with the conventional bridge costing more to construct. The estimated costs were based only on construction and material costs. Item costs were based on the most recent DOTD letting information because actual detailed bid items for the semi-integral bridges were not available [11]. The estimated costs did not consider the possible additional costs of long-term maintenance to strip seal joints, time savings attributed to omitting strip seal joints, and indirect benefits resulting from a smoother ride over the jointless bridge.

Based on DOTD records, the actual total construction cost for Bridge I-2 in 1998 was $2,770,425. Using an inflation rate of 3 percent, a similar semi-integral bridge constructed in 2003 would have cost $3,211,682.

Table 23
Semi-integral/conventional cost comparison

Structural Item	Bridge Type		Cost	
	Bushley Bayou I-2 (A)	**Conventional (B)**	**Item**	**Difference (B - A)**
Girders	Type III Class 'P(m)' concrete	Type III Class 'P(m)' concrete	$55 per ln. ft. ($180 per ln. m)	None
Slab	7.5 inch (191 mm) Class 'AA' concrete	7.5 inch (191 mm) Class 'AA' concrete	$357 per cu. yd. ($442 per cu. m)	None
Approach Slabs	12 inch x 40 feet (305 mm x 12.2 m) Class 'AA' concrete	10 inch x 40 feet (254 mm x 12.2 m) Class 'AA' concrete	$357 per cu. yd. ($442 per cu. m)	-$3,912
Expansion Joints	Yes	No	$4.00 per lbs. ($1.80 per kg)	-$14,373
Strip Seal Joints	No	Yes	$95 per ln. ft. ($368 per ln. m)	+$49,366
Abutments	Class 'A' concrete	Class 'A' concrete	$357 per cu. yd. ($442 per cu. m)	None
Piers	Class 'A' concrete	Class 'A' concrete	$357 per cu. yd. ($442 per cu. m)	None
Piles	30 in. (750 mm) precast Class 'P' concrete	30 in. (750 mm) precast Class 'P' concrete	$70 per lin. ft. ($274 per ln. m)	None
Geotextile	425 sq. yd. (506 sq. m)	None	$0.80 per sq. yd. ($1.26 per sq. m)	-$638
Geogrid	375 sq. yd. (446 sq. m)	None	$4.00 per sq. yd. ($4.78 per sq. m)	-$2,132

CONCLUSIONS

In the United States, 35 of the 50 states have constructed integral (jointless) bridges. Eleven states reported their overall experience with integral bridges as being very good to excellent and twenty-one states say their experience has been good to satisfactory. With regard to worldwide usage of integral bridges, the United Kingdom Highways Agency Standard now recommends that any new bridge less than 197 feet (60 m) long should be integral. Several Canadian provinces including Alberta, Quebec, Nova Scotia and Ontario have constructed jointless bridges, and most have reported good to satisfactory experiences with their use.

In general, the most reported potential problems in integral abutment bridges include:

- An increase of lateral earth pressure on the integral abutments due to seasonal summer expansion of the bridge superstructure.
- Incremental or permanent buildup (ratcheting) of lateral pressure on the integral abutments resulting from the annual thermal cycle's effects on the bridge superstructure.
- Excessive settlement of the ground surface adjacent to the abutments resulting from seasonal winter contraction associated with the bridge superstructure that could produce voids under the approach slab or settlement of the adjacent pavement.

Louisiana DOTD semi-integral prototype bridges have their deck and approach slabs cast integral with the backwalls, but not the abutments. The design includes a continuous vertical annular space (gap) behind the backwall. The gap is created by the construction of a geosynthetic-reinforced embankment beneath the approach slab. This gap eliminates the potential for many the aforementioned problems associated with integral bridges.

Based on a review of the available design and maintenance records and the results of the field inspections, all six semi-integral abutment bridges and the four comparable conventional bridges examined in this study are in relatively good condition regardless of their age, length, traffic, and location. According to DOTD records, they would be ranked as very good to excellent. On a scale of 0 to 9, they rank as either 8 or 9.

The rideability of all 10 bridges was rated as good to very good. All four comparable conventional bridges have a mild bump at the interfaces between the approach slab and bridge deck and between the approach slab and roadway. Rubber seal fillers along the

expansion joints were either partially or fully loose in all four conventional bridges, particularly in Bridge C-3.

Field inspections of the semi-integral bridges indicated that all gaps were constructed as specified in the design drawings and are performing satisfactory. The design drawings of all 6 semi-integral bridges indicate a design gap of 6 inches (152 mm). However, some differences were observed in the gap size with depth and location in all six bridges. The gap size varied from 1.75 to 6 inches (45 to 152 mm), with an average gap size of 3.5 inches (89 mm). A larger gap of 14 inches (350 mm) was measured through some of the weep holes along the backwall of Bridge I-1. The differences in gap size are likely due to the movement of the embankment face following the removal of the construction forms. Some debris (concrete, gravel, geogrid, etc.) found at the bottom of the annular space at random locations appears to have fallen down during construction. Some debris was also found at more shallow depth in Bridge I-5. The detected amount of debris was insignificant in all the bridges and should not cause any concern.

A 1-inch (25 mm) horizontal gap (separation) was detected under the approach slab near the backwall in some of the semi-integral bridges. The exact extent of the separation along the approach slab was not established due to the limited number of inspection holes drilled in the approach slab. This separation is likely due to settlement of the geosynthetic-reinforced embankment and/or the underlying natural subsoils. This observation could lead to the conclusion that some loss of support has occurred over a segment of the approach slab. Therefore, a weak joint (internal hinge) placed at about the quarter span point of the approach slab away from the backwall could be included in future designs to minimize the potential for overstressing the top of the backwall. This weak joint has been implemented in the design of Bridge I-2 through a saw-cut joint.

Geodetic surveys were performed along the spans of all semi-integral bridges. Bridges I-1, I-2, and I-5 have the largest grade difference along their approach slabs of about 2 to 3 inches (51 to 76 mm). The remaining semi-integral bridges have a grade difference of less than 0.5 inch (13 mm). With the exception of Bridge I-1, all of the approach slabs' maximum grade differences are near the midspan point. Bridge I-1 has a lower grade with distance away from backwall, which is consistent with the design grade.

Bridge I-1 was designed without an open joint at the end of the approach slab. The bridge has repeatedly expanded and pushed the adjacent asphalt pavement away from the approach slab, creating a mound of asphalt and an open joint at the pavement edge. This condition produced a bump at the end of the bridge. Periodically, the asphalt mound was

removed and the opening was filled with asphalt by the DOTD district office. All subsequent semi-integral bridges eliminated this problem by the inclusion of a sleeper slab and a joint at the roadway interface.

Bridges I-3 and I-4 are presently in good condition, but could develop future problems due to the placement of an incompressible granular material in the vertical gap between the embankment face and the backwall as specified in the design drawings. The short spans of these bridges and the fact that the fill material was probably not fully compacted would likely minimize the impact of longitudinal movements of the superstructure. This condition does not exist in the remaining bridges.

A conventional structural analysis was performed on the semi-integral Bridge I-2. Results of the analysis indicated that all of the calculated stresses in the various structural components of the bridge are at or below the calculated allowable values. Accordingly, the bridge design is satisfactory from a conventional structural analysis viewpoint. This conclusion is supported by field inspection of the bridge, which indicated no signs of distress in the integral superstructure or the abutments.

The settlement analysis of the pile-supported bridge piers of Bridge I-2 indicated that long-term settlement of the pier should be approximately 0.2 to 0.5 inch (5 to 13 mm). Field inspections and available maintenance records of Bridge I-2 indicate that the piers did not experience any measurable settlement, lateral movement, or rotation. These results should be expected considering the precompressed character of the cohesive subsoils encountered at the bridge site.

A settlement analysis was also made on the approaches of Bridge I-2 due to self-weight of the approach slab and the underlying embankment. The calculated long-term settlement was about 0.5 to 1 inch (13 to 25 mm). Field measurements indicated a difference in grade of about 1 to 2 inches (25 to 51 mm) at the edge of the approach slab. A higher grade difference of about 3 inches (76 mm) was measured at a distance of about 10 feet (3.1 m) away from the roadway edge. These grade differences could be due to high or low local survey points on the approach slab or due to construction or survey error.

A geotechnical analyses indicated that the present design of the geosynthetic-reinforced embankment is satisfactory and on the conservative side for fair to good (medium stiff to stiff) soil subgrade conditions. This is due to the relatively small height of the embankment and the precompressed character of the subsoils. It is understood that this

conservative design was necessary to create the vertical annular space (gap) between the embankment face and the backwall.

A finite element parametric study was performed on Bridge I-1. Five parameters were considered in this analysis that included uniform temperature increase with roller supports assumed at the boundaries, uniform temperature increase with hinge supports, a temperature gradient, approach slab settlement, and bridge skew angle. As a given parameter was varied, all others properties of the bridge components were set to the design value.

Review of the finite element results indicated that the various components of Bridge I-1 were at or below allowable stress levels for all cases, excluding the case of approach slab settlement. The calculated stresses at the top surface of the backwall indicated that cracking would occur at the connection with the approach slab settlement. The connection could become overstressed in compression due to about 1.1 inches (30 mm) of settlement at the far end of the approach slab. This condition is the most important factor affecting the semi-integral abutment performance and, therefore, it should be considered in the design of the various structural components of the superstructure. Based on the results of the FEM temperature analysis, the gap as designed and constructed in Bridge I-1 is sufficient in terms of width. Seasonal temperature changes anticipated at the bridge location should not cause bridge expansion in excess of the provided gap. Thus, the abutment should not be subjected to lateral earth pressure across the backwall beneath the approach slab.

The cost/benefit analysis showed that the difference in cost between the existing Bridge I-2 and a comparable conventional bridge of similar dimensions and spans is approximately $28,311, with the conventional bridge costing more. The estimated costs were based on construction costs and do not consider any additional costs due to long-term maintenance of strip seal joints, time savings attributed to omitting strip seal joints and indirect benefits resulting from a smoother ride over the jointless bridge.

In summary, the overall results of the study indicated that the existing six prototype semi-integral bridges are performing well and according to the design specifications. In view of this as well as the positive results of the cost/benefit analysis, it could be concluded that the present DOTD semi-integral bridge design is structurally sound and cost effective. Therefore, the use of this type of bridge should be continued and promoted by DOTD, with minor adjustments to account for local soil conditions at a given site. The present design is innovative and incorporates the recommendations of many researchers, which address the potential problems of integral and semi-integral bridges. The important features of the present DOTD design that should be maintained in future designs include:

- Casting the approach slab with the bridge deck and backwalls as one integral structure eliminates the potential for abutment movement or rotation.
- Using a geosynthetic-reinforced embankment with an MSE face creates a vertical gap that eliminates lateral pressure transfer to the backwall.
- Using a sleeper slab and an expansion joint at the end of the approach slab eliminates the effects of seasonal thermal variations on the adjacent roadway pavement.
- Using a non-plastic material for embankment construction with the front segments of the top and bottom lifts filled with stone, provides an excellent drainage medium in the gap area behind the backwall.

RECOMMENDATIONS

As previously discussed, all six DOTD semi-integral abutment prototype bridges are performing well, except for two minor concerns with Bridges I-1, I-3, and I-4. Two alternatives could permanently address the asphalt-curling problem in Bridge I-1. First, a joint could be cut in the asphalt at the end of each approach slab. The joint should be approximately 2.5 inches (6.5 cm) wide to accommodate thermal movements of the concrete superstructure. This joint could then be filled with a compressible joint material to improve the ride across the end of each approach slab. Alternatively, a sleeper slab could be constructed to support the end of the approach slab, with an open joint between the approach slab and sleeper slab filled with compressible joint material. Construction of either repair should be done at ambient temperatures of at least 50° F (10° C). The latter alternative was adopted in all subsequent semi-integral bridges. Bridges I-3 and I-4 need to be inspected periodically for cracking, particularly the connection between the approach slab and the backwall.

Based on the results of the study, use of the present design of semi-integral abutment bridges could be continued throughout Louisiana in areas where the soils conditions are fair to good. These sites include those with predominantly cohesive soils of at least a medium stiff consistency or those with predominantly granular character where the anticipated long-term settlements are tolerable. All future semi-integral bridge designs should consider the following:

1. Creating and maintaining a continuous vertical annular space (gap), at least 6 inches (150 mm) wide, behind the backwall. The gap should not be filled with conventional fill material. This would allow the backwall to freely move longitudinally and reduce the risk of future problems due to thermal variations.
2. While a larger gap is specified than what is necessitated by the design to accommodate construction conditions, contractors should be attentive during removal of the construction forms along the face of the embankment to reduce the potential for lateral movement of the embankment face into the backwall and the possibility of closure of the gap.
3. Contractors should attempt to reduce the amount of fallen debris inside the annular space behind the backwall. Some insignificant amount of debris was detected in the gaps of some of the bridges. EPS geofoam blocks placed in the gap space would also eliminate the potential for this problem.

4. It is mandatory that a sleeper slab and an open compressible joint follow the approach slab.

5. Maintaining good drainage behind the backwall through weep-holes, such as those in Bridge I-1, or placing perforated drainage pipe in the gravel at the bottom lift of the geosynthetic-reinforced embankment is recommended. Good drainage reduces the potential for water pressure buildup behind the backwall. The conditions inside the gap could also be evaluated through the weep-holes during routine inspections.

6. Moderate length bridges could include expansion dams or finger joints to reduce the jointless bridge length, as is the case in Bridge I-2.

7. Designing a weak joint or "internal hinge" in the approach slab at some distance away from the backwall, e.g., about one-quarter of the approach slab length, is recommended. This design would enable the approach slab to safely span as a cantilever over the gap while accommodating any future settlement. If excessive settlement does occur, the short segment of slab up to the weak joint would act as a cantilever while the remainder of the approach slab would be supported on the embankment surface. In Bridge I-2, the weak joint was constructed with a saw cut joint. Field inspection of this bridge found that, to date, the week joint has performed well but the joint has not.

It is recommended that a detailed parametric study be performed in the future to investigate the effects of other design parameters on the performance of semi-integral abutment bridges. These parameters may include girder type, span, width, deck thickness, size of gap, loads, skew, abutment height, etc. Each case in the parametric study would require redesign of the reinforcement of the abutment, slab, and girders as necessary for that particular case. Results of the parametric study would be used in refining the present design methodology and developing additional design recommendations.

It is further recommended that the future FEA study focus on the slab/supporting soil system interaction. For example, the present semi-integral bridge design allows for longitudinal movement due seasonal temperature variations. The field investigation revealed some separation exists between the approach slab and the underlying geosynthetic-reinforced embankment near the backwall. A preliminary FEA analysis found that lack of vertical support close to the backwall would increase the stresses in the approach slab at the haunch area just prior to overcoming the interface bond. However, the approach slab must then be designed as a structural element for some distance, as it is no longer a slab on grade. The

potential for loss of support under an approach slab due to embankment settlement is accounted for in the present DOTD design by assuming that only one-half the approach slab span is soil supported. In Bridge I-2, a week joint was created to address this concern. The optimal distance between the backwall and the weak joint could be ascertained through the proposed FEA study.

ACRONYMS, ABBREVIATIONS, & SYMBOLS

2-D = Two dimensional
3-D = Three dimensional
α_x = Thermal expansion coefficient of concrete
ϕ = Soil angle of internal friction
γ = Unit weight of a soil
ΔT = Temperature increase
Δz = Longitudinal displacement
μ_{xy} = Posisson's ratio of concrete
σ_{xx} = Stress in x plane
σ_{yy} = Stress in y plane
σ_{zz} = Stress in z plane
τ_{xy} = Shear stress in xy plane
τ_{yz} = Shear stress in yz plane
τ_{xz} = Shear stress in xz plane
cu. = Cubic
e_o = Void ratio of a soil
in. = Inch
f_c' = Compressive strength of concrete
ft. = Foot
kg = Kilogram
lbs. = Pounds
lin. = Linear
q_u = Undrained compressive strength of a cohesive soil
m = Meter
mm = Millimeter
^oC = Degrees Celsius
^oF = Degrees Fahrenheit
pcf = Pounds per cubic foot
psi = Pounds per square inch
psf = Pounds per square foot
w = Unit weight of reinforced concrete
yd. = Yard
AASHTO = American Association of State Highway and Transportation Officials
APDL = ANSYS Parametric Design Language
ASTM = American Society for Testing and Materials

AVG = Average
C_c = Compression Index of a cohesive soil
C_u = Undrained cohesion of a cohesive soil
DOT's = States' Departments of Transportation
DOTD = Louisiana Department of Transportation and Development
E = East
E_x = Elastic modulus of concrete
EPS = Expanded polystyrene
FEA = Finite element analysis
FEM = Finite element method
FHWA = Federal Highway Administration
LL = Plastic Limit
LTRC = Louisiana Transportation Research Center
NW = Northwest
OCR = Over consolidation ratio
PCI = Portland Concrete Institute
PI = Plasticity Index
PL = Plastic Limit
SE = Southeast
USCS = Unified Soil Classification System
W = West

REFERENCES

1. PCI, *The State of the Art of Precast / Prestressed Integral Bridges*, Precast / Prestressed Concrete Institute, Chicago, IL, 2001.
2. Stark, T.D., Arellano, D., Horvath, J.S. and Leshchinsky, D., Guidelines for Geofoam Applications in Embankment projects, Final Report, NCHRP, Transportation Research Board, national Research Council, Project No. 24-11, 2003.
3. Kurin, J. and Alampalli, S., *Integral Abutment Bridges: Current Practices in the United States and Canada*, Report FHWA/ NY/ SR-99/ 132, Transportation Research and Development Bureau, Jun. 1999.
4. State of Louisiana Department of Transportation and Development Baton Rouge, *Louisiana Standard Specifications for Roads and Bridges*, DOTD 03-07-7002, 2000.
5. American Association of State Highway and Transportation Officials (AASHTO), *Standard Specifications for Highway Bridges*, Sixteenth Edition, American Association of State Highway and Transportation Officials, Washington, D.C., 1996.
6. American Society for Testing and Materials (ASTM), *Annual Book of ASTM Standards, Soils and Rock*, Vol. 4.0, 2004.
7. Federal Highway Administration (FHWA), *Guidelines for Design and Construction of geosynthetic Mechanically Stabilized Earth Slopes on Firm Foundations,"* U.S. Department of Transportation, SA-93-025, 1993.
8. MesaPro, Computer Program for Analysis of Mechanically Stabilized Earth Walls, Ver. 1.0, Tensar Earth Technologies, Inc., 1998.
9. ANSYS, Engineering Analysis System User's Manual, Swanson Analysis System, Inc.
10. Weather Underground, http://www.wunderground.com/
11. State of Louisiana Department of Transportation and Development, 'Letting Information: Bid Item Weighted Unit Prices', 2003.
12. Cernica, J.N., *Geotechnical Engineering: Soil Mechanics.* John Wiley & Sons, Inc., New York, NY, 1995.
13. Koerner, R.M., *Design with Geosynthetics*. Simon & Schuster, New Jersey 1998.
14. State of Louisiana Department of Transportation and Development, *Louisiana Dept. of Transportation and Development Bridge Design Manual*, Fourth English Edition, Version. 1.1, 2002.

15. Briaud, J.L., James, R.W. and Hoffman, S.B., *Settlement of bridge approaches (The bump at the end of the bridge)*, Synthesis of Highway Practice 234, National Academy Press, Washington, D.C., U.S.A., 1997, pp 75.

16. Burdette, E.G., Ingram, E.E., Goodpasture, D.W. and Deatherage, J.H., *Behavior of Concrete Integral Abutments*, Concrete International, Jul 2002, pp. 59-63.

17. Burke, M.P., Jr., *Cracking of Concrete Decks and other Problems with Integral Type Bridges*, Transportation Research Record No.1688, Transportation Research Board, 1999, pp. 131-138.

18. Burke, M.P., Jr., *Integral Bridges*, Transportation Research Record, No.1275, Transportation Research Board, 1990, pp. 53-61.

19. Dagher, H.J., Elgaaly, M., and Kankam, J., *Analytical Investigation of Slab Bridges with Integral Wall Abutments*, Transportation Research Record No. 1319, Transportation Research Board, 1991, pp. 115-125.

20. Edgar, T.V., Puckett, J.A. and D'Spain, R.B., *Effects of geotextiles on lateral pressure and deformation in highway embankments*, Geotextiles and Geomembranes, Elsevier Science Ltd., London, U.K., Vol. 8, No. 4, 1998, pp. 275-292.

21. Helwany, S.M., WU, J.T. and Froessl, B., *GRS Bridge Abutments-an effective means to alleviate bridge approach settlement*, Geotextiles and Geomembranes, Journal of the International Geotextile Society, Vol. 21, 2002.

22. Kamel, M.R., Benak, J.V., Tadros, M.K., and Jamshidi, M., *Application of Precast Prestressed Concrete Piles in Integral Abutment Bridges*, Fourth International Bridge Eng. Conf., Transportation Research Board, 1995, pp. 146-157.

23. Misty, V.C., *Integral Abutment and Jointless Bridges*, Conf. on High Performance Steel Bridge, National Bridge Research Organization, 2000.

24. Mourad, S. and Tabsh, S.W., *Deck Slab Stresses in Integral Abutment Bridges*, Journal of Bridge Engineering, May 1999, pp. 125-130.

25. Precast/Prestressed Concrete Institute, *Precast Prestressed Concrete Bridge Design Manual*, MNL-133-97, Precast/Prestressed Concrete Institute, Chicago, IL, 1997.

26. Reid, R.A., Soupir, S.P. and Schaefer, V.R., *Use of fabric reinforced soil walls for integral abutment bridge and treatment*, Proc. of the Sixth International Conf. on Geosynthetics, R.K. Rowe (ed.), Industrial Fabrics Association International, Roseville, MN, USA, 1998, pp. 1-11.

27. Thippeswamy, H.K. and GangaRao, H.V.S., *Analysis of In-Service Jointless Bridges*, Transportation Research Record, No. 1476, Transportation Research Board, 1995, pp. 162-170.

28. Thippeswamy, H.K., GangaRao, H.V.S., and Franco, J.M., *Performance Evaluation of Jointless Bridges*, Journal of Bridge Eng., ASCE, Oct. 2002, pp. 276-289.

29. Van Lund, J.A. and Brecto, B.B., *Jointless Bridges and Bridge Joints in Washington State*, Transportation Research Record, No. 1688, Transportation Research Board, 1999, pp. 116-123.

30. Wassweman, E.P., *Design of Integral Abutments for Jointless Bridges*, Structure, May 2001, pp. 24-33.

31. Card, G.B. and Carder, D. R., *A literature review of the geotechnical aspects of the design of integral bridge abutments*, Project Report 52, Transport Research Laboratory, Crowthorne, Berkshire, U.K, 1993.

32. Carr, S.P., "Comparison between Jointless and Conventional Bridges,"' Thesis submitted to Tulane University Civil and Environmental Engineering, 2004.

33. Das, C.S., Bakeer, R.M., Zhong, J. and Schutt, M.A., *Assessment of Mitigating Embankment Settlement with Pile-Supported Approach Slabs*, Louisiana Transportation Research Center, Summary Report, 1999.

34. Thomas Telford Online, *http://www.t-telford.co.uk/html/.*

35. TRB, *Highway Capacity Manual*, Special Report 209, 3rd Edition Update, National Research Council, Washington, D.C., 1994.

APPENDIX A

Selected Photographs Of Bridge Sites

Figure 49
Bridge C-1

Figure 50
Bridge C-1

Figure 51
Bridge C-1

Figure 52
Bridge C-1

Figure 53
Bridge C-1

Figure 54
Bridge C-2

Figure 55
Bridge C-2

Figure 56
Bridge C-3

Figure 57
Bridge C-3

Figure 58
Bridge I-1

Figure 59
Bridge I-2

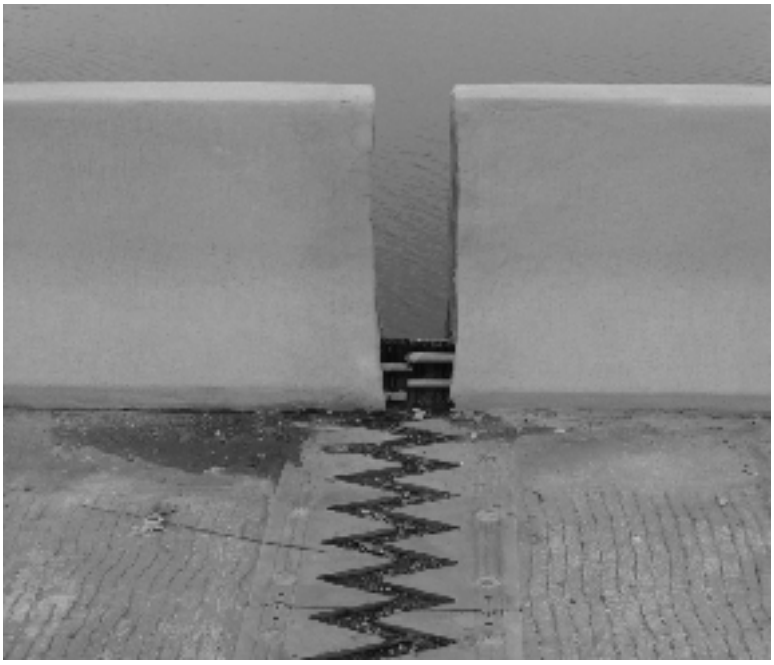

Figure 60
Bridge I-2

Figure 61
Bridge I-3

Figure 62
Bridge I-3

Figure 63
Bridge I-3

Figure 64
Bridge I-3

Figure 65
Bridge I-4

Figure 66
Bridge I-5

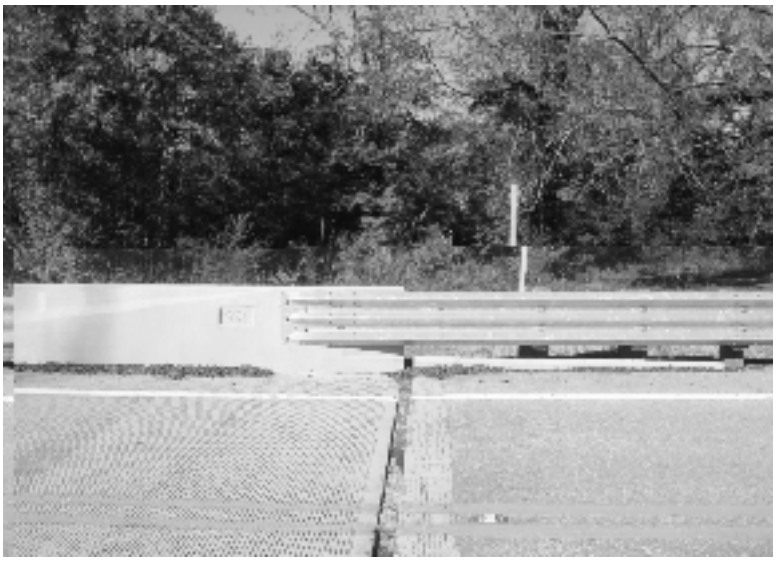

Figure 67
Bridge I-5

APPENDIX B

Finite Element Model Verification

The Finite Element Model

The FEA mesh used in this preliminary study modeled the backwall and approach slab. The abutment was held fixed against translation at the deck/girder connection. The boundary at the bottom of the abutment was modeled as a series of rollers in the longitudinal direction. The interface between the approach slab and the geosynthetic-reinforced embankment was also modeled as a series of rollers in the longitudinal direction.

The model was loaded with the equivalent loads of the approach slab/backwall interface at the time of interface failure. The shear forces that developed at the interface were lumped into small, concentrated loads at the bottom nodes of the approach slab. The load was then stepped from zero to the value at failure when bonding was overcome and slip did occur. All concrete structural elements (approach slab and backwall) were modeled with 3-D cubic elements (ANSYS Solid65). The cracking and crushing capabilities of the Solid65 element were activated in this analysis. This allowed for tracking of crack development and detection of their locations within the concrete element. Several reinforcement techniques were available for the Solid65 element. The discrete approach was selected for the analysis. Link8 elements were used to represent the longitudinal reinforcement in the approach slab. The backwall was assumed to be fully fixed along its boundary with the bridge and the approach slab was assumed to be simply supported in the vertical direction.

Convergence

Convergence was studied by decreasing the size of the concrete element as a function of the slab depth. A Concrete Element Dimensioning Factor (CEDIMFAC) available in the APDL program was activated. CEDIMFAC set the target size of the concrete element. The geometry was generated as two rows of concrete elements in a three-dimensional space. The longitudinal reinforcement on the slab was modeled as Link8 elements running throughout the common nodes between these two rows of concrete elements.

Convergence of the solution was achieved as long as the concrete did not crack. Numerical instabilities developed in analyses that had medium to high values of adhesion and friction. These instabilities occurred because, when a concrete element fail, ANSYS multiplied the stiffness of the concrete element by a very small reduction factor (essentially zero). As loads were still being applied to the element with no stiffness, the force/convergence criterion could not be met and the solution diverged. If cracks are expected, the smallest concrete element size recommended for concrete structures should be in the range of 1.5 to 2 inches (37 to 51 mm) because the length of the cracks can reach two to three times the largest aggregate size present in the concrete. If the concrete does not crack, any size could be selected for the concrete element provided that it does not exceed the

limitations set fourth by ANSYS (32,000 elements in the ResearchFS version) and by the computer platform.

As previously discussed, convergence was studied by decreasing the size of the concrete element and measuring the variation of the critical stress point in the system. Table 24 describes the variation of this stress in terms of the CEDIMFAC parameter (the size of the element defined by the depth of the approach slab/CEDIMFAC). The trendline of CEDIMFAC versus stress is given in figure 68. By setting CEDIMFAC to zero, one can find that absolute convergence occurs at a CEDIMFAC equal to 34. However, this is extremely computationally intensive. The solution for the system at CEDIMFAC = 22 took 7 hours on a 2.4 GHz personal computer with 768 MB of DDR Ram. The solution time would increase exponentially as the element size decreases. By inserting a value of 34 for CEDIMFAC back into the original equation, an error estimate can be found for a given solution. Use of a trendline permits the analysis to be performed at lower CEDIMFAC with acceptable accuracy. Using the trendline and estimating the actual stress in the system under absolute convergence conditions could be used to calculate the accuracy of the results.

Table 24
Convergence curve for FEA model

CEDIMFAC	Max. Tensile Stress psi (kPa)	% Error
6	145 (1,000)	29
8	149 (1,027)	27
10	161 (1,110)	21
12	170 (1,117)	17
14	172 (1,130)	16
16	180 (1,182)	12
18	186 (1,221)	9
22	194 (1,274)	5
34	205 (1,347)	0

1 psi = 145.93 MPa

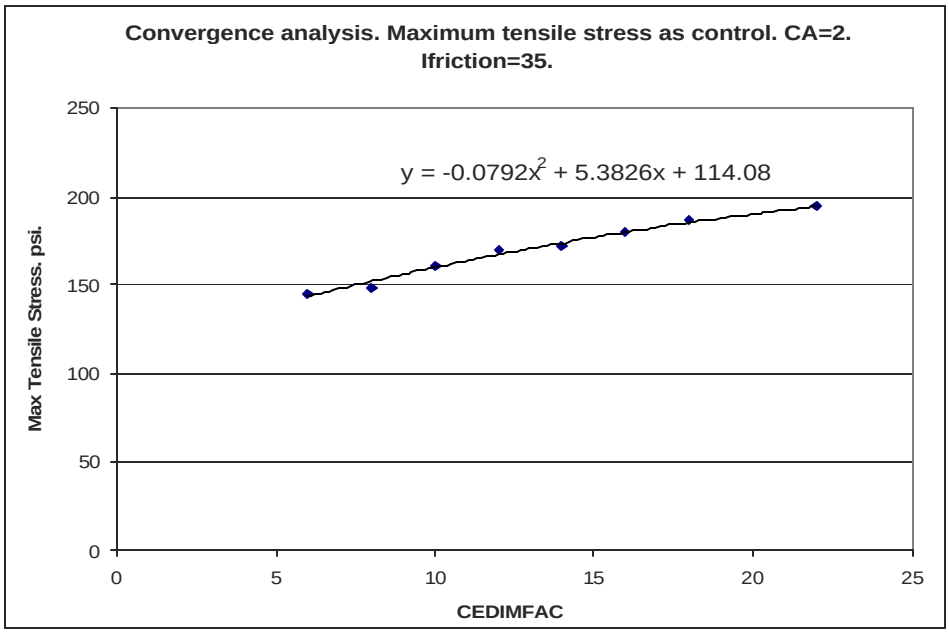

1 psi = 6.895 kPa

Figure 68
Variation of stress in terms of the CEDIMFAC parameter

Initial Finite Element Results

A typical stress distribution resulting from the finite element analysis is presented in figure 69 for illustrative purposes. An analysis with a CEDIMFAC = 10, Ca = 2.5 psi, and IFRICTION = 25, revealed the following stress distribution (note that the stresses are expected to be 20 percent higher in the fully converged case). All stresses are in psi units. A parametric study was performed to determine the effect of changing the haunch angle. The results are shown in table 25. Note that for small values of the haunch angle, the critical stress point is moved to the backwall. A few of the initial cases show cracks in the system and stress redistribution (CEDIMFAC=12, ca=3, IFRICTION=2.5). Figures 70 and 71 are examples of such cases. The circle in figure 71 indicates locations of cracking.

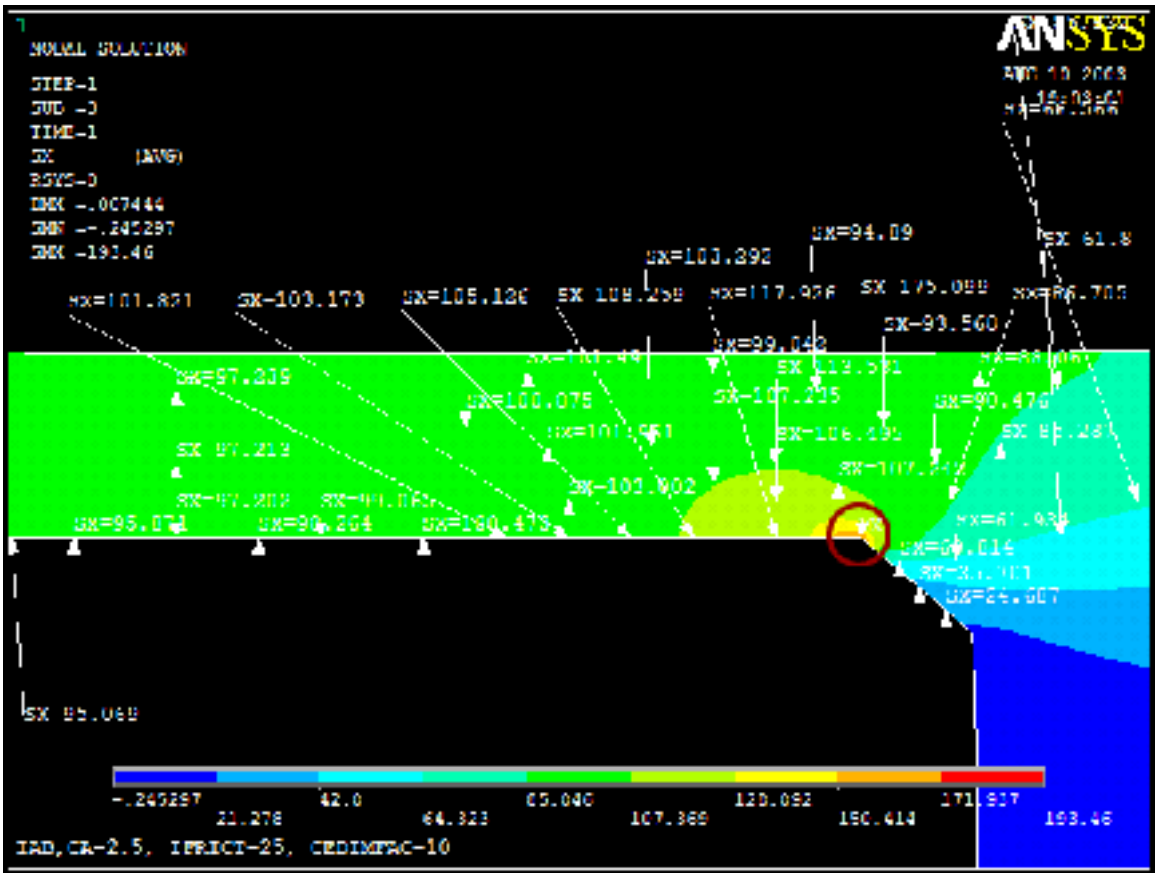

Figure 69
Stress distribution with CEDIMFAC=10, Ca = 2.5 psi & IFRICTION = 25

Table 25
Effect of changing the haunch angle

Haunch Angle	Maximum Stress (MPa)	Maximum Stress at Haunch/Backwall (MPa)
0	216 (2)	----
5	242 (2)	111
15	173.72 (1)	126.4
30	154.31	154.31
40	162.95	162.95
45	169.95	169.95
50	169.5	169.5
60	177.869	177.869
(1) Max stress occurs at haunch/backwall connection		
(2) Max stress at slab/backwall interception		

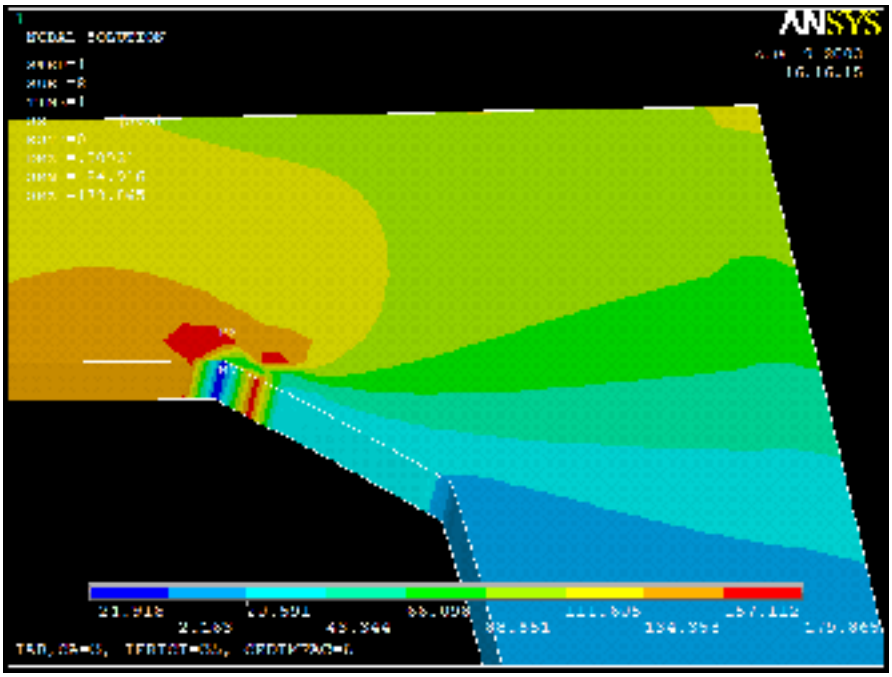

Figure 70
Cracks in the system

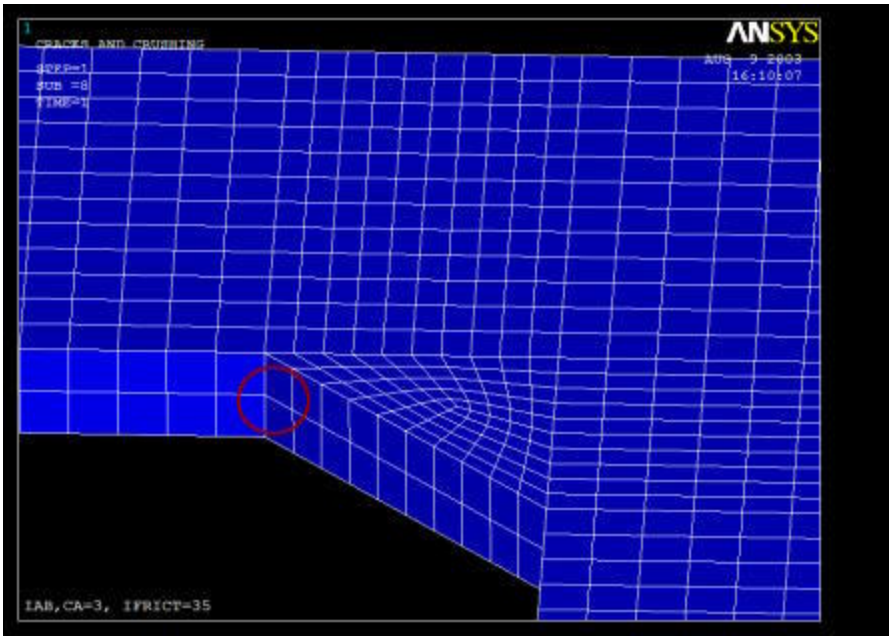

Figure 71
Another view of the cracks in the system

APPENDIX C
Typical STAAD–III Input File

Five-Span and Four-Span Continuous Live Load

```
            ************************************************
            *                                              *
            *           S T A A D - III                    *
            *           Revision 23.0                      *
            *           Proprietary Program of             *
            *           Research Engineers, Inc.           *
            *           Date=    MAR  6, 2004              *
            *           Time=    10:34:13                  *
            *           Build No.    1007.01.02            *
            *      USER ID:                                *
            ************************************************
```

```
     1. STAAD SPACE
     2. INPUT WIDTH 72
     3. UNIT FEET KIP
     4. *CONTLL.STD
     5. JOINT COORDINATES
     6. 1     0.00      0.00    0.00
     7. 2     8.00      0.00    0.00
     8. 3    16.00      0.00    0.00
     9. 4    24.00      0.00    0.00
    10. 5    32.00      0.00    0.00
    11. 6    40.00      0.00    0.00
    12. 7    48.00      0.00    0.00
    13. 8    56.00      0.00    0.00
    14. 9    64.00      0.00    0.00
    15. 10   72.00      0.00    0.00
    16. 11   80.00      0.00    0.00
    17. 12   88.00      0.00    0.00
    18. 13   96.00      0.00    0.00
    19. 14  104.00      0.00    0.00
    20. 15  112.00      0.00    0.00
    21. 16  120.00      0.00    0.00
    22. 17  128.00      0.00    0.00
    23. 18  136.00      0.00    0.00
    24. 19  144.00      0.00    0.00
    25. 20  152.00      0.00    0.00
    26. 21  160.00      0.00    0.00
    27. 22  168.00      0.00    0.00
    28. 23  176.00      0.00    0.00
    29. 24  184.00      0.00    0.00
    30. 25  192.00      0.00    0.00
    31. 26  200.00      0.00    0.00
    32. 27  208.00      0.00    0.00
    33. 28  216.00      0.00    0.00
    34. 29  224.00      0.00    0.00
    35. 30  232.00      0.00    0.00
    36. 31  240.00      0.00    0.00
    37. 32  248.00      0.00    0.00
    38. 33  256.00      0.00    0.00
    39. 34  264.00      0.00    0.00
    40. 35  272.00      0.00    0.00
    41. 36  280.00      0.00    0.00
```

42.	37	288.00	0.00	0.00
43.	38	296.00	0.00	0.00
44.	39	304.00	0.00	0.00
45.	40	312.00	0.00	0.00
46.	41	320.00	0.00	0.00
47.	42	328.00	0.00	0.00
48.	43	336.00	0.00	0.00
49.	44	344.00	0.00	0.00
50.	45	352.00	0.00	0.00
51.	46	360.00	0.00	0.00
52.	47	368.00	0.00	0.00
53.	48	376.00	0.00	0.00
54.	49	384.00	0.00	0.00
55.	50	392.00	0.00	0.00
56.	51	400.00	0.00	0.00
57.	52	408.00	0.00	0.00
58.	53	416.00	0.00	0.00
59.	54	424.00	0.00	0.00
60.	55	432.00	0.00	0.00
61.	56	440.00	0.00	0.00
62.	57	448.00	0.00	0.00
63.	58	456.00	0.00	0.00
64.	59	464.00	0.00	0.00
65.	60	472.00	0.00	0.00
66.	61	480.00	0.00	0.00
67.	62	488.00	0.00	0.00
68.	63	496.00	0.00	0.00
69.	64	504.00	0.00	0.00
70.	65	512.00	0.00	0.00
71.	66	520.00	0.00	0.00
72.	67	528.00	0.00	0.00
73.	68	536.00	0.00	0.00
74.	69	544.00	0.00	0.00
75.	70	552.00	0.00	0.00
76.	71	560.00	0.00	0.00
77.	72	568.00	0.00	0.00
78.	73	576.00	0.00	0.00
79.	74	584.00	0.00	0.00
80.	75	592.00	0.00	0.00
81.	76	600.00	0.00	0.00
82.	77	608.00	0.00	0.00
83.	78	616.00	0.00	0.00
84.	79	624.00	0.00	0.00
85.	80	632.00	0.00	0.00
86.	81	640.00	0.00	0.00
87.	82	648.00	0.00	0.00
88.	83	656.00	0.00	0.00
89.	84	664.00	0.00	0.00
90.	85	672.00	0.00	0.00
91.	86	680.00	0.00	0.00
92.	87	688.00	0.00	0.00
93.	88	696.00	0.00	0.00
94.	89	704.00	0.00	0.00
95.	90	712.00	0.00	0.00
96.	91	720.00	0.00	0.00

97. MEMBER INCIDENCES

98.	1	1	2
99.	2	2	3
100.	3	3	4
101.	4	4	5
102.	5	5	6
103.	6	6	7
104.	7	7	8
105.	8	8	9
106.	9	9	10
107.	10	10	11
108.	11	11	12
109.	12	12	13
110.	13	13	14
111.	14	14	15
112.	15	15	16
113.	16	16	17
114.	17	17	18
115.	18	18	19
116.	19	19	20
117.	20	20	21
118.	21	21	22
119.	22	22	23
120.	23	23	24
121.	24	24	25
122.	25	25	26
123.	26	26	27
124.	27	27	28
125.	28	28	29
126.	29	29	30
127.	30	30	31
128.	31	31	32
129.	32	32	33
130.	33	33	34
131.	34	34	35
132.	35	35	36
133.	36	36	37
134.	37	37	38
135.	38	38	39
136.	39	39	40
137.	40	40	41
138.	41	41	42
139.	42	42	43
140.	43	43	44
141.	44	44	45
142.	45	45	46
143.	46	46	47
144.	47	47	48
145.	48	48	49
146.	49	49	50
147.	50	50	51
148.	51	51	52
149.	52	52	53
150.	53	53	54
151.	54	54	55
152.	55	55	56
153.	56	56	57

```
   154. 57   57        58
   155. 58   58        59
   156. 59   59        60
   157. 60   60        61
   158. 61   61        62
   159. 62   62        63
   160. 63   63        64
   161. 64   64        65
   162. 65   65        66
   163. 66   66        67
   164. 67   67        68
   165. 68   68        69
   166. 69   69        70
   167. 70   70        71
   168. 71   71        72
   169. 72   72        73
   170. 73   73        74
   171. 74   74        75
   172. 75   75        76
   173. 76   76        77
   174. 77   77        78
   175. 78   78        79
   176. 79   79        80
   177. 80   80        81
   178. 81   81        82
   179. 82   82        83
   180. 83   83        84
   181. 84   84        85
   182. 85   85        86
   183. 86   86        87
   184. 87   87        88
   185. 88   88        89
   186. 89   89        90
   187. 90   90        91
   188. SUPPORTS
   189. 1 51 91 FIXED BUT FX MZ
   190. 11 21 31 41 61 71 81 FIXED
   191. MEMBER RELEASES
   192. 1 51 START MZ
   193. 50 90 END MZ
   194. UNIT INCHES
   195. MEMBER PROPERTY AMERICAN
   196. 1 TO 90 PRI AX 1068.5 AY 315 AZ 266 IX 18440 IY 343770 IZ 343938
   197. CONSTANT
   198. E 4696 ALL
   199. DENSITY CONCRETE ALL
   200. UNIT FT KIP
   201. LOAD 1 LIVE LOAD
   202. JOINT LOAD
   203. 1 FY -1.0
   204. LOAD 2 LIVE LOAD
   205. JOINT LOAD
   206. 2 FY -1.0
   207. LOAD 3 LIVE LOAD
   208. JOINT LOAD
   209. 3 FY -1.0
```

```
   210. LOAD 4 LIVE LOAD
   211. JOINT LOAD
   212. 4 FY -1.0
   213. LOAD 5 LIVE LOAD
   214. JOINT LOAD
   215. 5 FY -1.0
   216. LOAD 6 LIVE LOAD
   217. JOINT LOAD
   218. 6 FY -1.0
   219. LOAD 7 LIVE LOAD
   220. JOINT LOAD
   221. 7 FY -1.0
   222. LOAD 8 LIVE LOAD
   223. JOINT LOAD
   224. 8 FY -1.0
   225. LOAD 9 LIVE LOAD
   226. JOINT LOAD
   227. 9 FY -1.0
   228. LOAD 10 LIVE LOAD
   229. JOINT LOAD
   230. 10 FY -1.0
   231. LOAD 11 LIVE LOAD
   232. JOINT LOAD
   233. 11 FY -1.0
   234. LOAD 12 LIVE LOAD
   235. JOINT LOAD
   236. 12 FY -1.0
   237. LOAD 13 LIVE LOAD
   238. JOINT LOAD
   239. 13 FY -1.0
   240. LOAD 14 LIVE LOAD
   241. JOINT LOAD
   242. 14 FY -1.0
   243. LOAD 15 LIVE LOAD
   244. JOINT LOAD
   245. 15 FY -1.0
   246. LOAD 16 LIVE LOAD
   247. JOINT LOAD
   248. 16 FY -1.0
   249. LOAD 17 LIVE LOAD
   250. JOINT LOAD
   251. 17 FY -1.0
   252. LOAD 18 LIVE LOAD
   253. JOINT LOAD
   254. 18 FY -1.0
   255. LOAD 19 LIVE LOAD
   256. JOINT LOAD
   257. 19 FY -1.0
   258. LOAD 20 LIVE LOAD
   259. JOINT LOAD
   260. 20 FY -1.0
   261. LOAD 21 LIVE LOAD
   262. JOINT LOAD
   263. 21 FY -1.0
   264. LOAD 22 LIVE LOAD
   265. JOINT LOAD
```

```
   266. 22 FY -1.0
   267. LOAD 23 LIVE LOAD
   268. JOINT LOAD
   269. 23 FY -1.0
   270. LOAD 24 LIVE LOAD
   271. JOINT LOAD
   272. 24 FY -1.0
   273. LOAD 25 LIVE LOAD
   274. JOINT LOAD
   275. 25 FY -1.0
   276. LOAD 26 LIVE LOAD
   277. JOINT LOAD
   278. 26 FY -1.0
   279. LOAD 27 LIVE LOAD
   280. JOINT LOAD
   281. 27 FY -1.0
   282. LOAD 28 LIVE LOAD
   283. JOINT LOAD
   284. 28 FY -1.0
   285. LOAD 29 LIVE LOAD
   286. JOINT LOAD
   287. 29 FY -1.0
   288. LOAD 30 LIVE LOAD
   289. JOINT LOAD
   290. 30 FY -1.0
   291. LOAD 31 LIVE LOAD
   292. JOINT LOAD
   293. 31 FY -1.0
   294. LOAD 32 LIVE LOAD
   295. JOINT LOAD
   296. 32 FY -1.0
   297. LOAD 33 LIVE LOAD
   298. JOINT LOAD
   299. 33 FY -1.0
   300. LOAD 34 LIVE LOAD
   301. JOINT LOAD
   302. 34 FY -1.0
   303. LOAD 35 LIVE LOAD
   304. JOINT LOAD
   305. 35 FY -1.0
   306. LOAD 36 LIVE LOAD
   307. JOINT LOAD
   308. 36 FY -1.0
   309. LOAD 37 LIVE LOAD
   310. JOINT LOAD
   311. 37 FY -1.0
   312. LOAD 38 LIVE LOAD
   313. JOINT LOAD
   314. 38 FY -1.0
   315. LOAD 39 LIVE LOAD
   316. JOINT LOAD
   317. 39 FY -1.0
   318. LOAD 40 LIVE LOAD
   319. JOINT LOAD
   320. 40 FY -1.0
   321. LOAD 41 LIVE LOAD
```

```
322. JOINT LOAD
323. 41 FY -1.0
324. LOAD 42 LIVE LOAD
325. JOINT LOAD
326. 42 FY -1.0
327. LOAD 43 LIVE LOAD
328. JOINT LOAD
329. 43 FY -1.0
330. LOAD 44 LIVE LOAD
331. JOINT LOAD
332. 44 FY -1.0
333. LOAD 45 LIVE LOAD
334. JOINT LOAD
335. 45 FY -1.0
336. LOAD 46 LIVE LOAD
337. JOINT LOAD
338. 46 FY -1.0
339. LOAD 47 LIVE LOAD
340. JOINT LOAD
341. 47 FY -1.0
342. LOAD 48 LIVE LOAD
343. JOINT LOAD
344. 48 FY -1.0
345. LOAD 49 LIVE LOAD
346. JOINT LOAD
347. 49 FY -1.0
348. LOAD 50 LIVE LOAD
349. JOINT LOAD
350. 50 FY -1.0
351. LOAD 51 LIVE LOAD
352. JOINT LOAD
353. 51 FY -1.0
354. LOAD 52 LIVE LOAD
355. JOINT LOAD
356. 52 FY -1.0
357. LOAD 53 LIVE LOAD
358. JOINT LOAD
359. 53 FY -1.0
360. LOAD 54 LIVE LOAD
361. JOINT LOAD
362. 54 FY -1.0
363. LOAD 55 LIVE LOAD
364. JOINT LOAD
365. 55 FY -1.0
366. LOAD 56 LIVE LOAD
367. JOINT LOAD
368. 56 FY -1.0
369. LOAD 57 LIVE LOAD
370. JOINT LOAD
371. 57 FY -1.0
372. LOAD 58 LIVE LOAD
373. JOINT LOAD
374. 58 FY -1.0
375. LOAD 59 LIVE LOAD
376. JOINT LOAD
377. 59 FY -1.0
```

```
   378. LOAD 60 LIVE LOAD
   379. JOINT LOAD
   380. 60 FY -1.0
   381. LOAD 61 LIVE LOAD
   382. JOINT LOAD
   383. 61 FY -1.0
   384. LOAD 62 LIVE LOAD
   385. JOINT LOAD
   386. 62 FY -1.0
   387. LOAD 63 LIVE LOAD
   388. JOINT LOAD
   389. 63 FY -1.0
   390. LOAD 64 LIVE LOAD
   391. JOINT LOAD
   392. 64 FY -1.0
   393. LOAD 65 LIVE LOAD
   394. JOINT LOAD
   395. 65 FY -1.0
   396. LOAD 66 LIVE LOAD
   397. JOINT LOAD
   398. 66 FY -1.0
   399. LOAD 67 LIVE LOAD
   400. JOINT LOAD
   401. 67 FY -1.0
   402. LOAD 68 LIVE LOAD
   403. JOINT LOAD
   404. 68 FY -1.0
   405. LOAD 69 LIVE LOAD
   406. JOINT LOAD
   407. 69 FY -1.0
   408. LOAD 70 LIVE LOAD
   409. JOINT LOAD
   410. 70 FY -1.0
   411. LOAD 71 LIVE LOAD
   412. JOINT LOAD
   413. 71 FY -1.0
   414. LOAD 72 LIVE LOAD
   415. JOINT LOAD
   416. 72 FY -1.0
   417. LOAD 73 LIVE LOAD
   418. JOINT LOAD
   419. 73 FY -1.0
   420. LOAD 74 LIVE LOAD
   421. JOINT LOAD
   422. 74 FY -1.0
   423. LOAD 75 LIVE LOAD
   424. JOINT LOAD
   425. 75 FY -1.0
   426. LOAD 76 LIVE LOAD
   427. JOINT LOAD
   428. 76 FY -1.0
   429. LOAD 77 LIVE LOAD
   430. JOINT LOAD
   431. 77 FY -1.0
   432. LOAD 78 LIVE LOAD
   433. JOINT LOAD
```

```
   434. 78 FY -1.0
   435. LOAD 79 LIVE LOAD
   436. JOINT LOAD
   437. 79 FY -1.0
   438. LOAD 80 LIVE LOAD
   439. JOINT LOAD
   440. 80 FY -1.0
   441. LOAD 81 LIVE LOAD
   442. JOINT LOAD
   443. 81 FY -1.0
   444. LOAD 82 LIVE LOAD
   445. JOINT LOAD
   446. 82 FY -1.0
   447. LOAD 83 LIVE LOAD
   448. JOINT LOAD
   449. 83 FY -1.0
   450. LOAD 84 LIVE LOAD
   451. JOINT LOAD
   452. 84 FY -1.0
   453. LOAD 85 LIVE LOAD
   454. JOINT LOAD
   455. 85 FY -1.0
   456. LOAD 86 LIVE LOAD
   457. JOINT LOAD
   458. 86 FY -1.0
   459. LOAD 87 LIVE LOAD
   460. JOINT LOAD
   461. 87 FY -1.0
   462. LOAD 88 LIVE LOAD
   463. JOINT LOAD
   464. 88 FY -1.0
   465. LOAD 89 LIVE LOAD
   466. JOINT LOAD
   467. 89 FY -1.0
   468. LOAD 90 LIVE LOAD
   469. JOINT LOAD
   470. 90 FY -1.0
   471. LOAD 91 LIVE LOAD
   472. JOINT LOAD
   473. 91 FY -1.0
   474. PERFORM ANALYSIS
```

```
          P R O B L E M   S T A T I S T I C S
          -----------------------------------

     NUMBER OF JOINTS/MEMBER+ELEMENTS/SUPPORTS =    91/   90/   10
     ORIGINAL/FINAL BAND-WIDTH =    1/    1
     TOTAL PRIMARY LOAD CASES  =   91, TOTAL DEGREES OF FREEDOM =   492
     SIZE OF STIFFNESS MATRIX =    5904 DOUBLE PREC. WORDS
     REQRD/AVAIL. DISK SPACE =  12.57/ 1053.8 MB,  EXMEM = 1958.5 MB

  ++ Processing Element Stiffness Matrix.             10:34:17
  ++ Processing Global Stiffness Matrix.              10:34:17
  ++ Processing Triangular Factorization.             10:34:17
```

```
  ++ Calculating Joint Displacements.                10:34:17
  ++ Calculating Member  Forces.                     10:34:18
```

475. PRINT ANA RES

APPENDIX D

Geogrid Specification Sheet

Product Specification - Structural Geogrid UX1400MSE

Tensar Earth Technologies, Inc. reserves the right to change its product specifications at any time. It is the responsibility of the specifier and purchaser to ensure that product specifications used for design and procurement purposes are current and consistent with the products used in each instance. Please contact Tensar Earth Technologies, Inc. at 800-836-7272 for assistance.

The structural geogrid shall be an integrally formed grid structure manufactured of a stress resistant high density polyethylene material with molecular weight and molecular characteristics which impart: (a) high resistance to loss of load capacity or structural integrity when the geogrid is subjected to mechanical stress in installation; (b) high resistance to deformation when the geogrid is subjected to applied force in use; and (c) high resistance to loss of load capacity or structural integrity when the geogrid is subjected to long-term environmental stress.

The structural geogrid shall accept applied force in use by positive mechanical interlock (i.e. by direct mechanical keying) with: (a) compacted soil or construction fill materials; (b) contiguous sections of itself when overlapped and embedded in compacted soil or construction fill materials; and (c) rigid mechanical connectors such as bodkins, pins or hooks. The structural geogrid shall possess sufficient cross sectional profile to present a substantial abutment interface to compacted soil or particulate construction fill materials and to resist movement relative to such materials when subject to applied force. The structural geogrid shall possess sufficient true initial modulus to cause applied force to be transferred to the geogrid at low strain levels without material deformation of the reinforced structure. The structural geogrid shall possess complete continuity of all properties throughout its structure and shall be suitable for reinforcement of compacted soil or particulate construction fill materials to improve their long term stability in structural load bearing applications such as earth retention systems. The structural geogrid shall otherwise have the following characteristics:

Product Type: **Integrally Formed Structural Geogrid**
Load Transfer Mechanism: **Positive Mechanical Interlock**

Product Properties

Load Capacity	**Units**	**MD Values**[1]
• True Initial Modulus in Use[2]	kN/m (lb/ft)	930 (66,110)
• Tensile Strength @5% Strain[2]	kN/m (lb/ft)	31 (2,130)
• Long-Term Allowable Load in Sands, Silts & Clay[3]	kN/m (lb/ft)	30.2 (2,070)
• Long-Term Allowable Load in Well Graded Sand[3]	kN/m (lb/ft)	29.3 (2,010)
• Long-Term Allowable Load in Aggregate[3]	kN/m (lb/ft)	28.8 (1,970)
Integrity of Product Structure		
• Junction Strength[4]	kN/m (lb/ft)	66 (4,520)
• Flexural Stiffness[5]	X1000 mg-cm	730
Durability		
• Resistance to Installation Damage[6]	%SC / %SW / %GP	95 / 93 / 90
• Resistance to Long Term Degradation[7]	%	100

Dimensions and Delivery

The structural geogrid shall be delivered to the jobsite in roll form with each roll individually identified and nominally measuring 1.33 meters (4.36 feet) in width and 76.2 meters (250.0 feet) in length. A typical truckload quantity is 224 rolls. On special request, the structural geogrid may also be delivered in specific lengths or widths to suit site specific engineering designs.

Notes

1. Unless indicated otherwise, values shown are minimum average roll values determined in accordance with ASTM D 4759. Brief descriptions of test procedures are given in the following notes. Complete descriptions of test procedures are available on request from Tensar Earth Technologies, Inc.
2. True resistance to elongation when initially subjected to a load measured via ASTM D5867 without deforming test materials under load before measuring such resistance or employing "secant" or "offset" tangent methods of measurement so as to overstate tensile properties.
3. The strength available for resisting force in long-term load bearing applications is determined by reducing ultimate tensile strength by [illegible] for installation damage, [illegible] in use, product integrity [illegible] and long-term product [illegible] per [illegible].
4. Load transfer capability measured via GRI GG2-87.
5. Resistance to bending force measured via ASTM D-1388, using specimens of [illegible] in length by [illegible] in width.
6. Resistance to loss of load capacity or structural integrity when subjected to mechanical installation stress in clayey sand (SC), well graded sand (SW), and crushed stone classified as poorly graded gravel (GP). The material shall be sampled in accordance with ASTM D5818 and load capacity measured in accordance with ASTM D5937.
7. Resistance to loss of load capacity or structural integrity when subjected to chemically aggressive environments measured via EPA 9090 immersion testing.

Tensar Earth Technologies, Inc.
5883 Glenridge Drive, Suite 200
Atlanta, Georgia 30328-5363
(800) 836-7271

February 1, 2004

This product specification supersedes all prior specifications for the product described above and is not applicable to any products shipped prior to February 1, 2004.